

A STUDY ON THE NAD(P)^+ TRANSHYDROGENASE FROM *AZOTOBACTER VINELANDII*

CENTRALE LANDBOUWCATALOGUS



0000 0092 0914

Dit proefschrift met stellingen van Johannes Krul, doctorandus in de Chemie, geboren te Rijswijk op 11 maart 1945, is goedgekeurd door de promotor, Dr. C. Veeger, hoogleraar in de Biochemie.

De Rector Magnificus van
de Landbouwhogeschool,
J.P.H. van der Want

Wageningen, 1 februari 1975

NN08201,625

J. Krul

A STUDY ON THE NAD(P)⁺ TRANSHYDROGENASE FROM *AZOTOBACTER VINELANDII*

Proefschrift

ter verkrijging van de graad van doctor in de landbouwwetenschappen,
op gezag van de Rector Magnificus, Prof.Dr.Ir. J.P.H. van der Want,
hoogleraar in de Virologie, in het openbaar te verdedigen op woensdag
21 mei 1975 des namiddags te vier uur in de Aula van de Landbouwhoge-
school te Wageningen

ISSN = 104346 - 03

**BIBLIOTHEEK
DER
LANDBOUWHOGESCHOOL
WAGENINGEN**

1. De door Middleditch et al. gesuggereerde samenhang tussen electronen-microscopische opnamen en sedimentatiegegevens van *Azotobacter vinelandii* transhydrogenase onder verschillende omstandigheden, is aan ernstige twijfel onderhevig.

Middleditch, L.E., Atchison, R.W. and Chung, A.E., J.Biol.Chem. 247 (1972) 6802; dit proefschrift.

2. Bij het bestuderen van de 'energy-charge' hypothese van Atkinson dienen meer dan tot nu toe gedaan is de *in vivo* condities te worden benaderd.

Atkinson, D.E., in *Metabolic Pathways* (Greenberg, D.E., ed.) 3rd Ed., Vol. 5, p. 1, Academic Press, New York 1971.
Purich, D.L. and Fromm, H.J., J.Biol. Chem. 248 (1973) 461.

3. De veranderingen in de DNA-afhankelijke RNA-polymerasen en het waargenomen RNA-synthese patroon tijdens de sporenkieming van *Rhizopus stolonifer* zouden kunnen wijzen op een meervoudige functie van het DNA-afhankelijke RNA-polymerase III.

Gong, C. and Van Etten, J.L., Biochim. Biophys. Acta 272 (1972) 44.
Roheim, J.R., Knight, R.H. and Van Etten, J.L., Develop.Biol. 41 (1974) 137.

4. De vorming van nitrogenase is niet uitsluitend gekoppeld aan het bacteriële stadium van *Rhizobium*.

Child, J.J., Nature 253 (1975) 350.
Scowcroft, W.R. and Gibson, A.H., Nature 253 (1975) 351.

5. De door Hemmerich gepostuleerde structuur van het flavine-zuurstof intermediair gevormd bij de oxidatie van gereduceerd flavine met moleculaire zuurstof is gebaseerd op onjuiste interpretatie van de experimentele gegevens.

Hemmerich, P., in 19. Mosbach Colloquium der Gesellschaft für Biologische Chemie, p. 249, Springer Verlag, Berlin-Heidelberg-New York, 1968.

6. De verklaring van Louie et al. voor de verandering van de polarisatiegraad van het aan *Pseudomonas aeruginosa* transhydrogenase gebonden flavine gaat voorbij aan de mogelijkheid van depolarisatie door energieoverdracht tussen de flavinemoleculen onderling.

Louie, D.D., Kaplan, N.O. and McLean, J.D.,
J.Mol.Biol. 70 (1972) 651.

7. De berekening van de standaardredoxpotentiaal van het superoxide radicaal zoals uitgevoerd door Rao et al. is principieel fout.

Rao, P.S. and Hayon, E., Biochem.Biophys.
Res.Commun. 51 (1973) 468.

8. De door Habib Ali et al. voorgestelde chemolitotrophe leefwijze van *Sphaerotilus discophorus* met Mn^{2+} als enige energiebron, kan niet verklaard worden uit de experimentele gegevens van deze auteurs.

Habib Ali, S. and Stokes, J.L., Antonie van
Leeuwenhoek 37 (1971) 519.
Van Veen, W.L., Antonie van Leeuwenhoek 38
(1972) 623.

9. De bepaling van oxalaat in urine volgens de methode van Menachè verdient geen aanbeveling.

Menachè, R., Clin.Chem. 20 (1974) 1445.

10. Artsen die lid zijn van de Koninklijke Nederlandse Maatschappij tot bevordering der Geneeskunst dienen krachtens hun kunstenaarschap bij werkeloosheid opgenomen te worden in de contraprestatie-regeling.

maart 1975

J.Krul.

Specialisatie kan iedere dag het leven zo gecompliceerd maken dat activiteit en leven niets meer met elkaar te maken hebben.

Ivan Illich in "Naar een
nieuwe levensstijl"

Aan de nagedachtenis van mijn vader

TEN GELEIDE

Dit proefschrift is tot stand gekomen via werk, verricht op het Laboratorium voor Biochemie van de Landbouwhogeschool Wageningen, onder leiding van Prof.Dr. C. Veeger.

Een ieder die, op zijn/haar specifieke wijze heeft bijgedragen aan het ontstaan van dit proefschrift, wil ik hierbij uitdrukkelijk bedanken.

Hierbij dienen allereerst mijn (ex)-collega's van de afdeling Biochemie genoemd te worden. Gelukkig heeft het contact met velen een bredere basis gekregen dan de puur vakmatige. De namen van de 'good old boys' Tjarda, Rob, Piet, Jaap, Ton en Hans dienen met ere vermeld te worden.

Hoewel in deze opsomming natuurlijk namen ontbreken, mag hieruit niet geconcludeerd worden dat de rest van de contacten slecht was, integendeel.

De vele 'passanten' die mij geholpen hebben in verschillende stadia van het onderzoek moeten ook genoemd worden zoals Harry Kuiper, Will Meyer, Jan de Jonge, Jan van der Hurk, Marina van Kalmthout-Kuiper, Piet Scheepens en Jan(tje) de Wit. Vooral van de twee laatstgenoemden zijn de onverstoortbaarheid en de shag onvergetelijk.

De gastvrijheid die mij verleend is op het Laboratorium voor Biochemie, afdeling Electronenmicroscopie, moet hier nog uitdrukkelijk genoemd worden. De zeer plezierige samenwerking met Prof.Dr. E.J. van Bruggen en Jan van Breemen zal ik niet licht vergeten.

Zoals al opgemerkt zijn er velen die ieder op hun terrein hun inbreng hebben gehad. Met name wil ik dan nog danken Mevrouw van den Anker van de Afdeling Tekstverwerking der Landbouwhogeschool voor het persklaar maken van de kopij, en de heer Bery J. Sachteleben, die de tekeningen maakte.

CURRICULUM VITAE

De schrijver van dit proefschrift werd op 11 maart 1945 geboren te Rijswijk (Z.H.). De lagere school werd bezocht in Rijswijk en Bennekom. Het HBS-B diploma werd behaald aan het 2e Chr. Lyceum te Zeist in 1962. In hetzelfde jaar begon de chemiestudie aan de Rijksuniversiteit te Utrecht, en in 1966 werd met goed gevolg het candidaatsexamen chemie g afgelegd. In 1968 volgde toen het doctoraalexamen (hoofdvak biochemie, bij Prof.Dr. L.L.M. van Deenen; bijvakken microbiologie, bij Prof.Dr. K.C. Winkler en hematologie bij wijlen Prof.Dr. C. Verloop).

Van 1 januari 1969 tot 1 mei 1974 is de auteur werkzaam geweest bij het Laboratorium voor Biochemie van de Landbouwhogeschool te Wageningen. Sedert 1 augustus 1974 is hij werkzaam als docent klinische en fysiologische chemie aan de School tot Opleiding van Laboratoriumpersoneel te Arnhem en Nijmegen.

CONTENTS

	page
List of Abbreviations	
1. Introduction	1
2. Materials and Methods	7
3. Purification and Properties	14
4. Studies on the equilibrium constant and properties of the pyridine nucleotides	37
5. Electron microscopic studies	54
6. Spectral properties	70
Summary	91
Samenvatting	94
References	97

LIST OF ABBREVIATIONS

A	absorbance
ADH	alcohol dehydrogenase
2'-AMP	adenosine 2'-monophosphate
ATCC	american type culture collection
ATP	adenosine 5'-triphosphate
CoASH	coenzyme A, reduced form
DTNB	(5,5'-dithiobis-[2-nitrobenzoic]acid), Ellmans reagent
E_{ox}	transhydrogenase oxidized form
EDTA	ethylene diamine tetra acetate
F	fluorescence intensity
FAD	flavine adenine dinucleotide, oxidized form
FMN	flavin mono nucleotide, oxidized form
F_o	initial fluorescence intensity
g	gravity
GLDH	glutamate dehydrogenase
G-6PDH	glucose-6-phosphate dehydrogenase
Hz	Herz
I	ionic strength
k	reaction constant
K_{eq}	equilibrium constant
K_D	dissociation constant of enzyme-substance complex
K_I	dissociation constant of enzyme-inhibitor complex
K_m	Michaelis constant
L-B plot	Lineweaver-Burk plot
Me^{2+}	divalent metal ions
min.	minutes
$NAD(P)^+$	nicotinamide adenine dinucleotide (phosphate) oxidized form
$NAD(P)H$	nicotinamide adenine dinucleotide (phosphate) reduced form
nm	nanometer
nmr	nuclear magnetic resonance
O.D.	optical density
\bar{p}	degree of fluorescence polarization

P_i	anorganic phosphate (potassium-)
PDC	pyruvate dehydrogenase complex
PEG	polyethylene glycol
r.p.m.	revolutions per minute
S	Svedberg constant
SDS	sodium dodecyl sulphate
S-NAD ⁺	thionicotinamide dinucleotide, oxidized form
τ	lifetime of the excited state
Tris	Tri(hydroxymethyl)amino methane
T.H.	transhydrogenase
TPP	thiamine pyrophosphate
v	velocity at a finite substrate concentration
V_{max}	maximum velocity at infinite substrate concentrations

1. INTRODUCTION

NADPH: NAD⁺ oxidoreductase (trivial name transhydrogenase) E.C. 1.6.1.1. activity is present in several species. It was first described by Colowick et al. (1952) in the bacterium *Pseudomonas aeruginosa*.

Bacterial transhydrogenase activity has since been found and studied in *Pseudomonas aeruginosa* (Colowick et al., 1952; Cohen, 1967; Cohen and Kaplan, 1970^a, 1970^b; Louie, Kaplan and McLean, 1972); *Azotobacter vinelandii*, (Kaplan et al., 1952; Van den Broek et al., 1968, 1970, 1971a, 1971b, 1971c, 1971d, thesis; Chung, 1970, 1972; Middleditch et al., 1971, 1972); *Rhodospirillum rubrum*, (Keister and Yike, 1966; Keister and Minton, 1969; Fisher and Guillory, 1971a, 1971b; Konings and Guillory, 1972; Ostroumov et al., 1973); *Rhodopseudomonas spheroides* (Orlando et al., 1966, 1970; Konings and Guillory, 1972); *Escherichia coli* (Murthy and Brodie, 1964; Bragg and Hou, 1968, 1972; Sweetman and Griffith, 1971; Fisher et al., 1970, 1971; Cox et al., 1971, 1972; Kanner and Gutrick, 1972) and *Micrococcus denitrificans* (Asano, Imai and Sato, 1967).

In higher organisms the mitochondrial transhydrogenase of the rat and beef heart has been studied extensively, mainly by the group of Kaplan (Kaplan et al., 1953; Kawasaki et al., 1964; Fisher et al., 1973) and the group of Ernster (Lee and Ernster, 1964, 1965, 1968; Rydström et al., 1970, 1971a, 1971b, 1972; Teixeira da Cruz et al., 1971).

Recently an ATP-stimulated reduction of NADP⁺ by NADH was reported to occur in the endosperms of a higher plant *Echinocystis macrocarpa* (Hasson and West, 1973). In chloroplasts of higher plants a light-dependent transhydrogenase activity associated with ferredoxin-NADP⁺ reductase has been discussed by Shen et al. (1963).

The physiological reaction catalyzed is

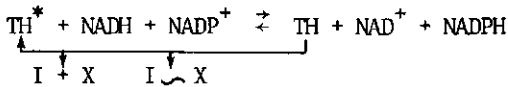


In general the rate of the reaction from the left to the right is much higher than the reverse reaction. In mitochondrial systems and in the bacteria *E. coli*, *Rhodospirillum rubrum*, *Rhodopseudomonas spheroides* and *Micrococcus denitrificans* the reaction from the right to the left is stimulated by high energy intermediates and ATP.

The equilibrium constant for the reaction

$$K_{eq} = \frac{[NADPH][NAD^+]}{[NADH][NADP^+]}$$

shifts in the presence of ATP from near unity towards a value of at least 500 (due to stoichiometric hydrolysis into ADP and phosphate, Lee and Ernster, 1964). It was proposed by Rydström et al. (1970) that the role of energy was to activate the enzyme; in a cyclic process the enzyme could be inactivated by NADH and $NADP^+$ and subsequently be reactivated according to the following scheme



In which TH^* is the active and TH is the inactive state of the enzyme, and $\text{I} \rightsquigarrow \text{X}$ represents a high-energy intermediate that can be hydrolysed into I + X. In the non-energy linked reaction, the substrates NADPH and NAD^+ activate the enzyme while NADH and NADP^+ inactivate it (Rydström, 1970). Kinetic studies of Rydström et al. (1971) on the energy-linked transhydrogenase revealed that energization is reflected primarily in an increase in the maximal velocity of the DT-reaction ($\text{NADH} + \text{NADP}^+ \rightarrow \text{NADPH} + \text{NAD}^+$).

This effect is accompanied by a decrease in the dissociation constants of the binary enzyme-substrate complex and an increase in the dissociation constant of the binary enzyme-product complex.

Support for the proposed role of $\text{I} \rightsquigarrow \text{X}$ was found in the fact that there is a competitive relationship between the substrates NAD^+ and NADPH on one hand and $\text{I} \rightsquigarrow \text{X}$ on the other hand in the transformation of inactive into active transhydrogenase.

Studies on the mitochondrial transhydrogenase with the stopped-flow technique (Fisher and Kaplan, 1973) showed that the activity of the non-energy-linked transhydrogenase is 50% lower in D_2O than in H_2O (at the optimal pD and pH respectively). It was suggested that dissociation of a proton from the energy-linked transhydrogenase system was required to induce conformational changes such that activation of the energy-dependent transhydrogenase occurs. Rydström (1972b) suggested that a protonation might be involved in the conversion of inactive transhydrogenase into the active form. The proton involved is probably not provided by the reduced substrate because there is no exchange of the nicotinamide C-4 proton with the medium. In D_2O membrane energy-dependent structural changes, as indicated by fluorescence enhancement of 8-aminonaphthalene-1-sulfonic acid, were nearly complete before the onset of transhydrogenation

(Fisher and Kaplan, 1973). It was suggested by Fisher and Kaplan (1973) that activation of the energy-linked transhydrogenase rate upon membrane energization is a function separate from the increase in the apparent equilibrium constant of the reaction.

A reversal of the energy-linked transhydrogenase reaction was demonstrated by the group of Skulachev (Grimius et al., 1970; Isaev et al., 1970) who showed that the reaction of $\text{NADPH} + \text{NAD}^+ \rightarrow \text{NADH} + \text{NADP}^+$ could be coupled to the transport of lipid soluble anions into the particles. Such a transport can also be observed on energization of the membrane by ATP or succinate. Van Stadt et al., (1971) showed that when the energy-linked reaction is reversed, there is an energy-dependent enhancement of ANS fluorescence, a red shift of the spectrum of cytochrome b and synthesis of ATP from ADP and phosphate.

The energy-dependent transhydrogenase of mammalian mitochondria cannot be resolved into a transhydrogenase part and an energy converting system. All attempts to purify this enzyme have led to irreversible loss of the energy-dependent reaction. However, a soluble protein fraction was obtained and purified from *Rhodospirillum rubrum* chromatophores (Fisher and Guillory, 1971a, 1971b) and from *E. coli* (Bragg and Hou, 1972) and found to enhance the ATP-driven energy-dependent transhydrogenase reaction, when added to depleted particles. Aerobic transhydrogenase activity (energy-dependent) in *E. coli* could be enhanced by an energy transfer factor prepared from rat-liver mitochondria (Fisher et al., 1970). No energy-dependent reactions have been observed so far in *Pseudomonas* and *Azotobacter*.

Studies with labeled substrates showed that the hydrogen transfer in the reactions catalyzed occurs without exchange of label to the medium. The transfer of hydrogen catalyzed by the mammalian transhydrogenase was found to be stereospecific for the 4A-atom of NADH but stereospecific for the 4B-atom of NADPH (Kawasaki et al., 1964; Lee et al., 1965). The stereospecificity of the *Rhodospirillum rubrum* system (Fisher and Guillory, 1971a) is the same as that of the mitochondrial system. The purified transhydrogenase from *Pseudomonas aeruginosa* (Louie and Kaplan, 1970) and the purified enzyme from *Azotobacter vinelandii* (Middleditch et al., 1971), however, shows a stereospecificity which differs from the mammalian and *Rhodospirillum* system. In the former the hydrogens are transferred from the 4-B position of NADH to the 4-B position of NADPH (see Fig. 1.1). It is not clear at the moment how enzymes from different sources which catalyze the same reaction can exhibit a different stereospecificity.

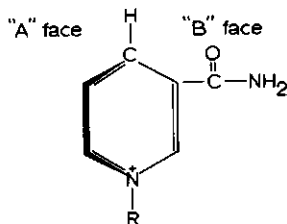


Fig. 1.1. Representation of the nicotinamide part of the nicotinamide adenine denucleotides. The figure represents the oxydized form of these nucleotides. Reduction at C-4 can take place either from the "A" or "B" side.

There seems to be a relationship, however, between the energy-linked character and the stereospecificity.

In the *Azotobacter* enzyme the transfer of label between NADH and NADP^+ proceeds in the absence of 2'-AMP, the *Pseudomonas* system, however, requires 2'-AMP for exchange between these substrates. In the reaction in which the reducing substrate does not contain a 2'-phosphate group, 2'-AMP is strongly activating in the *Pseudomonas* enzyme (Cohen and Kaplan, 1970a). Kinetic studies indicated that 2'-AMP plays an important role in the catalytic activity of the *Pseudomonas* enzyme (Cohen and Kaplan, 1970a). In the absence of 2'-AMP the reaction of $\text{NADPH} + \text{S-NAD}^+ \rightarrow \text{S-NADH} + \text{NADP}^+$ as catalyzed by the *Pseudomonas* enzyme showed a second order dependence on $[\text{NADPH}]$ and a first order dependence on $[\text{S-NAD}^+]$; in the presence of 0.5 mM 2'-AMP, a linear dependence on $[\text{NADPH}]$ and $[\text{S-NAD}^+]$ was observed. These experiments were interpreted in terms of enzyme activation by both NADPH and 2'-AMP. The reverse reactions $\text{NADH} + \text{S-NAD}^+ \rightarrow \text{S-NADH} + \text{NAD}^+$ and $\text{NADH} + \text{NADP}^+ \rightarrow \text{NAD}^+ + \text{NADPH}$ were strongly stimulated by 2'-AMP. The effect of 2'-AMP in this reaction was explained by postulating an increase in the rate of the reaction sequence leading to reduction of the enzyme by NADH. In the mitochondrial system 2'-AMP and 3'-AMP were found to be specifically inhibitory with respect to NAD(P)H, whereas adenine mononucleotides without a 2' (or 3') substituent are specifically inhibiting at the NAD(H) site (Rydström, 1972).

Several reaction mechanisms were proposed for the reactions catalyzed by the enzyme from different sources. Cohen et al. (1970) suggested a ping-pong mechanism for the *Pseudomonas* enzyme, whereas in later studies Louie et al. (1970) proposed a modified Theorell-Chance mechanism for this enzyme.

A rapid-equilibrium random bi-bi mechanism was proposed for the purified *Azotobacter* enzyme (Van den Broek et al., 1971). Teixeira da Cruz and Rydström (1971a, 1971b) proposed a Theorell-Chance mechanism for the non-energy linked as well as for the energy linked transhydrogenase reactions. As no exchange of label with the medium is found in the reactions catalyzed by all of these enzymes a short-living ternary complex is more likely than a ping-pong mechanism. Formation of a dead end complex of oxidized enzyme with NADP^+ was proposed for the *Pseudomonas* and the *Azotobacter* enzyme (Louie et al., 1970; Van den Broek et al., 1970, 1971). NADP^+ was also found to be a very potent inhibitor of the reaction $\text{NADP}^+ + \text{NADH} \rightarrow \text{NADPH} + \text{NAD}^+$. Van den Broek et al. (1971) suggested that the ratio of $\text{NADPH}/\text{NADP}^+$ is important in this reaction, because NADPH catalyzed its own formation, and maximum stimulation could be obtained at an initial 1 : 1 ratio of $\text{NADPH}/\text{NADP}^+$.

A very striking property of the purified bacterial non-energy dependent transhydrogenase is the strong tendency to form very long elongated structures (Louie et al., 1969, 1970, 1972; Van den Broek et al., 1971). The long strands of the *Pseudomonas* enzyme dissociate into regular substructures on the addition of 2'-AMP. As 2'-AMP also stimulates the rate of reduction of S- NAD^+ by NADH it was suggested that dissociation results in the exposure of sites buried in the elongated structures, thus promoting the binding of the substrates (Louie et al., 1972). The *Azotobacter* enzyme is dissociated at a higher pH (Middleditch et al., 1972) and by addition of NADP^+ (Van den Broek et al., 1971). 2'-AMP has no effect on the morphology of this enzyme. The connection between the association-dissociation phenomenon and the catalytic events of the *Azotobacter* enzyme is not very clear.

The physiological function of the transhydrogenases has been discussed extensively and several proposals were made. Kaplan et al., (1953, 1956) suggested that transhydrogenase furnishes a pathway for the oxidation of NADPH via the respiratory chain. Other proposals are based on the NADPH generating capacity of the energy-linked transhydrogenase. Thus NADPH which is formed via the energy-linked reaction could serve as a control of glutamate metabolism (Klingenberg and Slenczka, 1959; Papa et al., 1969). Also a possible role in the control of reductive synthetic processes was proposed, (Qualiariello et al., 1968; Bragg et al., 1972). Rydström et al. (1972) proposed, on the basis of the very potent inhibitions of the mammalian mitochondrial transhydrogenase reaction by long acyl-CoA compounds a regulatory role between oxidative break-down and reductive synthesis, possibly mitochondrial elongation, of fatty acids. For the

Azotobacter enzyme a possible role in the regulation of the transfer of reducing equivalents from pyruvate to either N_2 or O_2 via NADPH and NADH respectively was suggested (Van den Broek et al., 1968; Veeger et al., 1972).

A simple method for purifying *Azotobacter* transhydrogenase in high yield was developed by exploiting the strong polymerizing character of the enzyme (Chapter 3). Some properties of the transhydrogenase in crude extracts were investigated in order to compare these results with those of more purified preparations (Chapter 3). A pronounced effect of divalent metal ions on the catalytic activity (Chapter 3) and on the morphological appearance (Chapter 5) of the transhydrogenase was observed. The equilibrium constant for the transhydrogenase reaction is not energy dependent but is strongly affected by pH and ionic strength. These effects will be discussed with special attention to the chemical nature of the substrates and products involved (Chapter 4).

Although the *Azotobacter* and *Pseudomonas* enzymes have many features in common, some differences have been revealed by the studies of Van den Broek et al., (1970, 1971) and Louie et al. (1970, 1972). These differences are concerned mainly with their behaviour towards $NADP^+$ and 2'-AMP. Therefore, the effects of binding of these compounds to the *Azotobacter* enzyme have been examined in detail (Chapter 6). Earlier work had indicated that the enzyme accepts 4 reducing equivalents per mole of bound FAD (Van den Broek et al., 1971). The measurements which led to this conclusion have been repeated as a preliminary step towards determining the nature of the electron accepting groups; the earlier measurements were found to be in error (Chapter 6).

In general it must, however, be stated that the pronounced dissociating-associating character of the purified transhydrogenase gives a badly defined starting material for several studies. Especially binding studies sometimes suffer from irreproducible results probably as a consequence of using different preparations with a different degree of aggregation.

2. MATERIALS AND METHODS

2.1 MATERIALS

2.1.1 Enzymes

Transhydrogenase was purified from cell free extracts of *Azotobacter vinelandii* according to the methods described in Chapter 3. Most experiments were performed with enzyme obtained by a new purification method that includes a spontaneous aggregation of the enzyme. The purified enzyme was stored at 4°C in 50 mM Tris-HCl pH 7.6 containing 10 µg chloroamphenicol/ml to prevent bacterial growth. All experiments were performed with enzyme dialyzed against 50 mM Tris-HCl pH 7.6 unless stated otherwise.

Yeast alcohol dehydrogenase, yeast glucose-6-phosphate dehydrogenase, beef liver glutamate dehydrogenase and lactate dehydrogenase from rabbit muscle were purchased from Boehringer Mannheim.

2.1.2 Reagents

NAD⁺, NADH, NADP⁺, NADPH, S-NAD⁺, ATP, 2'-AMP, FAD, FMN, CoASH, TPP, bovine serum albumine and ovalbumine were obtained from Sigma Chemical Co. All reagents and chemicals used were of analytical grade. Solutions were made up in bidistilled water unless stated otherwise.

2.2 METHODS

2.2.1 Determination of activities and concentrations

The catalytic assays were carried out predominantly in 1 ml volume-1cm light path cuvettes in a Zeiss spectrophotometer PMQ II with diaphragm MF4, in combination with either a W + W 3011 recorder or a Honeywell Elektronik 16 high-speed recorder. Maximal absorbance changes at the highest substrate concentrations did not exceed 0.1-0.2 per minute.

Spectra were measured with a Cary model 14 or Cary model 16 double beam spectrophotometer in 1 cm light path cuvettes.

2.2.2 *Enzymatic assay of transhydrogenase, pyruvate dehydrogenase, NADH oxidase and NADPH oxidase activities*

The standard assay for transhydrogenase activity was performed in 50 mM Tris-HCl pH 7.6 containing 100 μ M S-NAD⁺ and 100 μ M NADPH in a final volume of 1 ml. The reaction was started by addition of enzyme in the appropriate dilution and the reaction was followed by measuring the absorbance increase at 398 nm due to the formation of S-NADH. An arbitrary unit of activity is defined as the optical density change per minute caused by 1 mg of the undiluted protein solution. The specific activity is defined as the number of μ moles product formed per minute per mg of protein, assuming a molar extinction coefficient of 11,300 M⁻¹ cm⁻¹ for S-NADH (Keister and Hemmes, 1966).

The activities with the physiologically normal substrates were studied in the presence of a regenerating system for one of the substrates. The enzymes of the regenerating systems were, if necessary, dialyzed to remove ammoniumsulphate. The reaction of NADPH + NAD⁺ \rightarrow NADH + NADP⁺ was studied using either glucose-6-phosphate dehydrogenase to regenerate NADPH or lactate dehydrogenase to regenerate NAD⁺. In the case of NADPH regeneration the cuvette contained 0.1 M Tris-HCl pH 7.6, 10 mM glucose-6-phosphate, excess glucose-6-phosphate dehydrogenase and pyridine nucleotides as indicated. When NAD⁺ was regenerated the cuvette contained 0.1 M Tris-HCl pH 7.6, 20 mM pyruvate and a small amount of lactate dehydrogenase (1 μ g/ml). If the concentration of the lactate dehydrogenase added is too high not only NADH but also NADPH will be oxidized (Navazio et al., 1957).

The reduction of NADP⁺ by NADH was measured with alcohol plus alcohol dehydrogenase to regenerate NADH. The cuvette contained 0.1 M Tris-HCl pH 7.6, 0.2 M ethanol, 5 mM neutralized semicarbazide-HCl, excess yeast alcohol dehydrogenase and pyridine nucleotides as required.

When the standard assay conditions were modified by additions of other materials care was taken that the regenerating system did not become rate limiting.

Unless stated otherwise the reactions were initiated by the addition of transhydrogenase and followed by measuring the change in absorbance at 340 nm. An extinction coefficient of 6,220 M⁻¹ cm⁻¹ at 340 nm was used for NADH and NADPH. Pyruvate dehydrogenase was measured with the NAD⁺-dependent assay as used by Schwartz et al. (1968). The mixture contained in a final volume of 1 ml, 0.05 M potassium phosphate buffer pH 8.0, 0.2 mM TPP, 1 mM MgCl₂, 2.4 mM cysteine-HCl or glutathione, 0.16 mM CoASH, 1 mM potassium pyruvate and 2.5 mM NAD⁺. The

reaction was started by the addition of pyruvate dehydrogenase and followed at 340 nm for the formation of NADH.

NAD(P)H-oxidase activity was measured by a modification of the method of Mackler and Green (1956). The cuvette contained 0.1 M Tris-HCl pH 7.6, 100 μ M NADH or NADPH in a final volume of 1 ml. Protein was added last and the disappearance of the reduced nicotinamide adenine dinucleotides was followed at 340 nm.

Anaerobic measurements of the transhydrogenase catalyzed reaction of NADH + NADP⁺ in cell free extracts were performed in cuvettes sealed with a Suba-seal rubber cap and flushed with argon. The reaction was started by the addition of oxygen-free NADP⁺ (100 μ M) by piercing the rubber serum cap with a syringe equipped with a hypodermic needle. The cuvette contained Tris-HCl 0.1 M at the required pH, 10 mM neutralized semicarbazide-HCl, 0.15 M ethanol, excess of alcohol dehydrogenase, excess of catalase, 100 μ M NADH and cell-free extract. The reaction was started when no absorbance change occurred at 340 nm upon shaking the cuvette, indicating that the NADH concentration had reached a constant level.

2.2.2.2 Determination of the equilibrium constant

Substrates at the indicated concentrations and transhydrogenase were incubated at 25°C in a thermostated waterbath. Samples were taken at different time intervals and the concentrations of the nucleotides present were measured. If no change of concentration of the substrates and products in the incubation mixture was observed over a period of at least 30 minutes the equilibrium situation was regarded as established.

The concentrations of the oxidized nucleotides were determined with samples of 2 ml which were removed from the incubation mixture and added with stirring to 0.5 ml 20% HClO₄. To this mixture 0.4 ml 0.5 M Tris-HCl pH 7.6 was added and the cool mixture (4°C) was neutralized by carefully adding a calibrated amount of 5 N KOH while stirring rapidly with a Whirlmix. The neutralized mixture (pH about 7-7.5) was centrifuged at 4°C, to remove the KClO₄ precipitate and the supernatant was analyzed for NAD⁺ and NADP⁺. Each oxidized nucleotide was determined by converting it quantitatively into the reduced form. NAD⁺ was assayed in a cuvette containing 0.1 M pyrophosphate-glycine buffer pH 8.5, 0.9 M ethanol, 10 mM neutralized semicarbazide-HCl pH 6.5 and 1 ml of the neutra-

lized sample in a final volume of 2.5 ml. The initial absorbance at 340 nm was noted and then excess of alcohol dehydrogenase was added. The absorbance at 340 nm was measured when it had reached a constant value, and the concentration of NADH was calculated, assuming a molar extinction coefficient for NADH of $6,220 \text{ M}^{-1} \text{ cm}^{-1}$. NADP^+ was measured in a cuvette containing Tris-HCl 0.1 M pH 8.0, 6 mM MgCl_2 , 1 mM glucose-6-phosphate and 1 ml of the neutralized sample, final volume 2.5 ml. Glucose-6-phosphate dehydrogenase was added in excess after (blank) corrections were made. The absorbance at 340 nm was taken when it reached a constant value and the NADPH formed was calculated.

The reduced nucleotides were measured by converting them quantitatively into the oxidized form. Samples of 1 ml from the incubation mixture were taken for the determination of the reduced nucleotides, and added to 0.5 ml 1 N KOH. This mixture was neutralized by addition of a calibrated amount of buffer containing 0.5 M glycyl-glycine - 0.4 M KH_2PO_4 - 0.1 M K_2HPO_4 under rapid stirring with a Whirlmix. The NADH and NADPH present in the neutralized sample was assayed in a single cuvette which contained 0.1 M Tris-HCl pH 8.0, 7.2 mM potassium-pyruvate, 18.7 mM ammonium-chloride, 6.8 mM α -oxoglutarate and 0.5 ml neutralized sample in a final cuvette volume of 1 ml. Blank corrections were made and lactate dehydrogenase was added in catalytic (0.5 $\mu\text{g}/\text{ml}$) amounts. Readings were made at 340 nm within 3 minutes after addition of this enzyme. The NADH oxidation by lactate dehydrogenase is very fast; however, addition of too high concentrations of the enzyme will cause some NADPH oxidation (Navazio et al., 1957). The NADPH was assayed by subsequent addition of glutamate dehydrogenase in excess. From the decrease in absorbance at 340 nm the NADH and NADPH concentrations were calculated. In all experiments the sum of the corresponding reduced and oxidized nucleotides should remain constant over the whole period of the experiment.

The equilibrium constant of the glutamate dehydrogenase catalyzed reactions was determined as follows. The starting mixture contained in buffer of variable ionic strength and pH 7.6 both reduced nucleotides (100 μM NADH and 100 μM NADPH), 270 μM α -oxoglutarate, 370 μM ammonium-chloride and 10 mM glutamate. The reaction was started by the addition of enzyme. Samples were taken and assayed as described above.

2.2.2.3 Determination of concentrations

Protein concentration was determined by the biuret method of Gornall et al. (1949) or by the microbiuret method of Itzhaki and Gill (1964). Calibration

curves were made with ovalbumine as a standard. The reduced nucleotides NADH and NADPH were measured at 340 nm for determination of the concentration, assuming an extinction coefficient of $6,220 \text{ M}^{-1} \text{ cm}^{-1}$. The oxidized nucleotides NAD^+ , NADP^+ and S-NAD^+ were assayed in cuvettes containing 1 M potassium cyanide assuming extinction coefficients for the CN^- -adducts of NAD^+ of $5,900 \text{ M}^{-1} \text{ cm}^{-1}$ at 327 nm, of NADP^+ $6,000 \text{ M}^{-1} \text{ cm}^{-1}$ at 327 nm and of S-NAD^+ of $10,000 \text{ M}^{-1} \text{ cm}^{-1}$ at 355 nm. (Pabst Laboratories circular OR-18, April 1961).

The concentration of SH groups was determined with the Ellman reagent DTNB (5,5'-dithiobis [2-nitrobenzoic acid]) assuming a molar extinction coefficient of $13,600 \text{ M}^{-1} \text{ cm}^{-1}$ at 412 nm for the reaction product 3-carboxylate-4-nitrothiophenolate (Ellman, 1959).

Solutions of dithionite used in the anaerobic titration experiments, were standardized by titration with flavin mononucleotide (FMN) assuming a molar extinction coefficient of $12,500 \text{ M}^{-1} \text{ cm}^{-1}$ (Dawson et al., 1969) at 445 nm. FMN was titrated with dithionite which was made up in anaerobic buffer in the titration assembly as described by Foust et al. (1969) and the concentration of the dithionite solution was calculated from the plot relating the absorbance change at 445 nm with the amount of dithionite added.

2.2.3 Absorption spectrophotometry

Absorption spectra were recorded on a Cary model 14 or Cary model 16 recording spectrophotometer in cells with 1 cm light path and corrected for the absorbance of the additions. The difference spectra were recorded with the 0-0.1 absorbance indicating slide wire; measurements were performed in tandem cells to correct for the absorbance of the added substances. During these measurements the slit remained relatively small and volume changes did not exceed 2% of the original volume.

Anaerobic titrations are performed under a nitrogen atmosphere in an anaerobic titration assembly as described by Foust et al. (1969). The apparatus consisted of three parts that could be made anaerobic separately; a modified quartz Thunberg cuvette, a burette and a reservoir for the titrant. Anaerobic conditions were obtained by repeated evacuation and refilling of the cuvette with oxygen-free nitrogen. The nitrogen was freed of oxygen by passing it through a column 125 x 10 cm filled with heated BASF R3-11 catalyst (80°C). The protein solution was kept in ice water during the evacuation procedure in order to avoid excessive foaming and evaporation. Volume losses due to evaporation were taken into account.

2.2.4 Fluorescence

Fluorescence emission and excitation spectra were recorded on a Hitachi Perkin Elmer MPF-2A spectrofluorometer equipped with a thermostated cuvette holder. The emission spectra were corrected for scatter of the solvent.

All transhydrogenase protein solutions scanned had an optical density not exceeding 0.200 at 440 nm.

Fully corrected excitation spectra were recorded as described by Chen (1967) using FMN as a quantum counter.

2.2.4.1 Polarization fluorescence

Polarization spectra of flavin fluorescence were obtained on a polarization spectrofluorimeter designed by Weber and Bablouzian (1966). The cuvette holder was thermostated at 25°C.

The degree of polarization of fluorescence, p , is defined as

$$p = (I_{\parallel} - I_{\perp}) / (I_{\parallel} + I_{\perp})$$
, with I_{\parallel} and I_{\perp} representing the fluorescence intensities parallel and perpendicular to the polarized excitation. A pair of Schott Jena type GG 495 or OG 530 filters was used to separate the emission from the excitation radiation. The degree of polarization could be directly read off from a DANA model 5403 digital voltmeter. The absolute accuracy varied between 0.005 and 0.01 depending on the signal intensity.

2.2.4.3 Fluorescence lifetime

The fluorescence lifetime was measured with a cross-correlation phase and modulation fluorometer as described by Spencer et al. (1969).

The apparatus was used operating at 60 Mc. The excitation wavelength was 440 nm and the emission wavelength was obtained by using cut off filters (Scott-Jena GG 495 or OG 530).

The phase delay of the fluorescence of the sample was measured relative to a glycogen scatter solution. The phase delay (δ) is related to the fluorescence lifetime (τ) according to $\tan \delta = 2\pi\nu\tau$ in which ν is the frequency used (60 Mc) and τ the fluorescence lifetime.

2.2.5 Ultracentrifugation

Sedimentation patterns were obtained using a MSE analytical ultracentrifuge. Sedimentation velocity runs were performed in 20 mm double sector cells at a

temperature of 18-21°C and rotor speeds between 10,000 and 25,000 r.p.m.. The sedimentation patterns were scanned with a MSE ultracentrifuge scanner either at 440 nm (optical density about 0.40) or at 290 nm (optical density about 0.30). The sedimentation coefficients were calculated according to the relation of Svedberg and Pederson (1940).

2.2.6 *Electron microscopy*

Enzyme preparations used in electron microscopy were negatively stained with 0.5% uranyl oxalate pH 6.4-6.7 at room temperature using the droplet method according to Mellema et al. (1967). The droplet of the cold enzyme solution was left on a carbon coated grid for 30-60 sec. and the non-absorbed molecules were removed with filter paper. The subsequent stained protein film was dried in air. Electron micrographs were taken at a magnification of 20,000 to 50,000 on a 35 mm film with a Philips EM 300 electron microscope operating at 80 KV, or a Jeol J.E.M. 100 B electron microscope operating at 60 KV.

Both instruments were provided with an anti-contamination device cooled by liquid nitrogen.

Kodak fine grain positive release (F.R.P. 426) film was used and development was performed at 29°C in Kodak HRP for 3-4 min.

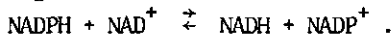
2.2.7 *N.M.R. spectroscopy*

The proton spectra of the reduced and oxidized nicotinamide adenine dinucleotides were recorded on a Varian XL-100-15D N.M.R. spectrometer operating at 100 MHz. The Fourier transform technique was used to acquire all spectra. Conditions were, acquisition time 3 sec, pulse width 30 μ sec and 50-100 transients. Most spectra were run at 1000 HZ spectral width, with peak positions being determined from the computer generated printout using DSS as internal standard. The nucleotides were dissolved in D₂O and neutralized with either NaOD or DCl and subsequently lypholized to remove exchangeable protons. The lypholized material was dissolved in D₂O at a concentration of approximately 10 mM. The solutions were freed of oxygen and left under a nitrogen atmosphere. Almost all values obtained in different runs are within 1 HZ of each other.

3. PURIFICATION AND PROPERTIES

3.1 INTRODUCTION

During their investigations on isocitrate dehydrogenase in extracts of *Pseudomonas fluorescens (aeruginosa)* Colowick et al. (1952) were able to demonstrate the presence of transhydrogenase activity. In later studies Kaplan et al. (1952, 1953) gave definite proof that the observed activity was a nicotinamide dinucleotide transhydrogenase activity by which reducing equivalents were reversibly transferred between the two nicotinamide dinucleotides according to the following reaction



In agreement with their predictions the pyridine nucleotide transhydrogenases were found to be widespread in nature. The activity was shown to be present in bacteria, higher plants and mammalian tissues. Two types of the enzyme were demonstrated: a) The energy-dependent enzyme in which ATP or an energized membrane enhances the formation of NADPH. In mammalian tissue this activity was first demonstrated by Klingenberg et al. (1961), Estabrook et al. (1961) and Danielson and Ernster (1963). In bacteria the energy-dependent activity was demonstrated in the following genera, *Rhodospirillum rubrum* (Keister and Yike, 1966), *Rhodopseudomonas spheroides* (Orlando, Sabo and Curnyn, 1966), *Escherichia coli* (Murthy and Brodie, 1964) and *Micrococcus denitrificans* (Asano, Imai and Sato, 1967). In higher plants this activity has been described for spinach chloroplasts (Shen et al., 1963), and in endosperms of *Echinocystis macrocarpa* (Hasson and West, 1973).

b) The non-energy-linked form. The latter form has been isolated and purified from *Pseudomonas* (Cohen et al., 1970) and *Azotobacter* (Van den Broek et al., 1969, 1971) in which until now the presence of the energy-linked activity could not be demonstrated. On the other hand in organisms which contain the energy-dependent form the non-energy-linked form is also present. Both activities are inhibited by the same inhibitors, triiodothyronine and thyroxine (Ball and Cooper, 1959; Kaplan and Ciotti, 1959; Hommes and Estabrook, 1963) while antibodies prepared against the purified non-energy-linked transhydrogenase inhibit not only the non-energy-linked but also the energy-linked transhydrogenase (Kawasaki et al., 1964). This indicates that the two activities presumably are due to one enzyme complex.

The role of transhydrogenase in cell metabolism is not very clear. A regulatory function in providing NADPH for biosynthesis was proposed (Bragg et al., 1972), or a regulatory function between the oxidative breakdown and reductive synthesis of fatty acids (Rydström, 1972).

In these studies mainly the properties of the *Azotobacter* enzyme in comparison with the enzyme isolated from *Pseudomonas* will be described. These enzymes have several features in common as already pointed out by Kaplan et al. (1953), Van den Broek et al. (1969, 1970, 1971) and Chung (1970).

The main differences are centered in the effects of 2'-AMP on the morphological structure and catalytic events of the *Pseudomonas* enzyme, whereas these effects are hardly present in the *Azotobacter* enzyme.

3.2 RESULTS AND DISCUSSION

3.2.1.1 Isolation and Purification of *Azotobacter* transhydrogenase

Since enzymes prepared by different purification methods were used, the purification methods used are summarized.

Method according to Van den Broek et al. (1971).

1. Frozen cells were thawed and washed several times with buffer (30 mM potassium phosphate pH 7.6). Cells were broken by ultrasonic treatment with a 100 Watt Ultrasonic Disintegrator MSE London 17 at 0-4°C. The cell suspension was freed from large cell fragments and insoluble material by centrifugation at 30,000 x g for 30 min. The resulting supernatant (referred to as cell-free extract) was used as the source of the enzyme. All further steps were performed at 4°C unless indicated otherwise. The cell-free extract was subsequently subjected to:
 2. Alcoholic heat treatment (5 vol %, 42°C, 15 min.).
 3. Ammonium sulphate fractionation between 30% and 50% saturation.
 4. The 30-50% fraction was dialyzed and treated batchwise with calcium phosphate gel. The transhydrogenase was eluted from the gel by 0.1 M potassium-phosphate buffer pH 7.6 containing 1 mM EDTA.
 5. The eluates of the previous step were concentrated by ammonium sulphate fractionation between 30%-50% saturation.
 6. After dialysis of the 30-50% fraction this solution was finally subjected to differential ultracentrifugation. If necessary this last step was repeated.

The purification resulted in an overall purification of 600-800 times (maximum specific activity 220-260 $\mu\text{moles min}^{-1} \text{mg protein}^{-1}$) and a yield of about 15%.

3.2.1.2 *Purification according to a new method*

1. Preparation of cell-free extract

All steps were performed at 0-4°C unless stated otherwise. The frozen cells (1 kg wet weight) were thawed and washed with 30 mM EDTA adjusted to pH 7.0 with potassium phosphate (acid sodium EDTA was neutralized with solid potassium phosphate). This washing was continued until the supernatant, obtained after centrifugation at 15,000 x g for 30 min., was clear. Cells were suspended (1 : 1 w/v) in 30 mM potassium phosphate buffer pH 7.6 containing 1 mM EDTA. The cells were either disrupted by ultrasonic treatment with a 100 Watt MSE ultrasonic Disintegrator London, or with an Aminco French Press equipped with a piston of 1" at 19,000 psi. The broken cell suspension was freed from large cell fragments and insoluble material by centrifuging for 30 min. at 36,000 x g.

2. Ammonium sulphate precipitation

The cell-free extract thus obtained was subjected to an ammonium sulphate precipitation. The solution was brought to 25% saturation by adding solid ammonium sulphate and after standing for 1 hour centrifuged at 36,000 x g for 30 min. Sometimes longer centrifugation times were necessary to obtain a solid precipitate.

3. Heat treatment

The supernatant of the previous step was diluted to a protein concentration of 6-8 mg/ml and 8-10% saturation of ammonium sulphate with 30 mM potassium phosphate buffer pH 7.6 containing 1 mM EDTA. The pH of the solution was, if necessary, brought to pH 7.0 with diluted KOH. The solution was heated for 15 min. at 60°C with continuous stirring. The heated solution was rapidly cooled in ice to 10°C and the denaturated protein was removed by centrifugation at 27,000 x g for 45 min.

4. Second ammonium sulphate precipitation

The resulting supernatant was brought to 45% saturation by adding solid ammonium sulphate. The pH was kept on pH 7.0 by adding diluted KOH when necessary. The solution was allowed to stand for 1 hour before centrifuging at 27,000 x g for 45 min. The grey-yellow ammonium sulphate precipitate was suspended as concentrated as possible in 50 mM Tris-HCl pH 7.3 containing 1 mM EDTA. This suspension was dialyzed for at least 24 hours against 3 times 2 liter of the same buffer.

Solubilization of highly polymerized transhydrogenase

The dialyzed protein fraction obtained in the previous step was centrifuged at 10,000 x g for 10 min. The resulting supernatant was subsequently centrifuged for 45 min. at 27,000 x g. Both precipitates contained a lot of grey insoluble material and the major part of the transhydrogenase activity. Both precipitates were resuspended with the aid of a Potter-Elvehjem in 0.1 M potassium phosphate pH 7.6 (total volume about 100 ml). To this turbid suspension NADP^+ was added in a final concentration of 0.5 mM and the solution was allowed to stand for at least two hours. This protein suspension was subsequently centrifuged at 10,000 x g for 10 min.

With a different batch of bacteria the enzyme could not be dissolved by the NADP^+ treatment. However, addition of 0.3 M β -mercaptoethanol resulted in a good solubilization of the polymerized transhydrogenase. Insoluble material was removed by centrifugation for 30 min. at 30,000 x g. The resulting solution was first dialyzed against 50 mM Tris-HCl pH 7.6 before the next step was performed. In both cases the resulting greenish-yellow solution contained nearly all transhydrogenase activity.

Differential centrifugation

The yellow supernatant of the previous step was centrifuged in a preparative ultracentrifuge (MSE No. 50) with an angle rotor at 200,000 x g. Although part of the enzyme sedimented as pellet after 5 min. the major part of the activity did so after 2 hours of centrifugation. In case the spectrum of the solubilized precipitates was not correct (mainly due to a contamination with a peak in the absorption spectrum at about 408 nm) the differential centrifugation was repeated. The whole purification method is summarized in Table 3.1.

The spectrum of the purified enzyme is similar with that as obtained by Van den Broek et al. (1971) in the presence of NADP^+ (Fig. 3.1). By anaerobic dialysis in the presence of glucose-6-phosphate and glucose-6-phosphate dehydrogenase the enzyme-bound NADP^+ is removed. However, the pure flavin character of the enzyme is sometimes obscured by the scatter of the turbidity which arises from the high degree of polymerization of the enzyme. The spectrum of a slightly turbid preparation in 50 mM Tris-HCl pH 7.6 is given in Fig. 3.2. No distinct peaks in the visible region are observed while the flavin band at 440 nm seems to be a shoulder of a band at 415 nm. This type of spectrum can be converted to the normal protein-flavin spectrum by

Table 3.1 Summary of the purification of *Azotobacter* transhydrogenase by the new procedure

Steps of purification	total vol. ml	total protein mg	protein mg/ml	activity units/mg	total activity	yield %	accumulative purification
1	2090	83,000	39,6	1.5	125,000	100	1
2	1700	32,000	18.8	3.5	112,000	93	2
3	5000	8,400	1.7	10	87,500	70	7
4	96	3,900	41	20	78,500	63	13
5	100	430	6.5	146	62,300	50	97
6	11.5	195	17.0	265	51,500	41	176

using a glycogen scatter solution as a reference or by calculation of the spectrum according to the method of Donovan (1969). Then the flavin character of the visible absorption band becomes clear (Fig. 3.2).

Addition of salt (potassium phosphate, potassium sulphate, potassium nitrate) also reconverts the ill-defined spectrum into a clear flavin-protein spectrum (Fig. 3.3). Apart from testing the purity of the enzyme on the basis of specific activity it was also checked by SDS-gel electrophoresis. Normal electrophoresis or ultracentrifuge experiments will only reflect the different association states in which the enzyme is present (see also Chapter 5).

In SDS-gel electrophoresis according to the method of Weber and Osborn (1969) the purified transhydrogenase appeared as a single band with neglectable impurities (Fig. 3.4). A minimum molecular weight of approximately 54,000 could be calculated which is in good agreement with that calculated from its flavin content 58,000-68,000 (Van den Broek et al., 1971).

3.2.2 Thiol groups in the enzyme

When the protein-SH groups are determined according to the method of Vallee (1972) in the presence of 2% SDS and 0.3 mM DTNB (see also Chapter 5) three reactive SH groups per mole of flavin are found. Without addition of the denaturing agent no reactive SH groups are found in the presence of either 0.3 mM or 10 mM DTNB. Thus the SH groups seem to be well protected in the native enzyme and only denaturation results in the reaction of DTNB with protein-SH groups.

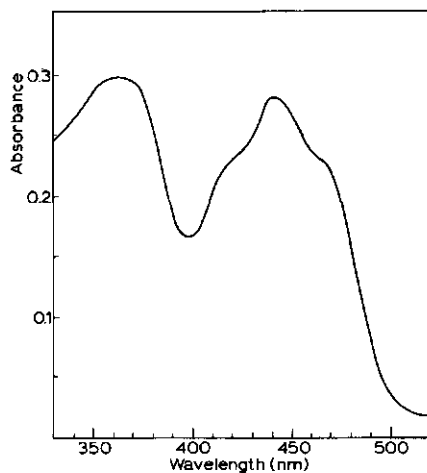


Fig. 3.1 Absorption spectrum of *Azotobacter* transhydrogenase after NADP^+ treatment before anaerobic dialysis. 1.2 mg of protein per ml in 50 mM Tris-HCl pH 7.6.

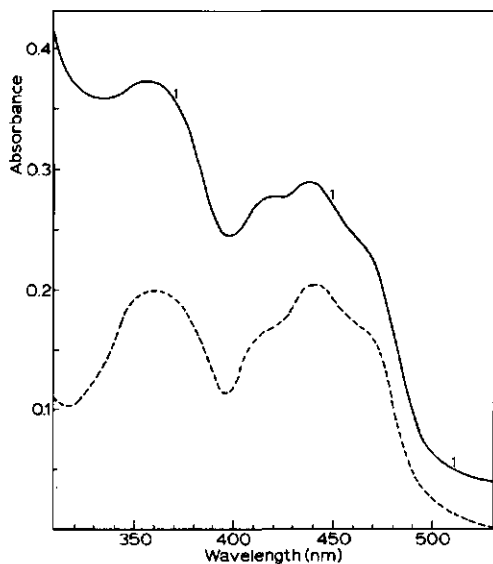


Fig. 3.2 Spectrum of purified highly polymerized transhydrogenase

- The enzyme dissolved in 50 mM Tris-HCl pH 7.6
- Addition of 10 mM potassium phosphate buffer pH 7.6 to 1
- .-. Addition of 40 mM potassium phosphate buffer pH 7.6 to 1

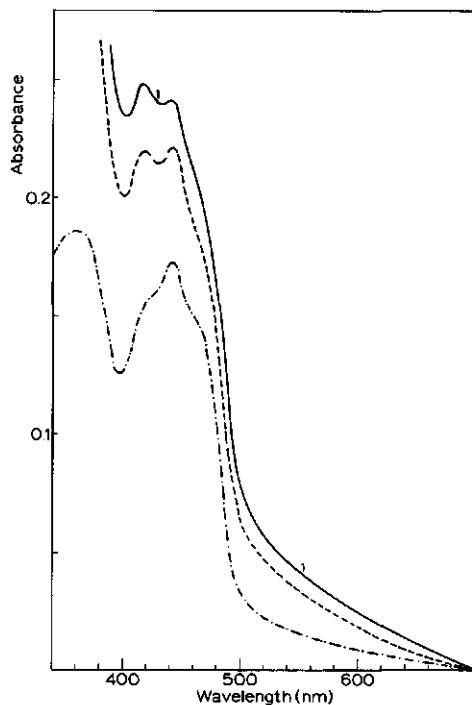


Fig. 3.3 Spectrum of purified highly polymerized transhydrogenase

- The enzyme dissolved in 50 mM Tris-HCl pH 7.6
- The enzyme spectrum as calculated from 1. by correction for the scatter

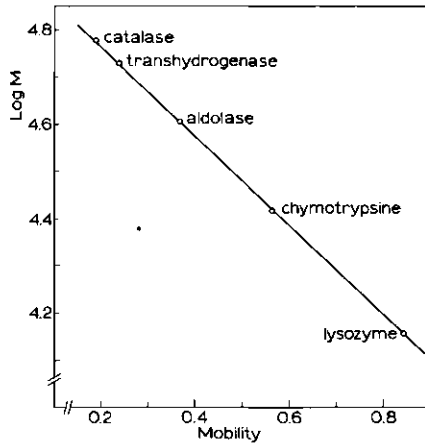


Fig. 3.4 SDS gel-electrophoresis for the determination of the minimal molecular weight of *Azotobacter* transhydrogenase.

Addition of 1 mM NADP^+ or 1 mM 2'-AMP does not change the number of reactive SH groups found either in the absence or presence of 2% SDS.

3.2.3 Effect of divalent metal ions on the association of transhydrogenase

In the early stages of these investigations on the purification method a very interesting property of the enzyme was discovered. An aggregation of the transhydrogenase molecules is induced if the protein solution, obtained after step 4 of the new purification method (except that EDTA is omitted in the washing procedure), is extensively dialyzed against 50 mM Tris-HCl pH 7.8 containing either 1 mM Mn^{2+} or 1 mM Ca^{2+} . The activity can be sedimented by centrifugation for 30 min. at 20,000 x g (Table 3.2). No activity is found in sediments from the control experiment (without Ca^{2+} or Mn^{2+}). It is found that the total amount of activity found after dialysis against 1 mM Mn^{2+} is always lower than the total activity present before dialysis. However, the specific activity increases considerably. This presumably cannot be explained by inactivation of the enzyme by Mn^{2+} since incubation of catalytic amounts of enzyme with 1 mM Mn^{2+} does not influence the activity for at least 48 hours. The decrease of the total amount of activity thus must be due to an artefact: probably the large two-dimensional aggregates do show a diffusion-limited reaction rate. The precipitate of Mn^{2+} -induced aggregation is very difficult to dissolve and it can only be suspended with the aid of a Potter-Elvehjem homogenizer. The sediments obtained by Ca^{2+} -induced aggregation are more soluble than those formed by Mn^{2+} . On this basis a new purification method was developed (Fig. 3.5).

Table 3.2 Effect of prolonged dialysis against 50 mM Tris-HCl pH 7.6 containing divalent metal ions (1 mM). The precipitates were resuspended with the aid of a Potter-Elvehjem.

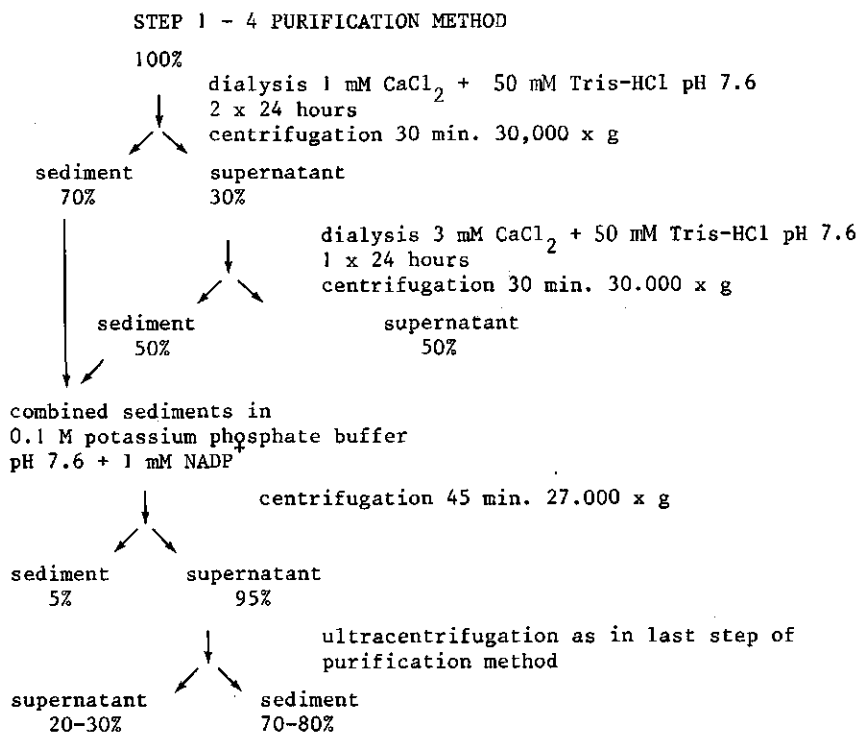
A: Effect of 1 mM Mn^{2+} ; B: Effect of 1 mM Ca^{2+}

Activities are measured as described under Materials and Methods.

Enzyme was dissolved in 50 mM Tris-HCl pH 7.6

FRACTION	A		B	
	specific activity expressed as relative activity	total activity %	specific activity expressed as relative activity	total activity %
Before centrifugation	1	100	1	100
Supernatant after centrifugation	0.15	13	0.45	40
Sediment after centrifugation	17	85	7	60

Percentages denote the amount of activity compared to the previous step.



The resulting transhydrogenase had a specific activity of about 200 $\mu\text{mol}/\text{min}/\text{mg}$ protein.

Fig. 3.5 Effect of Ca^{2+} on the polymerization during the purification of the transhydrogenase activity.

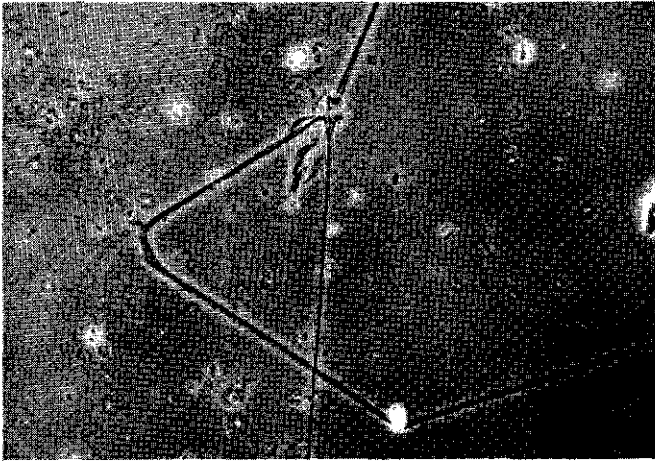


Fig. 3.6 Effect of the addition of ammonium sulphate to the highly purified transhydrogenase in 50 mM Tris-HCl pH 7.6. As soon as cloudiness appeared the solution was centrifuged for 5 min. at 10.000 x g. The sediment was carefully homogenized and phase contrast micrographs were taken x 812.

The dissociating effect of pH 9.0 and the reversible subsequent association upon lowering the ambient pH (Middleditch et al., 1972) was also tried in the purification procedure. The differences in state of aggregation are according to Table 3.3 not large enough to be of use in the new purification method.

3.2.4 *Ammonium sulphate induced precipitation*

It should be noticed that transhydrogenase can be precipitated with ammonium sulphate at various saturation levels, depending on the degree of polymerization. Transhydrogenase activity in crude extracts precipitates quantitatively at 45-50% saturation with ammonium sulphate at pH 7.6. However, highly purified transhydrogenase (spec.act. > 250 $\mu\text{mol}/\text{min}/\text{mg}$) under the same conditions precipitates almost quantitatively at a saturation level of 30%. This precipitate, partially solubilized, was examined under a phase contrast microscope (Fig. 3.6). Very big paracrystalline structures are present. These elongated structures resemble the filamentous structures seen under the electron microscope (Chapter 5) but are a few hundred times larger.

3.2.5.1 *Some characteristics of transhydrogenase in cell-free extract*

After ultrasonic treatment the major part of the transhydrogenase activity is found in the cell cytoplasm. Since this method of disruption is very drastic new artificial (sub)particles can be formed. In order to get some information how the transhydrogenase protein is present in the cell we have undertaken some studies on impure preparations.

Table 3.3 Effect of pH on the sedimentation behaviour of the enzyme. The precipitates were dissolved in 50 mM Tris-HCl pH 7.6 and homogenized if necessary in a Potter-Elvehjem tube. Activities are measured as described under Materials and Methods.

pH 9.0	specific activity expressed as relative activity	total activity %
1. Starting fraction brought to pH 9.0	1	100
2. Sed. after 2 hours at 100.000 x g	2.5	28
3. Supernatant after 2 hours at 100.000 x g	0.7	58
<hr/>		
pH 6.8		
4. Starting fraction is fraction 3 of the pH 9.0 treatment	1	100
5. Sed. after 2 hours at 100.000 x g	3.7	58
6. Supernatant after 2 hours at 100.000 x g	0.2	25

3.2.5.2 Osmotic shock procedure

The osmotic shock procedure as developed by Robrish and Marr (1962) offers a relatively mild procedure for disrupting the bacteria cells. Proteins that are soluble or loosely bound to membrane structures will be present in the supernatant of the burst cell material after the osmotic shock. The activities of transhydrogenase, pyruvate dehydrogenase (PDC), NADH oxidase and NADPH oxidase were tested. The oxidase activities are mainly particle-bound (Tissières et al., 1957), and thus can be used as markers for the particle-bound character of the transhydrogenase and PDC activities. The values presented here can only be regarded as qualitative because the osmotic shock procedure suffers from irreproducibility. This could be due to differences in age of the cells used in the different experiments. For instance, the *Azotobacter* cells very easily develop cysts, that are very rigid, at the end of the lag-phase (Wyss et al., 1961; Tchan et al., 1962). The permeability of the cell for glycerol may change during growth thus effecting the efficiency of the osmotic shock. Furthermore, the NAD(H)-linked activities in cell-free extracts are always somewhat obscured

Table 3.4 Distribution of several activities in *Azotobacter vinelandii*. After the osmotic shock procedure, the mixture was centrifuged at 10.000 x g for 20 min. The debris was resuspended in 50 mM Tris-HCl pH 7.6. Activities are measured as described under Materials and Methods. The NADH oxidase was measured in the absence of CN⁻.

	% of total activity present in supernatant of osmotic shock	% of total activity present in sonicatic debris of osmotic shock
Transhydrogenase	54	40
Pyruvate dehydrogenase dismutase assay	40	50
NADH-oxidase	15	85
NADPH-oxidase	7	90
Liberated protein %	15	82

by the presence of a very active NADH oxidase system that is KCN insensitive (Jones et al., 1967).

The data presented in Table 3.4 indicate that transhydrogenase and to a less extent pyruvate dehydrogenase is loosely bound to the cell structures. All activity of transhydrogenase sediments after 1½ hour at 144,000 x g, after working up the supernatant of the osmotic shock with ammonium sulphate (30-50%) dialysis and concomittant ultracentrifugation. In the supernatant of the osmotic shock some typical transhydrogenase structures (see Chapter 5) were found. This probably indicates that either the transhydrogenase is present as a large molecule in the cell or it starts to associate as soon as it is free from its natural environment.

3.2.5.3. Polyethylene glycol fractionation

Polson et al. (1964) introduced polyethylene glycol in the fractionation of proteins and viruses. Juckes (1971) investigated the parameters involved in this procedure. The limits of solubility decrease upon increase in size of the molecule.

Laurent et al. (1963) proposed that the mechanism of precipitation is one of exclusion of the protein from the solute by the polymer. This makes it reasonable to assume that the PEG concentrations at which precipitation occurs are

dependent on the difference between ambient pH and isoelectric point at a given ionic strength. Cell-free extract of *Azotobacter* was subjected to PEG precipitation in order to investigate whether interaction between transhydrogenase and pyruvate dehydrogenase is present under these conditions (Van den Broek et al., 1971). If so, considerable co-precipitation of the two activities can be expected. If no pronounced interaction is present precipitation at different saturation levels is expected as the isoelectric point for the purified transhydrogenase is 4.5 (Middleditch et al., 1972) and that of the purified pyruvate dehydrogenase complex is about 5.0 (Bresters et al., to be published). Cell-free extract is brought to pH 5.5 with diluted acetic acid and centrifuged for 30 min. at 36,000 x g. To the resulting supernatant subsequent additions of PEG were made. Precipitates obtained after stirring for 10 min. at 4°C and

Table 3.5 Precipitation of the transhydrogenase activity and pyruvate dehydrogenase activities at pH 5.5 in 30 mM potassium phosphate buffer by PEG 2000 30 mM. The precipitates were dissolved in 50 mM Tris-HCl pH 7.6 and if necessary homogenized in a Potter-Elvehjem tube. Activities are measured as described under Materials and Methods.

Fraction	total protein	PDC		TH	
	%	relative specific activity	Total activity %	relative specific activity	total activity %
Cell-free extract	100	1	100	1	100
Supernatant after pH 5.5	60	1.4	83	1.4	84
Sup. 2% w/v PEG	37	1.8	66	1.1	42
Sup. 3%	27	2.0	54	0.4	12
Sup. 4%	23	1.5	35	-	5
Sup. 5%	19	0.3	5.2	-	-
Sediment after pH 5.5	40	<0.01	4	0.4	16
Sed. 2%	21	0.7	14.5	1.9	40
Sed. 3%	9	0.8	7.5	2.7	26
Sed. 4%	3.7	4.8	18.0	-	-
Sed. 5%	3.5	6.7	24.0	-	-

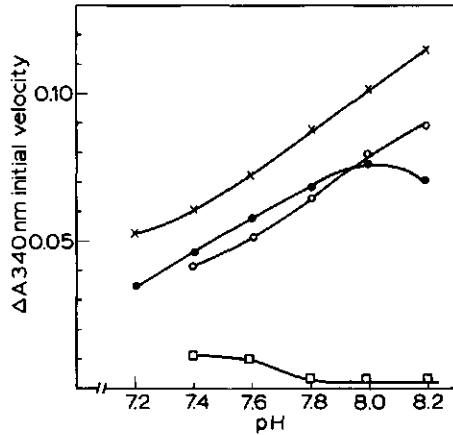


Fig. 3.7 Effect of Mn^{2+} and ATP on the transhydrogenase reactions of $NADH + NADP^+ \rightarrow NAD^+ + NADPH$. The reaction is carried out in 100 mM Tris-HCl pH 7.6 with 250 μM NADH and 100 μM $NADP^+$ as starting concentrations. As regenerating system alcohol plus alcohol dehydrogenase was used. Temp. 25°C.

●—● no extra additions; x—x plus 1 mM $MnCl_2$; □—□ plus 100 μM ATP;
○—○ plus 100 μM ATP and 1 mM $MnCl_2$.

centrifugation at 36,000 x g for 10 min. were tested for both activities. From Table 3.5 it is clear that transhydrogenase already precipitates at very low concentrations of PEG and within narrow limits. PDC precipitates even at a higher PEG concentration, unexpectedly, since the isoelectric point is higher than that of transhydrogenase. However, no closely parallel precipitation of the two activities is observed. The early precipitation of the transhydrogenase activity also indicates that the protein is relatively large under these conditions (Juckes, 1971). However, definite proof of the high molecular weight of transhydrogenase in crude extract might come from the band forming sedimentation technique suggested by Vinograd et al. (1963).

From the experiments with osmotic shock and polyethylene glycol precipitation no direct evidence was obtained about a close association between transhydrogenase and pyruvate dehydrogenase as suggested by Van den Broek et al. (1971).

3.2.6 Reactions catalyzed by cell-free extract

As measured with more purified transhydrogenase (Van den Broek et al., 1971) the reaction $NADP^+ + NADH \rightarrow NADPH + NAD^+$ is strongly inhibited by ATP. This inhibition is opposite to the response of an energy-driven reaction as in such a case stimulation can be expected (Danielson and Ernster, 1963). In order to

investigate the possible existence of an energy-driven transhydrogenase in crude extracts several studies were performed (see also Chapter 4),

Although Van den Broek et al. (1971) was unable to conduct the reaction of $\text{NADP}^+ + \text{NADH} \rightarrow \text{NADPH} + \text{NAD}^+$ in cell-free extracts it is found that it can be studied under strictly anaerobic conditions. The results show that the reaction rate is small compared to the reaction rate of a highly active CN^- -insensitive NADH oxidase. It was found that ATP is also strongly inhibitory to the reaction as catalyzed by cell-free extract. ATP inhibition increases at higher pH values and Mn^{2+} is very effective in counteracting this inhibition (Fig. 3.7). Under identical conditions a stronger ATP inhibition on the reaction catalyzed by cell-free extract than catalyzed by the highly purified enzyme is observed. At pH 7.6 hardly any inhibition is found at 25 mM ATP when the reaction is catalyzed by the pure enzyme whereas the reaction catalyzed by cell-free extract shows a minimal activity at this pH and concentration of ATP (Fig. 3.8). Van den Broek et al. (1969) reported a relatively strong inhibition of ATP with partially purified transhydrogenase. As the inhibition in cell-free extracts results immediately after the addition of the ATP a phosphorylation of the enzyme probably can be excluded. It must, therefore, be assumed that the catalytic properties of the enzyme change during purification.

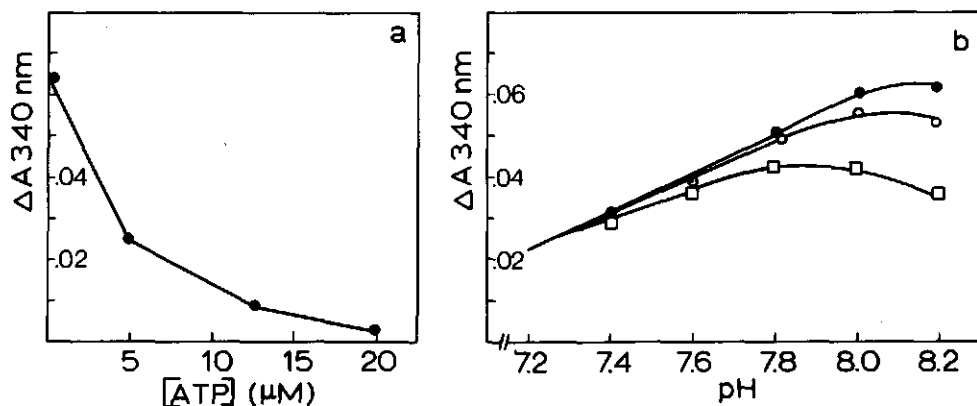


Fig. 3.8 Effect of ATP on the reduction of NADP^+ by NADH in 0.1 M Tris-HCl pH 7.6. $[\text{NADH}]$ 700 μM , $[\text{NADP}^+]$ 100 μM .

a. Anaerobic reaction catalyzed by cell-free extract in the presence of different ATP concentrations.

b. Reaction catalyzed by pure enzyme in the presence and absence of different ATP concentrations at different pH.

●—● no extra additions; ○—○ 5 μM ATP; □—□ 25 μM ATP.

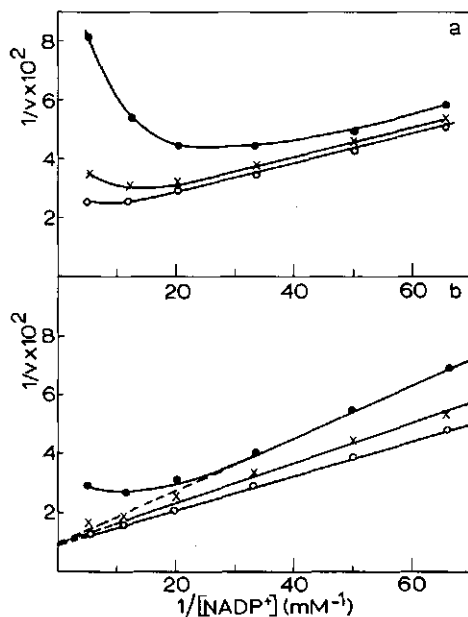


Fig. 3.9 Reduction of NADP^+ by NADH in 50 mM Tris-HCl pH 7.6 in the absence and presence of MnCl_2 .

a. $1/v$ vs. $1/[\text{NADP}^+]$ plot at low $[\text{NADH}]$ and at different MnCl_2 concentrations.

$[\text{NADH}]$ 18 μM , ●—● no MnCl_2 , x—x 200 μM MnCl_2 , ○—○ 1 mM MnCl_2 .

b. $1/v$ vs. $1/[\text{NADP}^+]$ plot at high $[\text{NADH}]$ and at different MnCl_2 concentrations.

$[\text{NADH}]$ 180 μM , ●—● no MnCl_2 , x—x 200 μM MnCl_2 , ○—○ 1 mM MnCl_2 . Temp. 25°C.

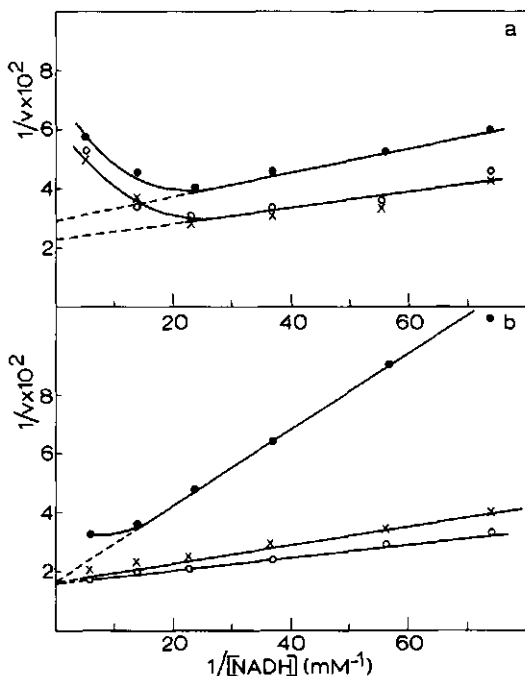


Fig. 3.10 Reduction of NADP^+ by NADH in 50 mM Tris-HCl pH 7.6 in the absence and presence of MnCl_2 .

a. $1/v$ vs. $1/[\text{NADH}]$ plot at low $[\text{NADP}^+]$ and at different MnCl_2 concentrations.

$[\text{NADP}^+]$ 20 μM , ●—● no MnCl_2 , x—x 200 μM MnCl_2 , ○—○ 1 mM MnCl_2 .

b. $1/v$ vs. $1/[\text{NADH}]$ plot at high $[\text{NADP}^+]$ and at different MnCl_2 concentrations.

$[\text{NADP}^+]$ 200 μM , ●—● no MnCl_2 , x—x 200 μM MnCl_2 , ○—○ 1 mM MnCl_2 . Temp. 25°C.

3.2.7. Metal induced effects on the reaction $\text{NADH} + \text{NADP}^+ \rightarrow \text{NADPH} + \text{NAD}^+$

A more detailed kinetic study about the metal induced effects in the reaction $\text{NADH} + \text{NADP}^+ \rightarrow \text{NAD}^+ + \text{NADPH}$ revealed several interesting phenomena. In accordance with Van den Broek et al. (1971) it is found that the reaction is inhibited by high concentrations of both substrates. Raising the concentration of the second substrate diminishes the inhibition. Addition of metal ions (Mn^{2+}) gives a

stimulation of the reaction rate in all cases. At high concentrations of the fixed substrate V does not change by the metal induced stimulation (Fig. 3.9.b and 3.10.b). At a low and fixed concentration of NADH the substrate inhibition due to NADP^+ is very effectively counteracted by Mn^{2+} (Fig. 3.9.a). However, at a low fixed concentration of NADP^+ the NADH substrate inhibition is hardly affected by Mn^{2+} (Fig. 3.10.a). This clearly points to the fact that the binding of NADP^+ is more affected than the binding of NADH. A possible kinetic explanation can be found in the fact that in the formulas for a rapid ternary complex mechanism (Theorell-Chance) with substrate inhibition by both substrates the K_B ($B=\text{NADP}^+$) is much lowered in the presence of Mn^{2+} while K_A is less affected.

Stimulation by other metal ions was also observed. Thus Co^{2+} , Ca^{2+} and Mg^{2+} also act as a stimulator on the reaction. In case of Co^{2+} the sulphate salt was used and as a reference potassium sulphate was taken (Fig. 3.11).

Van den Broek et al. (1971) reported a Mg^{2+} stimulation of the *Azotobacter* transhydrogenase catalyzed reaction $\text{NADP}^+ + \text{NADH} \rightarrow \text{NADPH} + \text{NAD}^+$. Rydström et al. (1973) reported about the Ca^{2+} stimulation in the same reaction as catalyzed by the *Pseudomonas* enzyme. The mechanism of the metal induced stimulation is

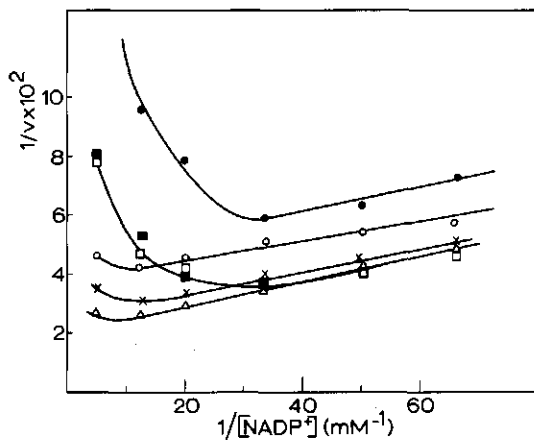


Fig. 3.11 Reduction of NADP^+ by NADH in 50 mM Tris-HCl pH 7.6 in the presence of different divalent metal ions. $1/v$ vs. $1/[\text{NADP}^+]$ plot with $[\text{NADH}]$ fixed at 18 μM . ■—■ no extra additions, ●—● 1 mM K_2SO_4 , ○—○ 1 mM CoSO_4 , □—□ 1 mM MgCl_2 , ×—× 1 mM CaCl_2 , Δ—Δ 1 mM MnCl_2 . Temp. 25°C.

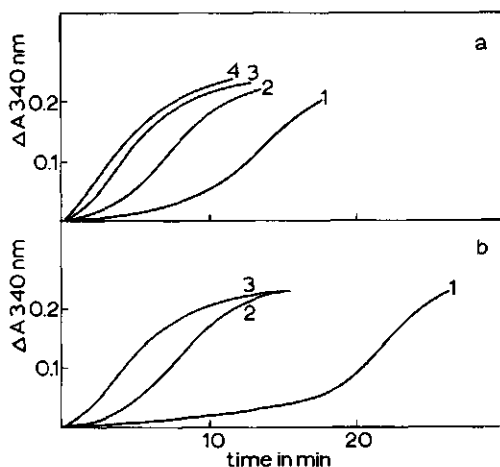


Fig. 3.12 Effect of a fifty fold dilution of concentrated enzyme (1 mg/ml) in 0.1 M potassium phosphate buffer pH 7.6.

a. with 100 mM Tris-HCl pH 7.6 and b. with H₂O (to 0.02 mg/ml).

From the diluted protein solution at different time intervals after dilution samples were taken and the reaction of NADH + NADP⁺ (25 μM + 50 μM) was measured.

- a. 1. directly after dilution with Tris-HCl
 2. 2 min. after dilution
 3. 250 min. after dilution
 4. 24 hours after dilution
- b. 1. directly after dilution with H₂O
 2. 160 min. after dilution
 3. 24 hours after dilution

not very clear at the moment. As especially the NADP⁺ inhibition is reversed it might be proposed that chelation of the 2'-phosphogroup of NADP⁺ by Mn²⁺ (Colman et al., 1972) prevents the inhibitory binding of this nucleotide. However, since Mg²⁺ and Co²⁺ both stimulate the reaction of NADP⁺ with NADH, but no complex formation of these metals with the secondary phosphogroup is found (Apps, 1973; Toreilles, 1973) the chelation of the 2'-phosphogroup seems of minor (or no) importance. Moreover, the NADH inhibition is also partially reversed. It seems more likely to assume that these effects are related to the metal induced morphological (conformational) changes of the protein (Chapter 4), by which especially the NADP⁺ binding place is affected.

3.2.8 Effect of salt

The reaction $\text{NADH} + \text{NADP}^+ \rightarrow \text{NADPH} + \text{NAD}^+$ shows a very pronounced lag where this

reaction is catalyzed by cell-free extract (section 3.2.6). With the more purified enzyme the lag observed is less clear (Van den Broek et al., 1971). As shown in Fig. 3.12 a pronounced effect of salt, (potassium phosphate or potassium sulphate) on the delay of the reaction is found. Upon diluting concentrated enzyme (1 mg/ml in 0.1 M potassium phosphate buffer pH 7.6) for the catalytic assay to about 0.02 mg/ml in water or 50 mM Tris-HCl pH 7.6 and the reaction started immediately after dilution, a long lag is observed. The lag shortens when the assay is performed with the same enzyme dilution standing for a longer period. Hardly any lag is observed when the reaction is performed with enzyme dialyzed against Tris-HCl to remove all phosphate present. Addition of salt (potassium phosphate or potassium sulphate) again introduces a lag. It thus can be concluded that divalent anions have a pronounced effect on the catalytic properties of the enzyme. Furthermore, these ions come off the protein only very slowly resulting in a more active conformation of the enzyme. As will be shown and discussed in Chapter 6 divalent anions bind to the enzyme and do influence the binding of NADP^+ . In this respect it is important to note that the regenerating system used in these reactions must be dialyzed to remove the ammonium sulphate present.

Van den Broek et al. (1971) reported a pronounced effect of phosphate on the

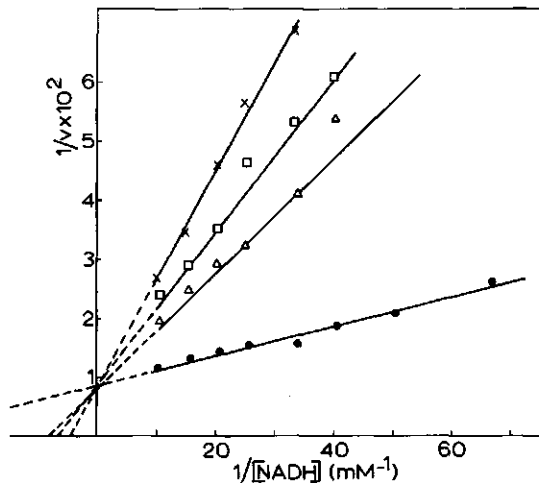


Fig. 3.13 Reduction of S-NAD^+ by NADH in 50 mM Tris-HCl pH 7.6 in the absence and presence of phosphate and 2'-AMP. $1/v$ vs. $1/[\text{NADH}]$ plot at $[\text{S-NAD}^+] 100 \mu\text{M}$. ●—● no extra additions, x—x plus 50 mM phosphate, □—□ plus 50 mM phosphate and 40 μM 2'-AMP, Δ — Δ plus 50 mM phosphate and 200 μM 2'-AMP. Temp. 25°C.

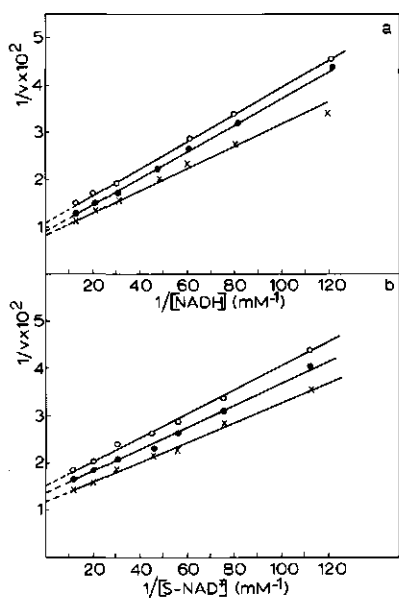


Fig. 3.14 Reduction of S-NAD⁺ by NADH in 50 mM Tris-HCl pH 7.6 in the absence and presence of 2'-AMP.

a. $1/v$ vs. $1/[NADH]$ plot. $[S-NAD^+]$ 43 μ M, x-x no extra additions; ●-● 1 mM 2'-AMP; ○-○ 2 mM 2'-AMP;

b. $1/v$ vs. $1/[S-NAD^+]$ plot. $[NADH]$ 41 μ M, x-x no extra additions; ●-● 1 mM 2'-AMP; ○-○ 2 mM 2'-AMP.

Temp. 25°C.

reduction of S-NAD⁺ by NADH depending on the pH. These authors also reported that 2'-AMP has a stimulating effect depending on the pH when the reaction of S-NAD⁺ + NADH is carried out in phosphate buffers. The stimulating effect of 2'-AMP in the presence of phosphate is also shown in Fig. 3.13. No stimulation but rather an inhibitory effect is found when 2'-AMP alone is used (Fig. 3.14). Both at constant donor and acceptor concentrations 2'-AMP inhibits the reaction non-competitively.

The salt induced inhibition of the reaction NADH + S-NAD⁺ is very interesting. In case of a constant acceptor concentration (S-NAD⁺) a competitive inhibition of salt (phosphate, sulphate, nitrate) towards the donor (NADH) is observed (Fig. 3.15 and 3.16). The apparent inhibition constants in the absence of 2'-AMP are for phosphate about 5 mM, for sulphate about 18 mM and nitrate about 50 mM. In the presence of 2'-AMP (100 μ M) the K_I 's for phosphate and sulphate are both higher namely 15 and 50 mM respectively, but in the presence of nitrate only some slight inhibition of 2'-AMP is observed and the K_I becomes about 40 mM. However, at a constant donor concentration phosphate and sulphate cause an inhibition that can be regarded as uncompetitive, while nitrate has a clearly different inhibitory effect which is non-competitive towards S-NAD⁺ (Fig. 3.17). In the presence of phosphate 2'-AMP (100 μ M) has a pronounced stimulatory effect but in the presence of NO₃⁻ hardly any effect of 2'-AMP is observed,

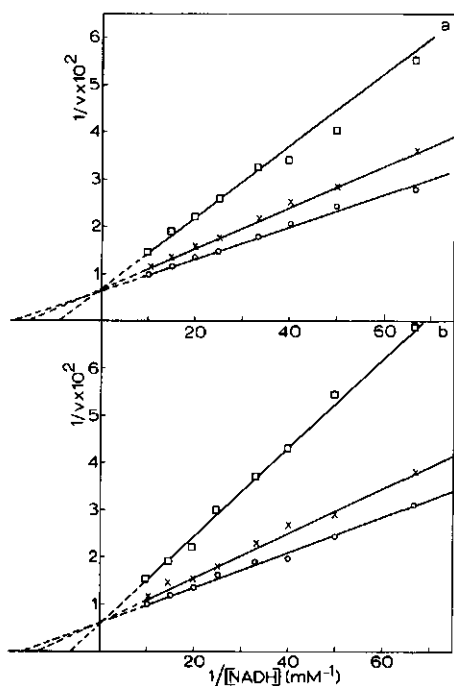


Fig. 3.15 Reduction of S-NAD⁺ by NADH in 50 mM Tris-HCl pH 7.6 in the absence and presence of nitrate and 2'-AMP.

a. $1/v$ vs. $1/[NADH]$ plot. [S-NAD⁺] 100 μ M, \circ — \circ no extra additions; \times — \times 15 mM KNO₃; \square — \square 60 mM KNO₃.

b. $1/v$ vs. $1/[NADH]$ plot. [S-NAD⁺] 100 μ M, \circ — \circ 100 μ M 2'-AMP; \times — \times 100 μ M 2'-AMP and 15 mM KNO₃; \square — \square 100 μ M 2'-AMP and 60 mM KNO₃. Temp. 25°C.

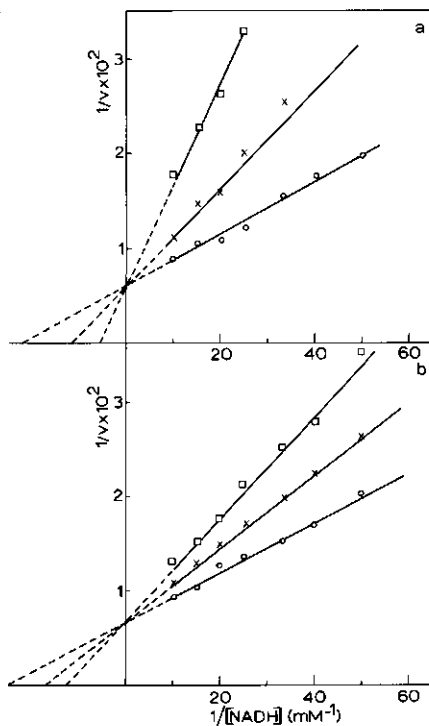


Fig. 3.16 Reduction of S-NAD⁺ by NADH in 50 mM Tris-HCl pH 7.6 in the absence and presence of phosphate and 2'-AMP.

a. $1/v$ vs. $1/[NADH]$ plot. [S-NAD⁺] 100 μ M, \circ — \circ no extra additions; \times — \times 5 mM phosphate; \square — \square 20 mM phosphate.

b. $1/v$ vs. $1/[NADH]$ plot. [S-NAD⁺] 100 μ M; \circ — \circ 100 μ M 2'-AMP; \times — \times 100 μ M 2'-AMP and 5 mM phosphate; \square — \square 100 μ M 2'-AMP and 20 mM phosphate. Temp. 25°C.

while the kinetic patterns remain unaltered. The effect of 2'-AMP on the spectral properties of the enzyme (chapter 6) shows that this nucleotide reverses the binding of phosphate to the oxidized enzyme. Van den Broek et al. (1971) reported that NADP⁺ effectively inhibits the reaction of NADH + S-NAD⁺ \rightarrow S-NADH + NAD⁺. At low fixed acceptor concentrations a tendency towards competitive inhibition was observed while at low NADP⁺ concentrations a tendency of uncompetitive inhibition towards S-NAD⁺ was found. For the *Pseudomonas* enzyme it was also found that low concentrations of NADP⁺ inhibit competitively towards NADH and non or uncompetitively towards the acceptor S-NAD⁺ (Cohen et al., 1970).

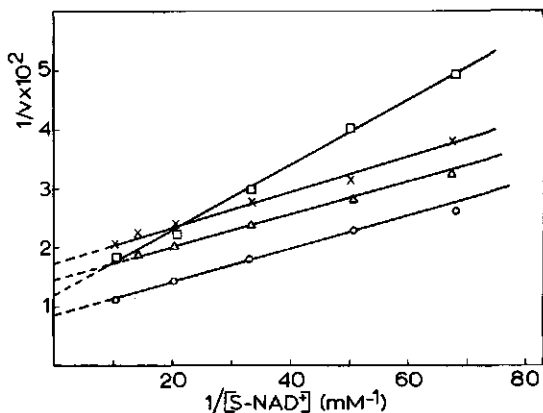


Fig. 3.17 Reduction of S-NAD⁺ by NADH in 50 mM Tris-HCl pH 7.6 in the absence and presence of different salts.

$1/v$ vs. $1/[S-NAD^+]$ plot. [NADH] 100 μ M, $\circ-\circ$ no extra additions; $\times-\times$ 20 mM potassium phosphate; $\Delta-\Delta$ 20 mM potassium sulphate; $\square-\square$ 60 mM potassium nitrate. Temp. 25^o C.

It seems that divalent anions do have the same effect on the kinetic picture. As it is found (Chapter 6) that phosphate has a pronounced effect on the absorption spectrum of the oxidized enzyme (comparable with the effect of NADP⁺) it seems reasonable to assume that the oxidized enzyme-phosphate complex can be regarded as a less active state of the oxidized enzyme. In view of the competitive inhibition of salt (phosphate, sulphate and nitrate) towards NADH and the binding of salt to the oxidized enzyme it can be concluded that NADH is presumably the first substrate bound to the enzyme. Rydström et al. (1971) also suggested that NAD(H) is the first substrate bound to the mammalian transhydrogenase.

The phosphate and sulphate inhibition patterns can be explained by either a ping-pong mechanism (formula 1) or a ternary complex mechanism in which the dissociation constant for the first substrate (K_A) is much smaller than the limiting Michaelis constant for the second substrate K_B (formula 2).

$$(1) \quad v = \frac{v_m}{1 + \frac{K_A}{A} + \frac{K_B}{B}}$$

$$(2) \quad v = \frac{V_m}{1 + \frac{K_A}{A} + \frac{K_B}{B} + \frac{\bar{K}_A K_B}{A \cdot B}}$$

in which A is NADH and B S-NAD⁺, K_A and K_B are the corresponding Michaelis constants and \bar{K}_A the dissociation constant for A.

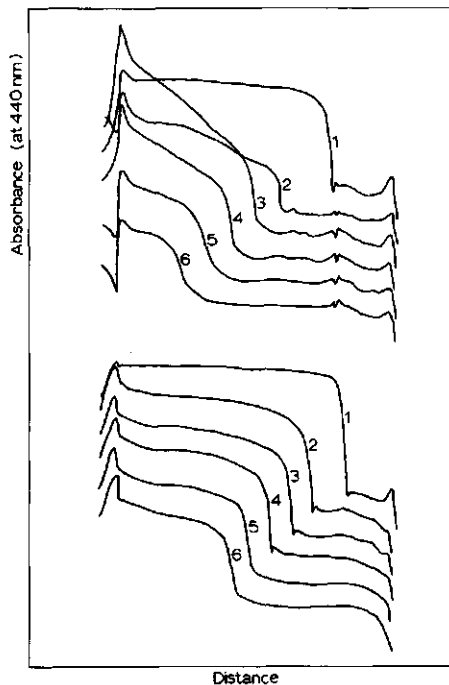


Fig. 3.18 Ultracentrifugal sedimentation patterns obtained with *Azotobacter* transhydrogenase. The enzyme (O.D. at 440 nm 0.400) was dissolved in 50 mM Tris-HCl pH 7.6 in the absence and presence of 1.0 M β -mercaptoethanol plus 5 mM EDTA. Rotor speed 35060 r.p.m. Temp. 20.1°C (+ 0.1).

- A. Patterns obtained in the absence of β -mercaptoethanol.
1. Directly after reaching rotor speed, full scale at 440 nm 0-10 O.D.
 2. After 360 seconds, full scale 0-1 O.D.
 - 3, 4, 5 and 6 after 600, 840, 1080 and 1350 seconds after reaching rotor speed, full scale 0-0.5 O.D.
- B. Patterns obtained in the presence of 1.0 M β -mercaptoethanol.
1. directly after reaching rotor speed, full scale at 440, 0-1.0 O.D.
 - 2, 3, 4, 5 and 6 after 240, 480, 720, 960 and 1200 seconds after reaching rotor speed.

If the effective concentration of E_{ox} is lowered by binding of salt in both cases an inhibition pattern as described for phosphate and sulphate can be expected according to the rules of Cleland (1963). In the formulas this means that K_A is affected by salt and as a consequence at variable A a competitive inhibition is found while at B variable K_A still changes with different salt concentrations, so that an uncompetitive inhibition results. However, the role of nitrate shows that a ping-pong mechanism is not very likely as no competitive inhibition towards the acceptor can be expected when K_A is altered. In the ternary complex mechanism it must be assumed that nitrate increases the \bar{K}_A relatively to the K_B so that no parallel lines are obtained for the double reciprocal plot of $1/B$ vs $1/v$.

3.2.9 Effect of β -mercaptoethanol

Under the electron microscope a pronounced dissociating effect of 0.1 M and 1.0 M β -mercaptoethanol upon the associated purified transhydrogenase was found (cf Chapter 4). If transhydrogenase is incubated with these concentrations of β -mercaptoethanol no decrease in catalytic activity in the reactions $NADH + S-NAD^+ \rightarrow S-NADH + NAD^+$ and $NADPH + S-NAD^+ \rightarrow S-NADH + NADP^+$ over a period of at least 60 min. is observed. Incubation at lower concentrations (10 mM) results in a gradual loss of activity presumably due to mixed disulfide bridge formation within the enzyme. The dissociative action of β -mercaptoethanol was confirmed by analytical ultracentrifuge experiments. The sedimentation pattern of an untreated protein sample is rather inhomogenous (Fig. 3.18) Addition of β -mercaptoethanol results in a much more flat plateau in the absorption patterns. The sedimentation coefficient for the slowest sedimenting material also changes from 50.0 S in the untreated sample towards 39.8 S in the presence of 1.0 M β -mercaptoethanol. This indicates that not only the big structures depolymerize but also that the smallest substructures in the presence and absence of β -mercaptoethanol are not comparable (see also Chapter 5).

4. STUDIES ON THE EQUILIBRIUM CONSTANT AND PROPERTIES OF THE PYRIDINE NUCLEOTIDES

4.1 INTRODUCTION

The equilibrium constant for the reaction between the two nicotinamide nucleotide couples, $K = \frac{[\text{NADPH}] \cdot [\text{NAD}^+]}{[\text{NADP}^+] \cdot [\text{NADH}]}$, was indirectly measured by Olsen and Anfinsen (1953) and Engel and Dalziel (1967) with the enzyme glutamate dehydrogenase. The constant was directly measured by Kaplan et al. (1953) with the aid of the non-energy linked transhydrogenase from mammalian tissue. The K-value was found to be near unity in agreement with the general idea that the two couples differ only slightly in standard redox potentials. Measurements of Engel and Dalziel (1967) indicate that the equilibrium constants of the NAD(H) and NADP(H) dependent reactions catalyzed by glutamate dehydrogenase show an ionic strength dependence.

The non-energy linked transhydrogenase from mammalian mitochondria catalyzes the reaction $\text{NADH} + \text{NADP}^+ \rightleftharpoons \text{NAD}^+ + \text{NADPH}$ with a higher maximal velocity from the right to the left than from the left to the right. In order to explain the value of the equilibrium constant near unity under these conditions Rydström (1970) proposed a mechanism in which the transhydrogenase protein could be activated and deactivated. In addition it was reported by Lee and Ernster (1964) that addition of ATP to the submitochondrial transhydrogenase causes a drastic shift in the K_{obs} from near unity to a value of about 500. Rydström et al. (1970) explained this by assuming activation of inactivated transhydrogenase at the expense of an energy-rich bond. Fisher and Kaplan (1973) suggested that the activation of the energy-dependent transhydrogenase reaction rate is a function separate from the increase in the apparent equilibrium constant of the reaction.

The observations on the mitochondrial transhydrogenase prompted us to investigate the equilibrium constant of the pyridine nucleotide couples established by crude extracts of *Azotobacter vinelandii* and purified preparations of the non-energy dependent transhydrogenase from this organism and also the effects of ATP and varying the initial ratios of the substrates. It will be shown that direct measurements of the equilibrium constant as defined above also reveal

an ionic strength dependence. This will be discussed in relation to the chemical nature of the pyridine nucleotides as revealed by N.M.R. studies. Furthermore, it will be discussed on the basis of the data in the literature that Rydström's calculation of the equilibrium constant is based on the wrong interpretation of kinetical data.

4.2. RESULTS AND DISCUSSION

4.2.1 *Effect of ionic strength and pH*

First the values of the equilibrium constant of the pyridine nucleotide couples as can be calculated from the data of Olsen and Anfinsen (1953), Engel and Dalziel (1967) and as measured by Kaplan et al. (1953) were reinvestigated with pure transhydrogenase.

It became clear that the thermodynamic equilibrium constant measured at a constant temperature depends on the ionic strength and the pH. At higher ionic strength (I) and lower ambient pH the K -values increase. The effect of ionic strength cannot be attributed to a specific ionic effect since it is independent of the kind of ion used to obtain the desired ionic strength (Table 4.1).

The effect of pH on the equilibrium constant was studied at constant ionic strength ($I = 0.01$) in potassium phosphate buffer of variable pH (Table 4.2). In order to exclude a specific enzyme effect the same equilibrium was studied using glutamate dehydrogenase as a catalyst. This enzyme is one of the few dehydrogenases which catalyze reactions with both nicotinamide nucleotides. The equilibrium was established by starting the reaction with both reduced nicotinamide nucleotides and the substrates present in the same mixture. After equilibrium was established, samples were taken and the mixture was heated to destroy the glutamate dehydrogenase. To the cooled (25°C) mixture transhydrogenase was added and by taking samples the new equilibrium constant was measured again (Table 4.3). The sum of the concentrations of the pyridine nucleotides is not the same before and after heating the mixture but this must be attributed to heat denaturation of the cofactors. The K -values observed in the reaction catalyzed by glutamate dehydrogenase and subsequently in the same medium by transhydrogenase are closely similar so that a specific enzyme effect can be excluded.

Since the ionic strength influences the equilibrium constant, the reaction between the pyridine nucleotides can be regarded as more or less ionic. For charged reactants the rate constant k shows a dependence on the charges of the

Table 4.1 Dependence of the equilibrium constant of the equilibrium $\text{NADPH} + \text{NAD}^+ \rightleftharpoons \text{NADP}^+ + \text{NADH}$ on the ionic strength. K-values as obtained in diluted buffer plus different salt concentrations at 25°C. The reaction was started with 150 μM NAD^+ + 150 μM NADPH and a catalytic amount of transhydrogenase. Samples were taken at different time intervals and assayed as described in Materials and Methods.

Buffer	Salt	pH	I	\sqrt{I}	K_{obs}	log K
Tris-HCl	KCl					
0.002 M						
	0	7.57	0.0015	0.039	0.33	-0.481
	5 mM	7.62	0.0061	0.078	0.35	-0.456
	10 mM	7.58	0.0115	0.107	0.38	-0.420
	20 mM	7.50	0.0216	0.146	0.43	-0.366
	50 mM	7.45	0.0516	0.227	0.48	-0.318
	100 mM	7.66	0.1014	0.318	0.54	-0.267

Table 4.2 Effect of the pH on K_{obs} at a constant ionic strength. The reaction was started with 200 μM NADPH + 200 μM NAD^+ and a catalytic amount of enzyme at 25°C. Samples were taken and assayed as described in Materials and Methods.

Buffer	pH	K_{obs}
potassium phosphate		
ionic strength 0.01	6.11	0.52
	6.53	0.44
	6.99	0.41
	7.45	0.38

Table 4.3 Equilibrium constant as established by glutamate dehydrogenase and subsequently by transhydrogenase in the same mixture. The reaction was started with glutamate dehydrogenase in the presence of 0.75 mM ammonium chloride, 0.27 mM α -oxoglutarate, 27 mM glutamate in 2 mM potassium phosphate buffer pH 7.6.

Enzyme	Equilibrium concentrations				K_{obs}
	NADH	NADPH	NAD^+	NADP^+	
+ glutamate dehydrogenase	45.5	27.0	84.0	96.0	0.52
heating (6 min. 80°C)	44.0	19.0	77.0	90.0	
+ transhydrogenase	40.5	23.0	80.0	86.0	0.53

reactants and the ionic strength as derived by Brönsted and Bjerrum (1922): $\ln k = \ln k_0 + 2Z_A Z_B \alpha \sqrt{I}$ (1), in which A and B are ions with charge Z_A and Z_B respectively; k and k_0 are the rate constants in the medium and at $I = 0$ respectively. The ionic strength I is defined as $I = 0.5 \sum_i c_i z_i^2$ in which c_i is the molarity of an ion and z_i its valency.

The numerical value of 2α in water at 25°C is 1.02. The simplifications that are used to derive this equation are only justified at low ionic strength and for point charges.

For the equilibrium situation defined in the introduction, this equation

changes into $\log K_{\text{obs}} = \log K_0 + A\sqrt{I}$ (2), in which $K_{\text{obs}} =$

$$\frac{[\text{NADPH}] \cdot [\text{NAD}^+]}{[\text{NADP}^+] \cdot [\text{NADH}]} ; K_0 \text{ is the equilibrium constant at } I = 0;$$

$$A = 2\alpha (Z_{\text{NADP}^+} \cdot Z_{\text{NADH}} - Z_{\text{NADPH}} \cdot Z_{\text{NAD}^+}).$$

A linear behaviour of $\log K_{\text{obs}}$ vs \sqrt{I} is observed at $I < 0.02$ using the data of Table 4.1 as plotted in Fig. 4.1. Extrapolation to zero ionic strength gives $K_{\text{obs}} = 0.30$. This corresponds to a difference in standard redox potential of the two pyridine nucleotide couples of 15 mV, the $\text{NADP}^+/\text{NADPH}$ couple being the more electronegative. The slope of the curve of $\log K$ vs \sqrt{I} is about one.

These results agree very well with the values obtained by Engel and Dalziel (1967) who studied the oxidative deamination of glutamate with each of both nicotinamide nucleotides separately, as catalyzed by glutamate dehydrogenase at pH 7.0 in phosphate buffers of varying ionic strength. The equilibrium

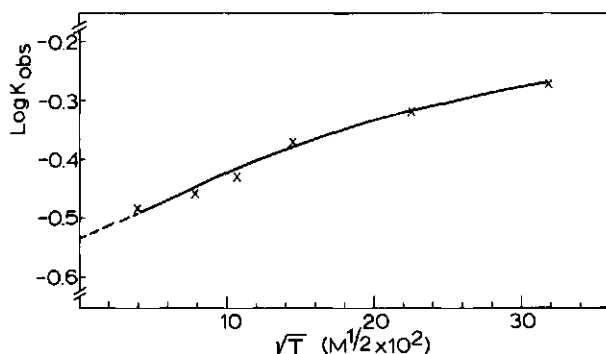


Fig. 4.1 Dependence of the equilibrium constant $[\text{NADPH}] \cdot [\text{NAD}^+] / [\text{NADH}] \cdot [\text{NADP}^+]$ on the ionic strength. The reaction was started with $150 \mu\text{M NAD}^+ + 150 \mu\text{M NADPH}$ and transhydrogenase in catalytic amounts. Temp. 25°C .

constant for the reaction catalyzed by glutamate dehydrogenase was defined as

$$\frac{[\text{NAD(P)H}] \cdot [\text{2-oxoglutarate}^{2-}] \cdot [\text{NH}_4^+] \cdot [\text{H}^+]}{[\text{NAD(P)}^+] \cdot [\text{glutamate}^{+2-}] \cdot [\text{H}_2\text{O}]}$$

For the NAD(H) dependent reaction $K_{(I=0)} = 0.64 \times 10^{-15}$ M and for the NADP(H) reaction $K_{(I=0)} = 0.193 \times 10^{-15}$ M was found. Thus $K_{(I=0)}$ for $\frac{[\text{NADPH}] \cdot [\text{NAD}^+]}{[\text{NADH}] \cdot [\text{NADP}^]}$ is 0.30 at 25°C and pH 7.0.

It can be derived from the results of Engel and Dalziel that the differences in slope of the linear parts of the two ionic-strength dependent curves is about one. This difference in slope reflects the dependence of the equilibrium constant of the pyridine nucleotide couples on the ionic strength.

The change of $\log K$ vs \sqrt{I} thus reflects differences in the effect of ionic strength on the two couples NAD^+/NADH and $\text{NADP}^+/\text{NADPH}$. The only chemical difference between the nucleotides is a secondary phosphate group in the adenine ribose of NADP(H) and attention must, therefore, be focused to this group.

The use of an ionic mechanism in these reactions needs to be justified. Such justification is unfortunately absent in the paper of Engel and Dalziel (1967). Recent N.M.R. data on the differences between NADH and NADPH and between NAD^+ and NADP^+ provide an explanation for the ionic strength dependence.

4.2.2 N.M.R. studies

In the past decade much work has been done on the conformation of the nicotinamide adenine dinucleotides in solution. From fluorescence studies of Weber (1957), Velick (1958) and Freed et al. (1967) N.M.R.-studies of Jardetzky et al. (1963); Jardetzki and Wade-Jardetzki (1966); Catterall et al. (1969); Hollis et al. (1969); Sarma and Kaplan (1969a, 1969b, 1970a, 1970b); Griffith et al. (1970) and Blumenstein and Raftery (1972, 1973), it has become clear that the nicotinamide adenine dinucleotides in aqueous solution can exist in a folded conformation. This conformation, in which intramolecular stacking exists between the two base pairs, is present in both the reduced and oxidized dinucleotides at neutral pH. The folding was found not to be a rigid two-state process (McDonald et al. 1972). As pointed out by Jacobus (1971) interesting, though sometimes conflicting, differences between the triphospho- and diphosphopyridine nucleotides have been reported (Sarma and Kaplan 1969a, 1970a, 1970b).

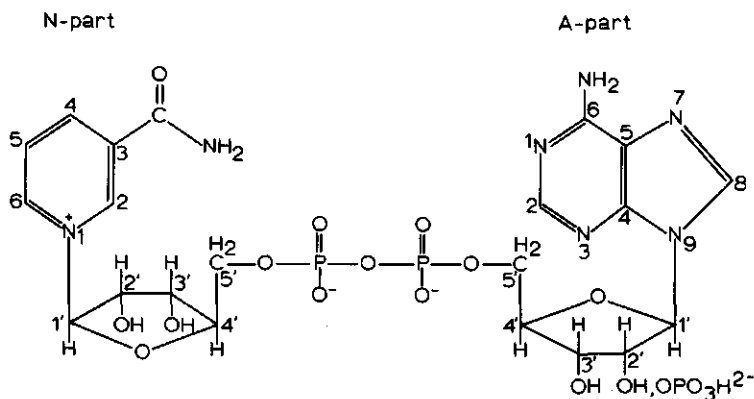


Fig. 4.2 The structure of NAD(P)⁺ and the numbering employed for the assignment of the various resonances. The proton resonances in the base parts are denoted as N-H1, A-H2 etc.; the proton resonance in the ribose attached to the bases are denoted as N-H1', A-H1' etc. The carbon resonances are denoted as N-C1, A-C1 etc. The ribose carbon resonances have an additional prime as in the proton resonances.

In the oxidized nucleotides the N-H4 proton (for nomenclature see Fig. 4.2) of β -NADP⁺ relative to β -NAD⁺ is shifted upfield. This shift is also present in the N-H2 and N-H6 protons. In the reduced nucleotides the N-H2 and N-H4 protons of NADPH are however found at lower field than those of NADH, whereas the N-H6 proton is found at higher field relative to the corresponding proton in NADH (Sarma and Kaplan, 1969). A possible conclusion from these N.M.R.-shifts that NADPH might be in a more open configuration than NADH can be regarded as somewhat premature as other subtle conformational changes can also give rise to shifts (Jacobus, 1971). It is, however, interesting that from fluorescence studies of Freed et al. (1967) it can be concluded that NADPH is in a somewhat more open configuration than NADH at comparable methanol concentrations.

In assuming an anti-conformation for the adenine-ribose glycosidic bond and a syn-conformation for the nicotinamide-ribose glycosidic bond, according to the definition of Donohue and Trueblood (1960), spacefilling models of the nucleotides were built (Sarma and Kaplan, 1970a). These authors proposed two possible helices (P and M helices) depending on the spiral direction of the backbone groups. In the M helix of the reduced triphosphopyridine nucleotide the 2'-phosphate group and the hydrogens of the CONH₂-side chain of the pyridine moiety can be hydrogen bonded (Sarma and Kaplan, 1970a). One negative charge of the phospho-group is thus in the vicinity of the B-proton of N-H4. In a

recent report Biellman and Samana (1973) provided evidence that an anti-conformation of the nicotinamide-ribose glycosidic bond is present in NAD^+ bound to horse liver alcohol dehydrogenase and dogfish lactate dehydrogenase. Examination of the space filling models reveals that in an anti-conformation the 2'-phosphate group can closely approach the 4A proton of NADPH in a M-helical form. Hydrogen bonding is no longer possible between the nicotinamide side chain and the 2'-phosphate group.

It has been shown by Schweizer et al. (1968) that in the adenine mononucleotides a phosphoryl group at the 2'-position of the adenine mononucleotide ribose has a greater effect in reducing the intermolecular base stacking than a similar group at the 3' or 5' position, especially in the dianionic form. These results are opposite to closer intramolecular stacking of NADP^+ compared with NAD^+ if proton shifts (Sarma and Kaplan, 1969a) are taken as indication for this type of interaction. Blumenstein and Raftery (1972) utilizing ^{31}P N.M.R. postulated electrostatic interaction between the positively charged nitrogen of the oxidized pyridine ring and a negative charged oxygen of the diphosphate backbone. No differences in the ^{31}P -chemical shifts of NAD^+ and NADP^+ were found. As the proton shifts in NMN (Sarma and Kaplan, 1969) and the carbon shifts (Blumenstein and Raftery, 1973) go in the same direction upon changing the pH it was postulated that the interaction of the phosphate backbone oxygen and the nitrogen can cause a redistribution of the charge around the whole pyridine ring. Thus the relative orientation of the nicotinamide with respect to the backbone can cause a different chemical behaviour of the ring protons. This means that not only stacking but also electrostatic interactions influence the shifts of the protons in the oxidized nucleotides. Examination of other data of Blumenstein and Raftery (1973) upon ^{13}C -natural abundance shifts of the nicotinamide carbons of NAD^+ and NADP^+ upon changing the pH, reveals some interesting facts not discussed by the authors. At pH 2.5 the ^{13}C -shifts of NAD^+ and NADP^+ are similar. At pH 7.5 for NAD^+ and 5.1 for NADP^+ the upfield shifts of the nicotinamide ring carbons of both compounds are still comparable. If, however, the pH of the NADP^+ solution is raised to 8.0 a further shift of all nicotinamide carbons is observed.

As the second ionization of the secondary phosphate group of NADP^+ has a pK around 6.1 this indicates that double and not single ionization of this group causes the nucleotides to behave differently in the ^{13}C -resonances of the pyridine ring. The ^{13}C -shifts of the adenine ring show, however, a somewhat different picture. From the data of Blumenstein and Raftery (1973) it can be

Table 4.4 Proton shifts of reduced and oxidized pyridine nucleotides induced by 1 M NaCl.

All resonances were taken with a Varian XL-100-15D with Fourier transform. The samples were lypholysed with D_2O to remove exchangeable protons. The pH of the oxidized nucleotides was adjusted with NaOD to pH 7.0. The reduced nucleotides have a pH of 7.9. All concentrations are about 10 mM. In B, + reflects the upfield shifts in the presence of salt compared to absence of salt and - reflects downfield shifts.

A				B				
Downfield proton shifts relative to the internal standard DSS in the presence of 1 M NaCl				Proton shifts of nucleotides in the presence relative to those in the absence of 1 M NaCl				
	NAD ⁺	NADP ⁺	NADH	NADPH	NAD ⁺	NADP ⁺	NADH	NADPH
N-H2	932.8	931.0	694.8	695.2	+3.3	+1.2	+2.4	+1.3
N-H6	916.6	917.8	-	-	+4.7	+4.6	-	-
N-H4	890.8	885.3	273.8	279.5	-0.3	+0.2	+2.0	+2.0
N-H5	821.5	820.3	-	-	+0.8	+1.3	-	-
A-H8	841.2	842.8	847.0	847.5	+3.1	+0.5	+2.9	+1.8
A-H2	818.4	817.3	825.3	826.5	-1	+1	+0.2	-0.2
N-H1 ¹	613.0	611.0	596.5	595.6	-1.1	+0.8	+4.1	+3.3
A-H1 ¹	600.8	605.0	613.3	620.5	+1.6	-2.9	+0.4	-0.5

found that the adenine ^{13}C -shifts of NAD⁺ at pH 7.5 and NADP⁺ at pH 8.0 are comparable. Comparison of the data of Blumenstein and Raftery (1973) on the difference in chemical shifts of the adenine part of NADP⁺ when the pH is changed from 5.1 to 8.0 and data of Ellis et al. (1973) on the difference in chemical shifts of the adenine part of NAD⁺ at pD5 and pD 7 shows that the molecules behave in an identical way. It seems reasonable to assume that these effects are mainly due to the disappearance of the protonation effect upon the A-N₁ and to the increase in ionization in the phosphate backbone as revealed by the shifts in A-H2, A-H6 and A-H8 respectively.

Some N.M.R. measurements have been performed to study the influence of 1 M NaCl upon the chemical shifts of the dinucleotides in 10 mM concentration in D_2O . The results are summarized in Table 4.5. The shifts are all relatively small (below 0.05 ppm) compared with those caused by overall stacking effects (Jardetzki et al., 1966; Catterall et al., 1969). In the oxidized nucleotides the N-H6 shows a remarkable shift in both nucleotides. This shift is less in the N-H2 protons. These shifts are consistent with the results of Blumenstein

and Raftery (1973) on the carbon shifts of NMN at decreasing pH (i.e. lower charge on the oxygen of the backbone). The N-H4 shows practically no shift and N-H5 shows only a small upfield shift. It thus seems unlikely that all these shifts are due to an increased stacking since in oxidized nucleotides one would expect to see shifts in all protons of the nicotinamide ring (Catterall et al., 1969). An effect of electrostatic origin seems a more likely explanation for these shifts. In the reduced coenzymes the N-H5 and N-H6 peaks were obscured by the HDO peak. The N-H2 and N-H4 protons show a comparable upfield shift. It is remarkable that the N-H4 protons in the reduced nucleotides do shift whereas hardly any shift was observed in the oxidized nucleotides. In the adenine part of NAD^+ the A-H8 moves further upfield than the corresponding proton in NADP^+ . The A-H2 proton of both compounds only shifts a small amount. Both the A-H8 and A-H2 protons are sensitive to stacking (Catterall et al., 1969), but A-H2 is more sensitive. The A-H8 proton of NAD^+ shows a much larger shift than that of NADP^+ . In the reduced nucleotides the A-H8 also shifts upfield. Here the difference between the shifts is smaller. The A-H2 proton in the oxidized and reduced dinucleotides shows hardly any shift. It seems reasonable to assume that in the proposed anti-conformation of the adenine-ribose (Schweizer et al., 1968) a reversal of a deshielding effect of an oxygen in the diphosphate upon the A-H8 is mainly responsible for this shift. It has been found recently (Tran-Din Son et al., 1973) that 2'-AMP shows a greater tendency than 5'-AMP to form a syn-conformation. Unfortunately 2'-5'-ADP was not investigated, but it is reasonable to assume that the adenine-ribose conformation in NADP^+ will be somewhat different than that of NAD^+ . The difference in the A-H8 shifts of NAD^+ and NADP^+ confirms this idea. As the adenine shifts and nicotinamide shifts are not comparable, these shifts cannot be attributed to stacking phenomena only.

It is interesting to compare the shifts in the ribose H' protons. In the A-H1' of both NADP^+ and NADPH downfield shifts are observed upon addition of salt. This is clearly attributable to a reversal of the shielding effect of the adjacent negative charge of the 2'-phosphate group. In both NAD^+ and NADH the A-H1' shows a small upfield shift. In the reduced dinucleotides upfield shifts in N-H1' are observed upon increasing the salt concentration. In the oxidized nucleotides, however, shifts in opposite direction are observed. According to the studies of Sarma and Kaplan (1968) and Catterall et al. (1969) both the A-H1' and N-H1' protons shift upfield as the pH or as the stacking increases. The downfield shift of the N-H1' in NAD^+ thus cannot be

explained by stacking phenomena alone. The combination of changes in stacking, changes in electrostatic interactions and changes in shielding make prediction and interpretation rather difficult. It is, however, clear that salt causes proton shifts that are different in NAD^+ compared to NADP^+ and NADH compared to NADPH . It is also clear that the conformation of the reduced and oxidized nucleotides must be different. Nevertheless one conclusion from data in the literature seems allowed, e.g. the ionization of the second 2'-phosphoryl-OH has a marked influence on the properties of the NAD(P)H couple. The translation of the shifts observed into subtle structural changes is difficult and intensive studies are necessary. In this respect two observations are of interest.

- 1) At high ionic strength the splitting of the N-H4 A and N-H4 B shifts of NADPH is less marked.
- 2) NADPH is a better coenzyme for lactate dehydrogenase at low pH (6.0) than at a higher pH value (Navazio et al., 1957).

Measurements of fluorescence lifetimes of the reduced nucleotides have been performed. The measurements were done with 100 μM of reduced nucleotides in the absence or presence of 1 M NaCl . No big differences between the behaviour of NADH and NADPH were found. In both cases the lifetime increased only a very small amount. This indicates that only slight changes occur in the stacking distance of the two base pairs and in the population of stacked molecules. Obviously these changes are too small to give a pronounced effect on the fluorescence lifetime of the excited state (see Table 4.5).

However, a systematic increase in lifetime is always observed upon addition of salt and this probably indicates destacking. The lifetime of the NADH excited state was always somewhat longer than that of the NADPH excited state.

Table 4.5 Fluorescence lifetimes of NAD(P)H in the absence and presence of 1 M NaCl . Measurements were performed at 35°C. The nucleotides were dissolved in distilled water.

100 μM NADH	100 μM $\text{NADH} +$ 1 M NaCl	100 μM NADPH	100 μM $\text{NADPH} +$ 1 M NaCl
0.45 nsec	0.48 nsec	0.43 nsec	0.46 nsec

This would agree with a somewhat more "open" character of the NADH compared to NADPH. However, the fluorescence data of Freed (1967) do point in the opposite direction. Possibly complex quenching by the secondary phosphate group in NADPH could account for the somewhat shorter lifetime observed.

4.2.3 *Mechanistic aspects*

As pointed out already, the dependence of the equilibrium constant on ionic strength and pH must be due to distinct differences between the di- and triphosphopyridine nucleotides; mainly due to the 2'-phospho-group. Studies on the structure revealed that this phospho-group might approach the N-C4 protons. The influence of the charges of the negative oxygens will cause these protons to behave differently from the N-C4 protons of NAD(H). The question how a slope of one can be obtained in the plot of $\log K$ vs \sqrt{I} remains to be answered.

Taking all charges into account (actually not permitted in the Brønsted approach used since the charges should be very close to each other) at pH 7.5 the diphosphate backbone carries two negative charges and the 2'-phosphate group also has two negative charges; in addition the oxidized nucleotides carry a delocalized positive charge (Dixon and Webb, 1964).

The net charges substituted in the slope-term of equation (2) give a value of 2. This value is not altered when the diphosphate backbone charges are omitted. If, however, of the negative charges only one of the two charges of the 2'-phosphate group is taken into account, the value of the theoretical slope becomes 1 in accordance to the experimental value. In the light of the N.M.R. data discussed previously this approach does not seem unreasonable. The effect of pH shows that a lowering of the charge, arising from the second ionization of the 2'-phospho group makes the couples NAD^+/NADH and $\text{NADP}^+/\text{NADPH}$ more equivalent since K increases. If the same numerical values for the charges of the nucleotides are substituted in the theoretical slopes of the glutamate dehydrogenase catalyzed reactions with NADH or NADPH, the theoretical values of 2 and 3 respectively agree fairly well with the experimental values (Engel and Dalziel, 1967) of 1.4 and 2.4 respectively.

All other numerical values for the dinucleotide charges give larger deviations of the theoretical values from the experimental ones.

The validity of the Brønsted-Bjerrum equation in two independent studies with different enzymes points to the fact that for thermodynamic equilibrium conditions, the negative charge of the second 2'-phosphoryl O^- must be very close to the positive pyridine ring in NADP^+ to give charge neutralization and to

influence the N-C4 of NADPH. This conclusion is necessary to satisfy the requirement of point charges. It follows that the charge of the first 2'-phosphoryl O^- must be a sufficiently large distance from the reactivity centre (N-C4) to be without effect. The N.M.R.-results of Table 4.4 suggest that this charge has a shielding effect on the proton of the ribose connected to the adenine ring. Such a condition can only be created in the folded form. In other words, the thermodynamic equilibrium is established by a reaction of the oxidized and reduced pyridine nucleotide couples in the folded form. In no other configuration the charges can be counted as has been done here, while in the open form the ionic strength should not influence the equilibrium constant. This conclusion, however, is only valid for the free coenzymes in thermodynamic equilibrium. It does not exclude the possibility that the coenzymes in either state bind to the enzyme in their open conformations.

4.2.4 *Shift of the observed equilibrium constant depending on initial concentration*

The equilibrium as reported in section 4.2.1 was reached starting from both directions with about equimolar concentrations of substrate. However, when the initial ratio of the substrates is changed, it is found that with a higher initial $[NAD^+]/[NADPH]$ ratio the thermodynamic equilibrium, as obtained with an initial 1:1 ratio, is no longer reached. In the reverse reaction the initial $[NADP^+]/[NADH]$ ratio does not influence the K_{obs} (Table 4.6). Upon addition of either NADH or NADPH the reaction restarts and the final values of K_{obs} approach those of K as given in Fig. 4.1 under the conditions of experiment (Table 4.7).

From Table 4.6 it is clear that NADPH is more effective than NADH in converting the enzyme into its catalytically active form. It must, however, be noticed that the values for K_{obs} under the extreme conditions of these experiments are only approximate because small variations in the actual NADPH concentrations cause relatively large shifts in the calculated equilibrium constant. In the cause of reactivation by NADH only small changes in the concentration of NADPH and $NADP^+$ are observed; however, the $[NADP^+]/[NADPH]$ ratio declines considerable. In order to explain the effects of changing the initial $[NAD^+]/[NADPH]$ ratio upon K_{obs} it is important to summarize briefly some of the kinetical data of this enzyme. From studies of Van den Broek et al. (1971) it is clear that $NADP^+$ is a very strong inhibitor of the reactions catalyzed by this enzyme. The oxidized enzyme forms a dead-end complex with $NADP^+$, a suggestion also made for the *Pseudomonas* enzyme (Cohen et al., 1970).

It was also shown that NADPH activates the reaction and enhances the rate of its own formation in the reaction of $\text{NADH} + \text{NADP}^+ \rightarrow \text{NADPH} + \text{NAD}^+$. This reaction shows a lag, which can be abolished by MgCl_2 and NADPH (Van den Broek et al., 1971). The highest rates of NADPH formation are obtained at about equal concentrations of NADPH and NADP^+ . It was thus suggested that the $[\text{NADP}^+]/[\text{NADPH}]$ ratio was of major importance in regulating the enzyme activity. From anaerobic titration experiments it is clear that in the presence of high concentrations of NADP^+ the reduction of the enzyme by NADH and NADPH is strongly retarded. From our experiments it is nevertheless clear that under unfavourable initial conditions the reaction can proceed, although slowly, towards equilibrium in those cases where enough NADPH is present to activate the enzyme. Equilibrium is reached even at a high final concentration of the inhibitor NADP^+ by starting the reaction with $\text{NADP}^+ + \text{NADH}$ in a 4:1 ratio. At equilibrium the $[\text{NADP}^+]/[\text{NADPH}]$ ratio becomes about 4-5 (Table 4.6).

Table 4.6 Dependence of the equilibrium constant of the pyridine nucleotide couples on starting conditions. K-values as obtained with different initial ratios of nucleotides at 25°C. Reaction was started with substrates at the indicated concentrations and a catalytic amount of enzyme. Samples were taken at different time intervals and assayed as described under Materials and Methods.

Buffer 0.1 M	Approximate starting concentrations (μM)				Final concentrations in equilibrium (μM)				K_{obs}
Tris-HCl	NADH	NADPH	NAD^+	NADP^+	NADH	NADPH	NAD^+	NADP^+	
pH 7.6		50	100		32.0	15.0	69.5	40.0	0.81
		50	150		37.1	11.7	114	41.5	0.89
		50	250		40.0	10.1	213	44.0	1.2
		50	500		44.5	8.5	461	45.0	1.8
		100	500		72.0	13.5	468	87.0	1.1
		500	500		290	210	232	302	0.55
		450	100		94.7	363	17.0	111	0.58
		500		100	427	61.6	89.0	23.1	0.56
		100		400	29.0	69.5	79.5	31.5	0.60
	0.02 M Tris-HCl pH 7.6		50	250		44.0	10.5	188	43.0
		250	50		47.0	191	6.0	52.0	0.47

Table 4.7 Effect of reduced substrates on the equilibrium constant of the pyridine nucleotide couples. The reaction was started with an initial ratio of $[NAD^+]/[NADPH]$ of about 10. Samples were taken at different time intervals and assayed as described in Materials and Methods.

Buffer	Addition after equilibrium		Equilibrium concentrations				K_{obs}
	NADH μM	NADPH μM	NADH μM	NADPH μM	NAD^+ μM	$NADP^+$ μM	
0.1 M Tris-HCl pH 7.6			44	10	500	44	2.6 I
		21 to I	68	13	482	62	1.5 II
		46 to I	91	16	459	85	0.95 III
		75 to I	109	20	437	108	0.74 IV
		100 to I	129	25	414	130	0.62 V
		150 to I	164	40	376	159	0.58 VI
			43	7	478	48	1.6 VII
		+ 92	128	10	483	44	0.86 VIII
		+196	218	14	484	39	0.80 IX
		+400	386	18	488	34	0.67 X

When the opposite reaction $NAD^+ + NADPH \rightarrow NADH + NADP^+$ is started with a high $[NAD^+]/[NADPH]$ ratio equilibrium is not reached while the $[NADP^+]/[NADPH]$ ratio at apparent equilibrium also becomes about 4-5. Thus it can be concluded that the reaction does not stop because of an unfavourable ratio $[NADP^+]/[NADPH]$. The data in Table 4.6 indicate that the $[NADP^+]/[NADPH]$ ratio is of less importance than the actual final NADPH concentration. A survey of all experiments performed leads to the interesting observation that independent of the $NADP^+$ -concentration the reaction reaches thermodynamic equilibrium as soon as the NADPH concentration exceeds a concentration of about 25 μM . An estimate shows that under the conditions of Table 4.7 a 50% decline of the value of K_{obs} is obtained at about 13 μM NADPH, a value in reasonable agreement with the reported K_m -value of NADPH of 15 μM .

4.2.5 Effect of ATP on the equilibrium constant

In order to determine whether the enzyme exhibits an energy-dependent reaction the equilibrium established by pure enzyme or cell-free extract in the presence of ATP was measured. In cell-free extract an ATP regenerating system was

present to maintain a constant level. No shift of the equilibrium constant was observed when the reaction was catalyzed by either pure enzyme or by cell-free extract (Table 4.8). ATP only inhibited the rate at which the equilibrium was reached. This result differs from the results obtained with mitochondrial particles; with this system ATP induces a very strong shift of the equilibrium constant from about unity towards 500 or more (Lee and Ernster, 1964). However, it cannot be excluded that the ultrasonic procedure used to prepare the cell-free extract of *Azotobacter vinelandii* destroys the energy-dependent transhydrogenase complex.

Table 4.8 Effect of ATP on the equilibrium constant as established by cell-free extract. The mixture was incubated anaerobically and samples were taken anaerobically with a syringe at different time intervals. The samples were assayed as described in Materials and Methods.

Reaction performed in 0.1 M Tris-HCl pH 7.6 (+ 1 mM potassium phosphate buffer)

A		Equilibrium concentrations			K_{obs}
Addition	NADH μM	NADPH μM	NAD^+ μM	NADP^+ μM	
---	205	101	309	266	0.57
---	212	104	310	264	0.56
1 mM ATP	187	96	275	238	0.59
1 mM ATP	178	85	300	240	0.60

B					
	NADH μM	NADPH μM	NAD^+ μM	NADP^+ μM	K_{obs}
---	165	130	192	260	0.58
---	174	130	183	266	0.52
1 mM ATP	168	137	193	257	0.61
1 mM ATP	165	137	194	264	0.61

A: Reaction of $\text{NADPH} + \text{NAD}^+$

B: Reaction of $\text{NADH} + \text{NADP}^+$

4.3 DISCUSSION OF USING KINETICAL DATA FOR THE CALCULATION OF THE EQUILIBRIUM CONSTANT

The non-energy linked transhydrogenase catalyzes the reaction $\text{NADH} + \text{NADP}^+ \rightleftharpoons \text{NAD}^+ + \text{NADPH}$ with a much higher maximal initial velocity from right to left than from left to right (Kaplan et al., 1953; Van den Broek et al., 1971). The value of the equilibrium constant is, however, near unity as reported by Kaplan et al, (1953) and in this chapter. The relationship between kinetic parameters and equilibrium constant is given by the Haldane equations. In general the Haldane equations of the reaction $A + B + C \xrightleftharpoons{K_{eq}} P + Q + R$ can be written as

$$K_{eq.} = \left(\frac{V_f}{V_b} \right)^n \frac{K_{(P)}K_{(Q)}K_{(R)}}{K_{(A)}K_{(B)}K_{(C)}}$$

in which V_f and V_b are the maximum rates of the forward and backward reactions respectively at infinite concentrations of all substrates and in the absence of products. The K 's may be either Michaelis constants or "inhibition"-constants (Cleland, 1963). For a rapid equilibrium random bi-bi mechanism as proposed by Van den Broek et al (1971) for the *Azotobacter* enzyme the Haldane relation is

$$K_{eq.} = \frac{V_f}{V_b} \frac{K_P \cdot K_Q}{K_A \cdot K_B} \quad \text{assuming independent binding of the substrates}$$

(Alberty et al., 1952). From the data of Van den

Broek et al. (1971) $K_{eq.} = 1.4$ can be calculated. This is in reasonably good agreement with the value of the equilibrium constant as measured directly, especially considering the extremely complex kinetic picture of the reaction of NAD^+ with NADPH , and the fact that enzyme inactivation occurs on the binding by NADP^+ at a site which differs from the catalytic site. In such a case deviations from the equilibrium constant can be expected (Cleland, 1963). From their kinetical data Teixeira da Cruz et al. (1971) calculated that the equilibrium constant for the mitochondrial non-energy linked transhydrogenase is 0.13, assuming a Theorell-Chance mechanism. It was found that the ratio $\frac{V_f}{V_b}$ differs in the presence or absence of a substrate regenerating system (Danielson and Ernster, 1963). Thus a correction was made for the equilibrium constant as calculated from kinetic data in the presence of a substrate regenerating system. It must, however, be emphasized that such a procedure is not correct since it cannot be assumed beforehand that all other constants in the Haldane relation remain constant. Furthermore, the equilibrium constant as calculated by Teixeira da Cruz et al. (1970)

$K_{eq.} = \frac{k_1 k_3 k_5}{k_2 k_4 k_6}$ does not agree with that calculated from the specific

Haldane relation for a Theorell-Chance mechanism:

$$K_{eq.} = \left(\frac{V_f}{V_b} \right)^3 \frac{K_P K_Q}{K_A K_B} \quad (\text{Cleland, 1963}); \text{ substitution of the values given}$$

in the paper of Teixeira da Cruz et al. (1971), gives a value of $K_{eq.} = 0.016$. It could be assumed that isomerization of EA in the forward and EQ in the backward reaction takes place. However, when binding of NADH as the first substrate in the reaction sequence of the forward reaction is accepted (Rydström, 1972), a reduction of the enzyme before the second substrate is bound or an unfolding of the NADH at the enzyme surface is implied.

In such a case the Haldane relation $K_{eq.} = \left(\frac{V_f}{V_b} \right)^3 \frac{K_P K_Q}{K_A K_B}$

for a Theorell-Chance mechanism is not valid. From these arguments it can be determined that a simple Theorell-Chance mechanism is not operating in the mitochondrial non-energy linked transhydrogenase. Also from the kinetic data given by Teixeira da Cruz et al. (1971) a similar argument can be derived. One of the specific criteria of a Theorell-Chance mechanism is, that the value of the ordinate of the intersection point of the Lineweaver-Burk plots at different donor and acceptor concentrations of the forward reaction has the same absolute value in the backward reaction. However, the actual value is negative with respect to the reaction $\text{NADPH} + \text{NAD}^+ \rightarrow \text{NADH} + \text{NADP}^+$, whereas in the reverse reaction the intersection point is on the ordinate.

5. ELECTRON MICROSCOPIC STUDIES

5.1 INTRODUCTION

In the past few years pure transhydrogenase from several bacterial sources has been examined by electron microscopy (Louie et al., 1969, 1970, 1972; Van den Broek et al., 1971; Middleditch et al., 1972). The pure enzymes isolated from *Pseudomonas aeruginosa* (Louie et al., 1969, 1970, 1972) and *Azotobacter vinelandii* (Van den Broek et al., 1971; Middleditch et al., 1972) have several morphological features in common.

Both exist as long helical-like structures of non-uniform length 50-1000 nm. As pointed out by Van den Broek (Van den Broek et al., 1971) the *Azotobacter* enzyme can be dissociated into shorter structures by the addition of 2 mM NADP^+ . A uniform size distribution of the dissociated molecules was not observed.

In the ultracentrifuge the peak with the highest sedimentation coefficient (88 S) disappeared but on the whole the solution remained polydisperse. Louie et al. (1970, 1972) reported on the drastic dissociating effect of 2'-AMP on the long helical structures of purified *Pseudomonas* transhydrogenase.

The reaction of $\text{NADPH} + (\text{S-})\text{NAD}^+ \rightleftharpoons \text{NADP}^+ + (\text{S-})\text{NADH}$ as catalyzed by the *Pseudomonas* enzyme proceeds readily from left to right, but it needs activation in the reverse direction. 2'-AMP was found able to enhance the enzyme activity in reactions in which the reducing substrate does not contain a 2'-phosphate group (Cohen and Kaplan, 1970). By a combination of electron microscopy and a band-forming sedimentation technique as suggested by Vinograd, Brunner, Kent and Weigle (1963) it became clear that:

1. in the absence of 2'-AMP long helical structures are present; length 50-500 nm and diameter 8-10 nm with $S_{20,w} \approx 110\text{S}$; not catalyzing the reaction of $\text{NADH} + \text{S-NAD}^+ \rightarrow \text{S-NADH} + \text{NAD}^+$, and
2. in the presence of 2'-AMP cylindrical structures are present; diameter 12 nm and height 10 nm with $S_{20,w} \approx 28-30\text{S}$; capable of catalyzing the reaction of $\text{NADH} + \text{S-NAD}^+ \rightarrow \text{S-NADH} + \text{NAD}^+$.

It was concluded that dissociation resulted in the exposure of sites that are buried within the helical structures thus promoting the catalytic activity in the NADH oxidizing reaction. It should however, be noted that although this dissociation results in a homogeneous population of cylinders, the diameter of

these cylinders does not fit in that of the original helices. Thus in addition to fragmentation, 2'-AMP also induces another conformational change not explicitly mentioned by the authors.

Middleditch et al. (1972) reported on the effect of pH on the structure of the *Azotobacter* enzyme. Their results show that a reversible pH-dependent association-dissociation process occurs. At pH 9.0 the enzyme is dissociated (7.4 S), while at pH 6.8 it shows the typical long strands (33.5 S). The activity of the enzyme was not affected by preincubation at these two pH values. It is, however, surprising that the sedimentation coefficient of the highly polymerized transhydrogenase was found to be 33.5 S compared with the much higher values reported by Louie et al. (1972), as both preparations show the same kind of elongated structures under the electron microscope. Van den Broek et al. (1971) reported a main peak in ultracentrifuge experiments of about 48 S and a minor peak with a sedimentation coefficient of 88 S. At high pH a non-homogeneous population was obtained with some threads still present. It cannot be understood that structures with a length of 10-100 nm and a diameter of 7 nm have such a very low sedimentation coefficient of 7.4 S. Evidently some of these constants must be in error.

A very interesting although catalytically inactive structure was reported by Middleditch et al. (1972). This structure looks like a paired rod and is devoid of all catalytic activity. The amino acid composition, however, agreed very well with that of native transhydrogenase.

The reasons for the association-dissociation behaviour of this enzyme are still unknown. Van den Broek et al. (1972) suggested that association can take place as soon as the pyruvate dehydrogenase is removed during the purification procedure; another possibility might be the removal of enzyme-bound NADP⁺ during purification, thus allowing the enzyme to associate (Van den Broek et al, 1971).

The effects observed by different authors prompted us to investigate different parameters involved in the association-dissociation phenomena. First, different steps of the purification were investigated in order to follow the association-dissociation behaviour. Second, in order to obtain information on the nature of the intermolecular interactions, salt concentrations were also varied. Third, the effect of the ambient pH was studied to compare the behaviour of this enzyme with the results as obtained by Middleditch et al. (1972).

As it was observed that divalent metal ions have a pronounced effect on the association, the influence of several divalent metal ions upon the electron-microscopic structures was investigated.

In order to compare the structures of the *Pseudomonas* enzyme (Louie et al., 1969, 1970, 1972) with the *Azotobacter* enzyme identical incubation conditions were taken before preparing the grids. It was found that β -mercaptoethanol has a very pronounced effect on the structure. Other thiol reducing agents were also taken in order to compare the different results. As 2'-AMP has such a distinct effect upon the association-dissociation of the *Pseudomonas* enzyme different conditions were screened with the *Azotobacter* enzyme to see whether comparable results could be obtained. The reported effects of NADP^+ and NADPH upon the *Azotobacter* enzyme (Van den Broek et al., 1971) were carefully re-examined to determine the critical concentrations involved in these processes.

These studies have been performed in collaboration with Prof. Dr. E.F.J. Van Bruggen and Mr. J.F.L. Van Breemen. Part of this work was done by Drs. S. Boonstra, all of the Laboratorium voor Biochemie, Rijksuniversiteit, Groningen, Nederland.

5.2 RESULTS

5.2.1 Screening of different purification steps

First, samples from the different steps of the purification procedure of Van den Broek et al. (1971), were screened for the presence of the thread-like structures of transhydrogenase. In the cell-free extract few filamentous structures of the typical transhydrogenase type can be observed. However, after heat treatment in the presence of alcohol the number of these structures increases considerably, and in parallel with an increase in purity of the enzyme.

5.2.2 Effect of NADP^+ and NADPH

Addition of NADP^+ to the purified enzyme causes dissociation of the filamentous structure of the enzyme as reported by Van den Broek et al. (1971). A closer investigation of this dissociating effect revealed that the NADP^+ concentration must be higher than $1 \mu\text{M}$. At a concentration of $10 \mu\text{M}$ the dissociation appears to be as complete as at a concentration of 1mM . Transhydrogenase can bind more than one molecule of NADP^+ ; the first NADP^+ molecule has a high affinity for the oxidized enzyme $K_D = 0.2-0.5 \mu\text{M}$ (Van den Broek et al., 1971). The results

suggest that the first molecule of NADP^+ bound, is the one responsible for the dissociation of the enzyme. In agreement with previous results (Van den Broek et al., 1971) the dissociating effect of NADP^+ on the enzyme can be effectively counteracted by the addition of NADPH. It is found, however, that the amount of NADPH needed to reassociate the enzyme depends on the NADP^+ concentration used to dissociate the enzyme. These results are summarized in Table 5.1. From the picture of the enzyme in the presence of 1 mM NADPH the structure looks like a flattened (double) helix. It can be seen that breakdown occurs along an oblique incision. The angle between the plane of incisions and the longitudinal direction is $50-60^\circ$. The periodicity of the helix is about 13-17 nm. The diameter is about 11 nm, the length being variable goes up to 1000 nm (Fig. 5.1).

5.2.3 Effect of 2'-AMP under different conditions

The very clear dissociating effect of 2'-AMP as seen in the case of the *Pseudomonas* transhydrogenase (Louie et al., 1972) was never found in the case of the *Azotobacter* enzyme (Middleditch et al., 1972; Van den Broek et al., 1971). In the present study no effect of 2'-AMP was found when the enzyme is dissolved in 50 mM Tris-HCl pH 7.6. However, some dissociation can be observed when 2'-AMP is added in the presence of phosphate but even under these conditions long strands (length > 100 nm) remain present. Phosphate alone has no effect. The dissociation products of the enzyme in the presence of 2'-AMP and phosphate are not as well defined as in the case of dissociated *Pseudomonas* enzyme (Louie et al., 1972). The substructures present are nearly all circular with a variable diameter of 8-16 nm (Fig. 5.2).

The sedimentation behaviour of the enzyme changes only slightly in the presence of 1 mM 2'-AMP. The sedimentation pattern shows a more homogeneous population of protein molecules in the presence than in the absence of 2'-AMP. However, the slowest sedimenting component (48 S) does not change.

These results indicate that 2'-AMP presumably binds to the enzyme only in the presence of phosphate, thereby causing some dissociation, in agreement with the effect of 2'-AMP on the spectral properties in the presence of phosphate (Chapter 6).

5.2.4 The effect of ambient pH

A wide range of pH values was taken (pH 4.2 - 9.5) in order to investigate the effects as reported by Middleditch et al. (1972). At pH 4.2 - 7.0 very long strands (up to 1000 nm) with a diameter of 11 nm are observed. At these pH

Fig. 5.1 Electron micrograph of purified transhydrogenase in the presence of 1 mM NADPH. The enzyme was diluted with 30 mM potassium phosphate buffer pH 7.6 containing 1 mM EDTA. Protein concentration 0.02 mg/ml. Negative staining with 0.5% uranyl acetate. x 296,000.

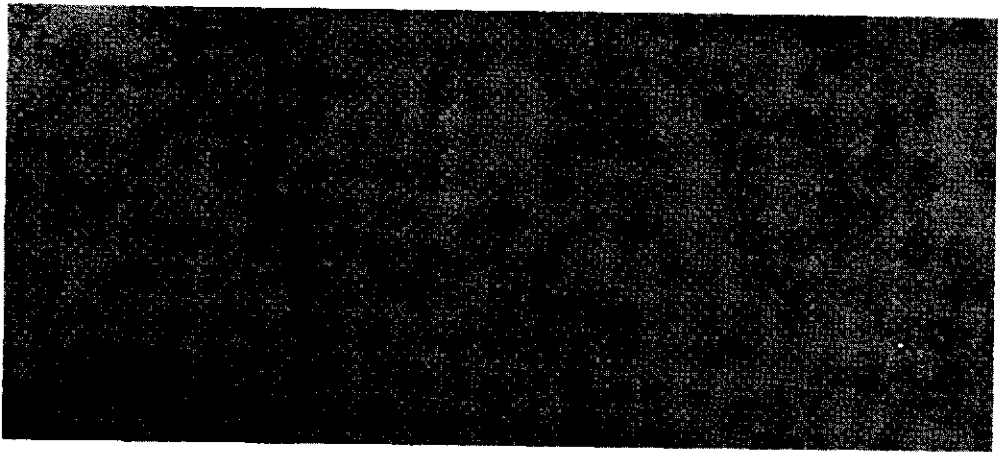
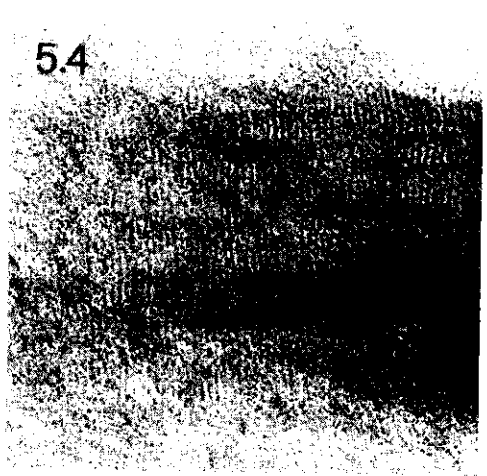
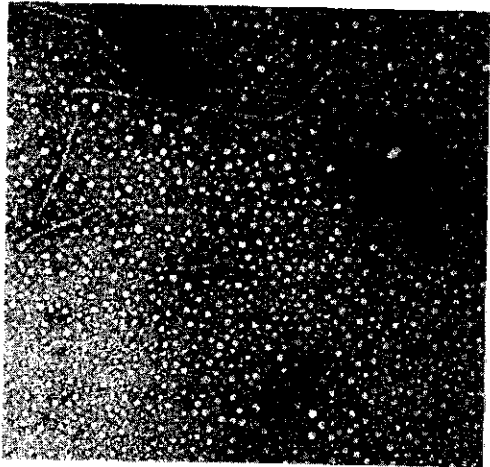
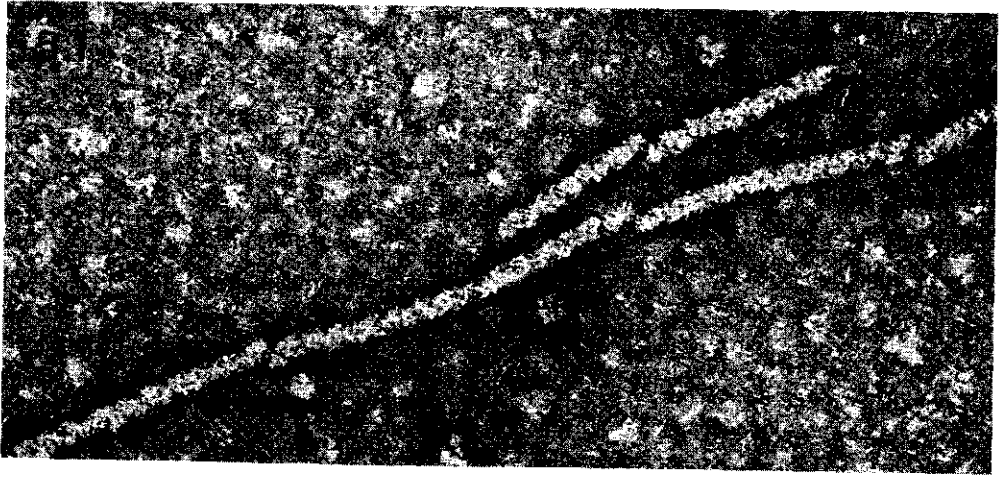
Fig. 5.2 Electron micrograph of purified transhydrogenase in the presence of 1 mM 2^1 -AMP and phosphate. The enzyme was dissolved in 50 mM Tris-HCl pH 7.6 containing 10 mM potassium phosphate buffer pH 7.6. Protein concentration 0.1 mg/ml. Negative staining with 2% uranyl acetate. x 77,700

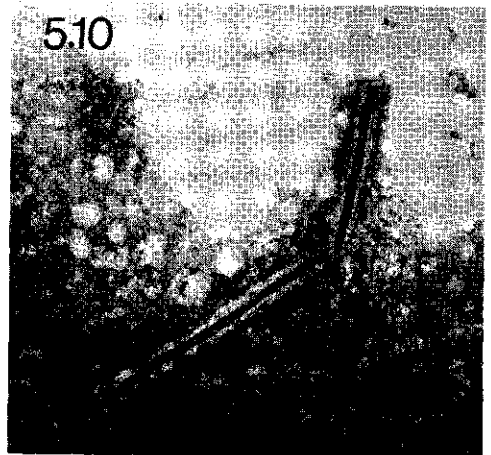
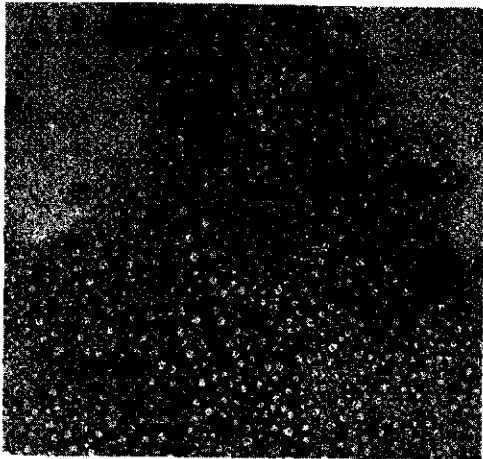
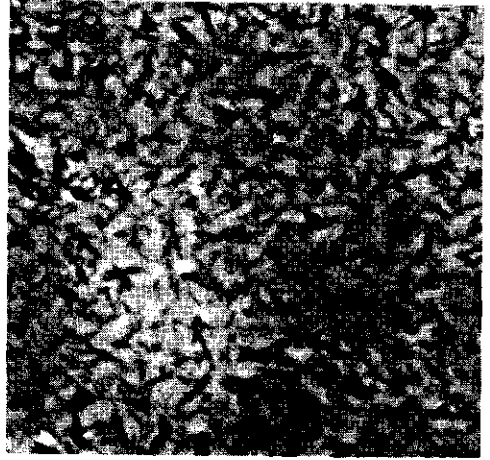
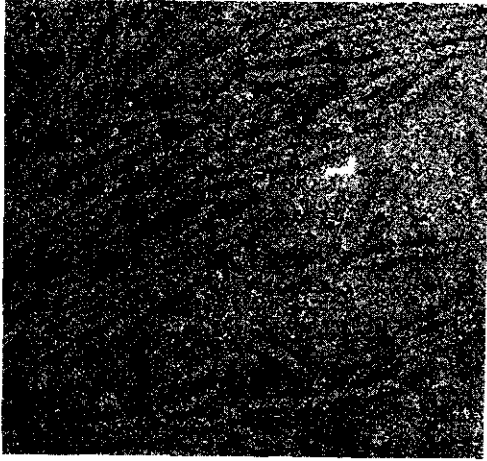
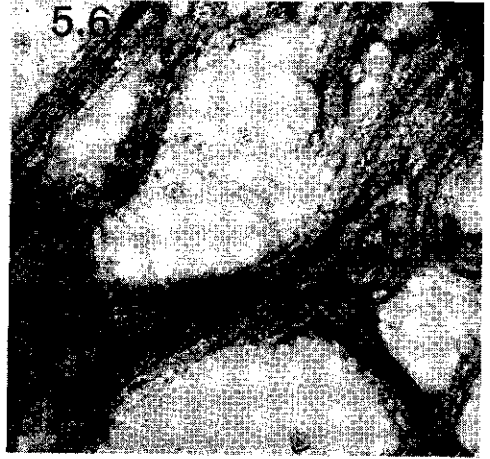
Fig. 5.3 Electron micrograph of purified transhydrogenase in the presence of 50 mM Tris-HCl pH 7.6 and 10 mM $MgCl_2$. The arrows indicate structures frequently seen. 1. rods; 2. striped rectangles; 3. rings; 4. circular fragments; 5. rozette-like structures. Protein concentration 0.02 mg/ml. Negative staining with 0.5% uranyl acetate. x 157,200.

Fig. 5.4 Electron micrograph of a crystalline transhydrogenase preparation. Crystallization was performed by adding a saturated ammonium sulphate solution at 4°C; at slight cloudiness the solution was allowed to set at 4°C. Negative staining with 0.5% uranyl acetate. x 314,400.

Fig. 5.5 Electron micrograph of purified transhydrogenase in the presence of 33% saturation ammonium sulphate. The enzyme was diluted with 30 mM potassium phosphate buffer pH 7.6 containing 1 mM EDTA to a protein concentration of 0.2 mg/ml. Subsequently this sample was diluted to 0.02 mg/ml in 30 mM potassium phosphate buffer pH 7.6 containing 2% glutaric aldehyd, 1 mM EDTA and 33% ammonium sulphate. Incubation time with the ammonium sulphate containing solution: 5 minutes. Negative staining with 5% uranyl acetate. x 204,000.

Fig. 5.6 Electron micrograph of purified transhydrogenase in 50 mM Tris-HCl pH 7.6 and in the presence of 10 mM $CoSO_4$. Protein concentration 0.1 mg/ml. Negative staining with 2% uranyl acetate. x 157,200.





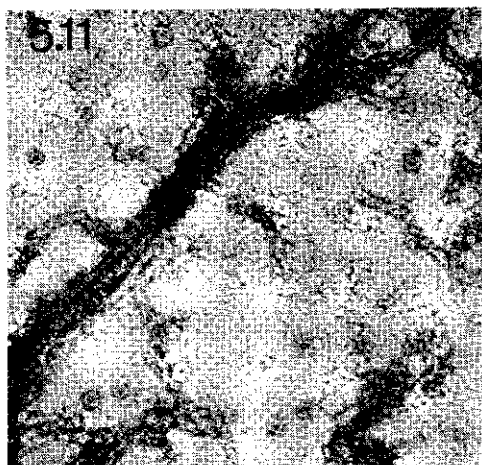


Fig. 5.7 Electron micrograph of purified transhydrogenase in 50 mM Tris-HCl pH 7.6 and in the presence of 10 mM $MgCl_2$. Negative staining with 2% uranyl acetate. x 157,200.



Fig. 5.8 Phase contrast micrograph of purified transhydrogenase in 50 mM Tris-HCl pH 7.6 containing 10 mM $MnCl_2$. x 1625.

Fig. 5.9 Electron micrograph of purified transhydrogenase in 50 mM Tris-HCl pH 7.6 containing 1.0 M β -mercaptoethanol and 5 mM EDTA. Negative staining with 2% uranyl acetate. x 77,700.

Fig. 5.10 Electron micrograph of a structure sometimes observed in preparations of purified transhydrogenase in 50 mM Tris-HCl pH 7.6. Negative staining with 2% uranyl acetate. x 157,200.

Fig. 5.11 Electron micrograph of a ladder-like structure present in preparations of purified transhydrogenase, after anaerobic dialysis in the presence of glucose-6-phosphate and glucose-6-phosphate dehydrogenase in 50 mM Tris-HCl pH 7.6. Negative staining with 2% uranyl acetate. x 157,200.

Fig. 5.12 Electron micrograph of purified transhydrogenase in 50 mM Tris-HCl pH 7.6 containing 10 mM $CaCl_2$. The arrow indicates the point of dissociation of the elongated structure into a rod-like structure. Negative staining with 2% uranyl acetate. x 157,200.

Table 5.1 Effect of the phosphopyridine nucleotides on the association-dissociation behaviour of the transhydrogenase molecules.
Experimental conditions as described under Materials and Methods (Chapter 2)

		NADP ⁺					
		0	0.1 μM	1 μM	10 μM	100 μM	1 mM
0	no dissociation	no dissociation	no dissociation	dissociation starts	dissociation	dissociation	dissociation
10 μM						dissociation remains	
100 μM					reassociation	reassociation	

NADPH

values also smaller structures are found like a striped rectangle (Fig. 5.3, structure 2). This kind of structure was also obtained upon incubation of *Pseudomonas* enzyme with 2'-AMP (Louie et al., 1972). Further circular fragments are present, ranging in diameter from 16 nm to 19 nm with some structural detail. At a high pH (9.5) no long strands are observed anymore. The maximal length then observed is about 50 nm.

5.2.5 *Effect of ammonium sulphate*

When the transhydrogenase protein is incubated at 33% saturation of ammonium sulphate microcrystalline structures are found, and they are clearly different from the original threads (Van den Broek et al., 1971). The original helical structures are rearranged into a kind of stacked-disk structures (Fig. 5.4). The effect of various ammonium sulphate concentrations was investigated by incubating the enzyme for short periods with salt and glutaraldehyd. At 10% saturation with ammonium sulphate and 2% glutaraldehyd a starting dissociation can be observed. The substructures arising from this treatment are of various kinds. Predominantly rozette-like structures of different diameter are found and occasionally also a striped rectangle. Incubation at 33% or 50% saturation results in very clear breakdown of the long strands at the oblique incisions that can be seen in the intact structures (Fig. 5.5). The pictures obtained after these treatments indicate that the microcrystalline structure, as found in Fig. 5.4 is formed by breakage of the threads into smaller segments, and subsequently rebuilding of these substructures into the stacked-disk structures with the perpendicular striping.

5.2.6 *The effect of divalent metal ions*

As has been discussed in Chapter 3, Mn^{2+} strongly enhances the rate of the reaction $NADH + NADP^+ \rightarrow NADPH + NAD^+$ in cell-free extracts (Veeger et al., 1973) and also can be used as a precipitant of the transhydrogenase. Addition of metal ions to purified transhydrogenase (Spec. act. 300 units/mg) revealed several interesting phenomena of the enzyme-metal interaction. The enzyme fraction used was a dissolved pellet obtained by centrifugation for 10 minutes at $200,000 \times g$ and containing very long strands. The purified enzyme (0.05 mg protein/ml) was incubated with a variety of metal cations: Mn^{2+} , Mg^{2+} , Co^{2+} , Ca^{2+} , Ba^{2+} and Zn^{2+} at a final concentration of 10 mM. Electron micrographs taken after either 5 minutes or 17 hours of incubation show no significant differences. In general it can be stated that no totally uniform effects are found, and that the effects seen under these different conditions might not

Table 5.2 Effects of the addition of divalent metal ions to the purified enzyme protein. The enzyme was suspended in 50 mM Tris-HCl pH 7.6. Further experimental conditions as described in Materials and Methods (Chapter 2).

10 mM	big bundles	structure 1	structure 2	structure 3	structure 4
Mn ²⁺	++	+	+	+	+
Mg ²⁺	++	+	+	+	+
Co ²⁺	++	+	+	+	+
Ca ²⁺	+	+	+	+	+
Ba ²⁺	+	+	+	+	+
Zn ²⁺	+	-	-	-	-

represent quantitatively the effects occurring. In the preparation technique used very big aggregates of threads can easily be rinsed off so that the amount of highly polymerized protein is underestimated.

Addition of Me²⁺ to the purified enzyme in general resulted in the formation of big bundles (Fig. 5.6). However, in these preparations also a lot of substructures are observed like rods, striped rectangles, rings, rozette-like structures and rings that are filled up (Fig. 5.3, structure 1, 2, 3, 4 and 5, respectively). The metal-induced effects are summarized in Table 5.2. The big aggregates formed under the influence of metal ions are of various kinds. A three-dimensional aggregation can be observed into ill defined big bundles (Fig. 5.6). In addition to this kind of aggregates a more regular arrangement is also found, in which the threads are arranged alongside one another and the oblique striping continues over several of them (Fig. 5.7). The latter arrangement contrasts with the microcrystalline structures found in the presence of 33% saturation of ammonium sulphate (Fig. 5.4), where a perpendicular striping in the stacked-disk structures is observed. The large structures remain when excess Me²⁺ is removed by dialysis.

The metal-induced effects as seen with purified enzyme are also observed with a less purified fraction. If protein obtained after step 4 of the new purification method (Chapter 3) is dialyzed against 50 mM Tris-HCl pH 7.6 containing 1 mM Mn²⁺ a greenish-yellow precipitate is obtained. Electron micrographs of this sediment showed the same kind of big aggregates as observed upon the incubation of pure enzyme with Me²⁺ (Fig. 5.6). Attempts to determine sedimentation coefficients for the metal-induced aggregates failed because all of the enzyme is

precipitated at 10,000 r.p.m. before measurements could be made. Phase contrast micrographs of Mn^{2+} and Co^{2+} aggregates showed small needle-like structures (Fig. 5.8).

5.2.7 *The effect of the thiol-reducing agents β -mercaptoethanol, reduced lipoamide and dithiothreitol*

β -Mercaptoethanol has a drastic effect on purified transhydrogenase. When 1.0 M β -mercaptoethanol is added to the enzyme (20 μ g/ml) the long strands are almost completely dissociated into smaller structures (Fig. 5.9). Dissociation starts already at a concentration of 10 mM β -mercaptoethanol, but here still long thread-like structures are present. The smaller structures as obtained by β -mercaptoethanol treatment are mainly circular fragments with a diameter of about 13 nm, but unfortunately their definition is poor (Fig. 5.9). Similar though less extensive effects are caused by either 0.1 M dithiothreitol or 0.1 M reduced lipoamide. The dissociating effect of β -mercaptoethanol was confirmed by sedimentation studies in the analytical ultracentrifuge which showed that the population of molecules becomes more homogeneous. The slowest sedimenting material in the untreated sample has a sedimentation coefficient of 50.0 S while the sample treated with β -mercaptoethanol shows a sedimentation coefficient of 39.8 S (Chapter 3).

5.2.8 *Some other structures*

The distinctive structures as already described by Middleditch et al. (1972) which look like a rigid pairwise arrangement of rods (about 10 nm apart), and are devoid of any catalytic activity, are also present in our preparations in low frequency (Fig. 5.10). These structures resemble the double helical rods and kinked tubes as described by Durham et al. (1972) in some preparations of tobacco mosaic virus protein.

Structures somewhat resembling the ladder-like structures as described by Van den Broek et al. (1971) were also present in some of the preparations in low frequency (Fig. 5.11). These preparations were freed of enzyme bound $NADP^+$ by anaerobic dialysis in the presence of glucose-6-phosphate and glucose-6-phosphate dehydrogenase. The ladder-like structures might represent an aspecific association of transhydrogenase with glucose-6-phosphate dehydrogenase or with some kind of impurity. It reflects, however, the ease of association of the transhydrogenase protein with other components.

5.3 DISCUSSION

The relation between the different polymeric structures and the catalytic activity of transhydrogenase is still not very clear. Preparations of purified *Azotobacter* enzyme with clearly different values for the sedimentation coefficient of the protein, as obtained by pH treatment, exhibit equal specific activity when measured under standard assay conditions (Middleditch et al., 1972). The S-value at pH 6.8 is 33.5 S for the long strands and a value of 7.4 S has been reported for the dissociation products of the enzyme at pH 9.0. However, at pH 9.0 still threads are present (Middleditch et al., 1972). Louie et al. (1972) on the other hand postulated an important role for the association-dissociation phenomenon obtained under the influence of 2'-AMP with *Pseudomonas* transhydrogenase. Highly purified transhydrogenase (119 S) dissociated in the presence of 2'-AMP into regular structures of about 30 S. At the same time the reaction of $\text{NADH} + \text{SNAD}^+ \rightarrow \text{NAD}^+ + \text{S-NADH}$ was strongly enhanced by this dissociation. It should, however, be noted that there is evidently a poor correlation between ultracentrifuge- and electron microscopic data. The long strands as obtained by Middleditch et al. (1972) have a diameter of 7 nm and are 30-800 nm in length; the structures of Louie et al. (1972) have a diameter of 8-10 nm and a length of 50-500 nm. These very comparable structures nevertheless show quite distinct sedimentation coefficients, 33.5 S (Middleditch et al., 1972) versus 110 S (Louie et al., 1972). The same discrepancy holds for the dissociation products after pH treatment (Middleditch et al., 1972) or 2'-AMP treatment (Louie et al., 1972). However, at the rotor speed (52,000 rpm) used by Middleditch et al. (1972) the largest structures probably have already precipitated before the maximum speed was reached and measurements are made. The data of Louie et al. (1972) are surprising in view of the fact that a non-homogeneous population of threads as observed in the electron microscope does give only a single sedimenting species, independent of the method used i.e. either the overlay technique or scanning for flavin absorbance at 440nm. With the overlay technique in non-homogeneous populations the fastest sedimenting active molecule will be measured, whereas in the scanning technique the moving boundary represents the slowest sedimenting material.

In contrast with the *Pseudomonas* enzyme the *Azotobacter* enzyme does not require 2'-AMP as an activator for the oxidation of NADH. The maximum rate of NADH oxidation, however, is always lower than the corresponding NADPH oxidation (Van den Broek et al., 1971). In studying the structures present in crude prepara-

tions i.e. cell-free extracts, practically no very large (up to 1000 nm) trans-hydrogenase structures were found. In cell-free extracts the reaction $\text{NADH} + \text{NADP}^+ \rightarrow \text{NAD}^+ + \text{NADPH}$ proceeds with a lag (Van den Broek et al, 1971; this thesis) and this lag could be due to a slow conversion of inactive (dissociated) enzyme into active (associated) enzyme. NADPH formed during this reaction strongly enhances the reaction rate (Van den Broek et al., 1971), thus suggesting an important role for the associated form in the reaction $\text{NADH} + \text{NADP}^+ \rightarrow \text{NADPH} + \text{NAD}^+$. Although such a postulate is supported by the electron microscopic patterns, it is nevertheless more likely that the stimulating effect of NADPH is caused by the counteracting effect of this nucleotide upon the strong inhibition by NADP^+ (Van den Broek et al., 1971). It is noteworthy that the dissociating effect of NADP^+ never results in a stimulation of the reaction of $\text{NADH} + \text{S-NAD}^+ \rightarrow \text{NAD}^+ + \text{S-NADH}$ (Van den Broek et al., 1971). No definite conclusions can be made on the effects of NADP^+ and (or) NADPH as the kinetic and (or) morphological effects cannot be separated in these experiments. Thus the role of 2'-AMP also remains obscure. Since it can, in part, act as a substrate analogue it is difficult to discriminate between a kinetic effect (i.e. reversal of NADP^+ inhibition) and a morphological effect. In order to prove a definite role on the catalytic activity, the dissociation must be brought about by agents which have no structural analogy with the substrates. Incubation of the enzyme in 1.0 M or 0.1 M β -mercaptoethanol leads to dissociation but subsequent determination of the catalytic activity under standard assay conditions did not reveal any influence on the initial rate of the reactions $\text{NADH} + \text{S-NAD}^+ \rightarrow \text{S-NADH} + \text{NAD}^+$ or $\text{NADPH} + \text{S-NAD}^+ \rightarrow \text{NADP}^+ + \text{S-NADH}$. It could be argued that reaggregation occurs during the assay of the catalytic activity. This is very unlikely since reassociation must be complete within 20-30 seconds at a protein concentration of 0.20 $\mu\text{g/ml}$. As metal ions do not have a uniform effect on the morphological structure it is not possible to relate directly specific morphological changes to the effects on the catalytic activity (Chapter 3). It is also possible that for instance Mn^{2+} reverses the strong NADP^+ inhibition in the reaction of $\text{NADH} + \text{NADP}^+ \rightarrow \text{NADPH} + \text{NAD}^+$ (Chapter 3). The action of Mn^{2+} might be a chelation of the secondary phosphate group present in NADP^+ as described by Colman et al. (1972). However, a direct influence of the metals on the conformation of the protein cannot be excluded as discussed in Chapter 3.

A survey of the different smaller structures found (Table 5.2) reveals some interesting features. It must be noted that not only association-dissociation

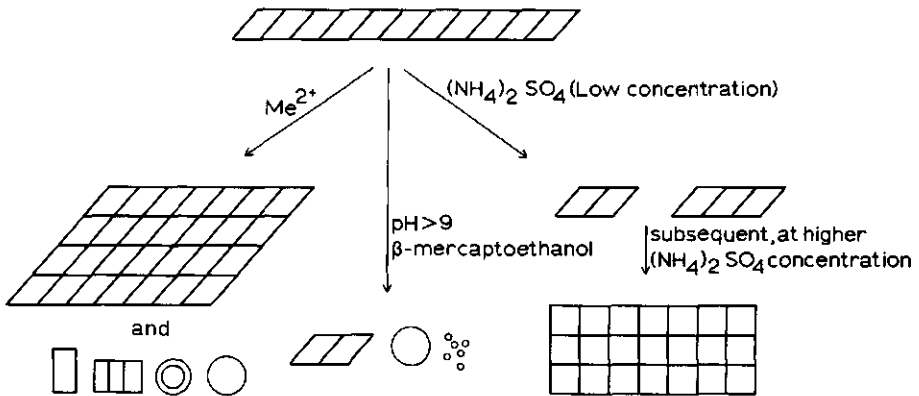


Fig. 5.13 Diagram of some of the different structures obtained from the long helical strand under different conditions. The structures drawn are only rough representations of the real structures and the magnitude of the different structures is not proportional to the real dimensions.

is observed but also distinct conformational changes. Thus, the perpendicular striping in the rectangles (Fig. 5.3, structure 2) strongly contrasts the oblique striping in the threads. The circular- or rosette-like structures observed (Fig. 5.3, structures 4 and 5) have quite different diameters and probably represent different aggregates of still smaller subunits of transhydrogenase. The ring-like fragments (Fig. 5.3, structure 3) might represent a projection of the striped rectangle as the diameters do agree fairly well (12 nm).

Dissociation at the end of a thread is occasionally observed (Fig. 5.12). The small segments dissociating from the threads look like small rods (or a parallelogram) of about (16-20 nm) - (6-7 nm). They can be accommodated into the spiral structure by placing them together under an angle of about $50-60^\circ$. In the presence of Ca^{2+} , Ba^{2+} and Mg^{2+} these structures are more frequently observed than in the presence of Co^{2+} or Mn^{2+} . Another projection of these structures can be a circular fragment with a diameter of 18 nm (Fig. 5.3, structure 4).

The metal-induced two-dimensional aggregation (Fig. 5.7) clearly shows that new binding sites for intermolecular aggregation are formed. As the oblique striping continues over several threads it is clear that the induced binding sites are formed at distinct places of the enzyme molecule thus allowing a regular

aggregation.

The different effects can be summarized as follows (Fig. 5.13).

It is interesting to note that the metal induced effects on the transhydrogenase molecules show some resemblance to the effect observed with the enzyme glutamine synthetase from *E. coli* (Valentine et al., 1968). Rapid addition of 10 mM Mn^{2+} , Mg^{2+} and Co^{2+} to this enzyme, pretreated with EDTA, resulted in an aggregation into very big bundles. Recently a purification method involving the formation of paracrystalline structures of this enzyme under the influence of Zn^{2+} was described (Miller, 1974).

6. SPECTRAL PROPERTIES

6.1 INTRODUCTION

It was established by Cohen et al. (1970) for the *Pseudomonas* transhydrogenase and by Van den Broek et al. (1971) and Middleditch et al. (1972) for the *Azotobacter* transhydrogenase that the enzyme contains flavin (FAD) as a prosthetic group. Under anaerobic conditions the enzyme-bound FAD is reduced by addition of NADH, NADPH and dithionite, but this reduction was not complete when performed with NADH or NADPH (Cohen et al., 1970; Van den Broek et al., 1971). The reduction of the *Pseudomonas* enzyme by NADH is activated by 2'-AMP (Cohen et al., 1970), whereas the NADH reduction of the *Azotobacter* enzyme proceeds without further addition (Van den Broek et al., 1971). From their spectral studies Van den Broek et al. (1971) concluded that the enzyme was completely reduced by 4 electrons per mole of flavin. This pointed to the existence of an additional redox active group, probably a disulfide, as was also found for the lipoamide dehydrogenase (Massey and Veeger, 1961), glutathione reductase (Massey and Williams, 1965) and thioredoxin reductase (Zanetti and Williams, 1967). However, in the case of the transhydrogenase reduction no stable 2-equivalent reduced state could be detected (Van den Broek et al., 1971).

Fluorescence studies showed that the enzyme has an emission maximum around 510 nm. This maximum shifts to lower wavelength by the addition of NADP^+ (Van den Broek et al., 1971). Binding of NADP^+ to the oxidized enzyme was also demonstrated by effects on the absorption, optical rotatory dispersion and circular dichroism spectra. These interesting spectral properties are further investigated and special attention is paid to the binding of 2'-AMP and NADP^+ to the oxidized enzyme.

6.2 RESULTS AND DISCUSSION

6.2.1 Effect of NADP^+ and salt on the fluorescence characteristics

Oxidized transhydrogenase shows a pronounced flavin fluorescence with an emission peak at about 510 nm. Free FAD, under the same conditions, shows an emission maximum around 520 nm. The shift towards shorter emission wavelength

of the protein-bound flavin points to a rather apolar environment for the transhydrogenase flavin (Song, 1969). The quantum yield of the protein-bound flavin is about 25% of the FMN quantum yield at equal optical density of the maxima under identical conditions 50 mM Tris-HCl, pH 7.6). Thus in contrast to the *Pseudomonas* enzyme (Louie et al., 1972) the quantum yield is rather high for the *Azotobacter* enzyme (free FAD has about 10% of the FMN quantum yield at equal optical density of the maxima under identical conditions (Velick, 1961)). The tryptophan fluorescence emission maximum is also shifted towards shorter wavelengths in the protein (340 nm) compared to the free tryptophan (350 nm) (uncorrected values). When the oxidized enzyme is titrated with NADP^+ an interesting series of changes of the flavin fluorescence emission intensity

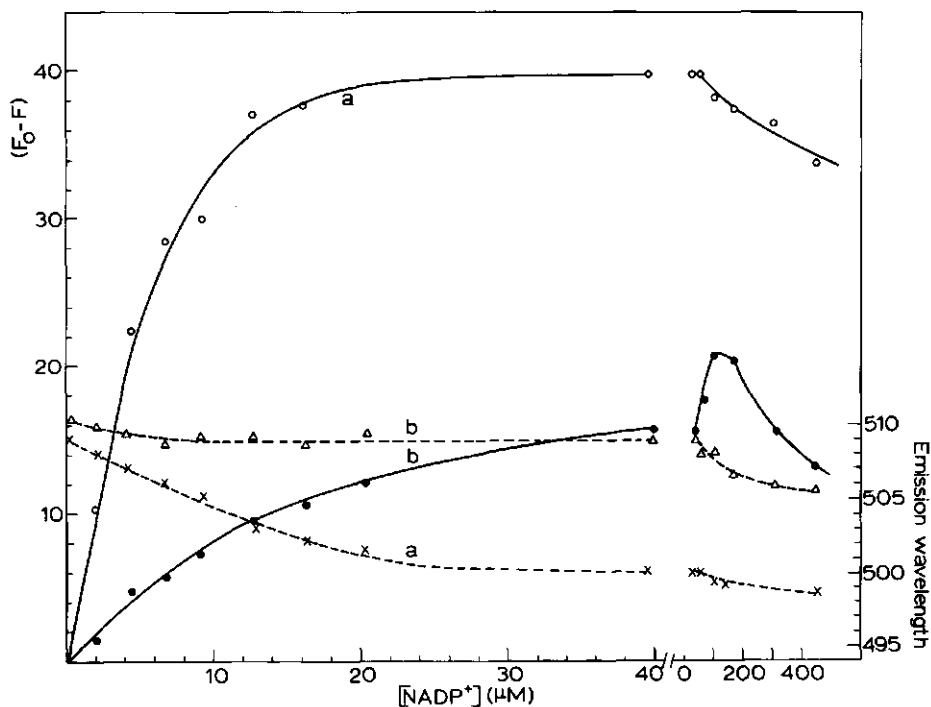


Fig. 6.1 Effect of NADP^+ on the flavin fluorescence of the oxidized transhydrogenase protein (10 μM) in 50 mM Tris-HCl pH 7.6. The fluorescence after the addition of phosphate (F_0) is taken as 100. Excitation wavelength 440 nm. Temp. 22°C.

- a. ○—○ quenching effect of NADP^+ in the presence of 10 mM potassium phosphate
 X—X shift of the fluorescence emission maximum
- b. ●—● quenching effect of NADP^+ in the absence of phosphate
 Δ—Δ shift of the fluorescence emission maximum

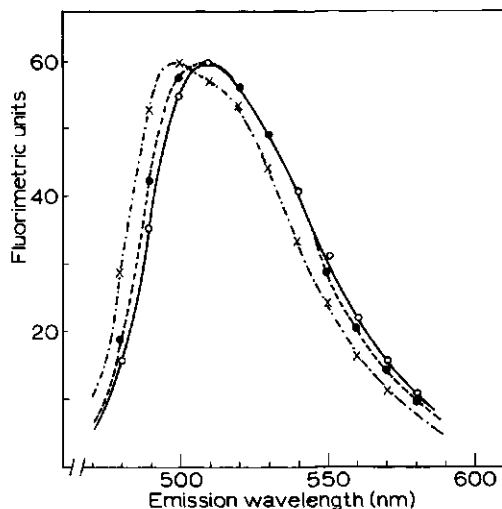


Fig. 6.2 Effect of NADP^+ in the absence and presence of phosphate on the shift of the flavin fluorescence emission maximum. The peaks are normalized to the same peak height. Excitation wavelength 440 nm. Temp. 22°C .

- enzyme in 50 mM Tris-HCl pH 7.6₊
- in the presence of 0.7 mM NADP^+
- X—·—X in the presence of 0.7 mM NADP^+ and 10 mM potassium phosphate

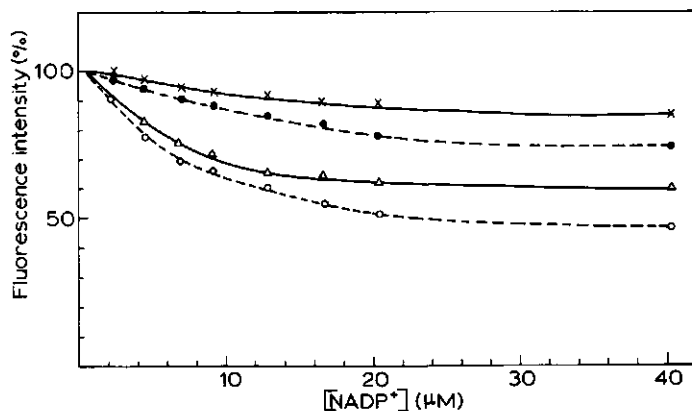


Fig. 6.3 Effect of NADP^+ in the presence and absence of phosphate on the transhydrogenase flavin fluorescence intensity at different excitation wavelengths. Emission at 510 nm. Temp. 22°C .

- X—X in the absence of phosphate excitation 440 nm
 - in the absence of phosphate excitation 295 nm
 - Δ—Δ in the presence of 10 mM potassium phosphate excitation 440 nm
 - in the presence of 10 mM potassium phosphate excitation 295 nm.
- The enzyme was dissolved in 50 mM Tris-HCl pH 7.6.

can be observed. (It must, however, be noticed that the enzyme must be freshly prepared because upon prolonged standing at 4°C the binding characteristics change with little change in specific activity).

In the presence of phosphate 10 mM (Fig. 6.1a) a maximal quenching of about 40% is observed upon the titration with NADP⁺ (starting emission intensity in the presence of phosphate taken as 100%) in accordance with the results of Van den Broek et al. (1971). However, only 20% decrease is observed upon titration with NADP⁺ in the absence of phosphate (Fig. 6.1b). At concentrations of NADP⁺ far exceeding a 1 : 1 stoichiometry a subsequent increase in the fluorescence emission intensity is found (Fig. 6.1a).

Upon titration with NADP⁺ not only a decrease and subsequent increase in fluorescence intensity is found but also a concomitant shift of the emission maximum towards shorter wavelengths. It must be noted that in the absence of phosphate the emission (511 nm) maximum is slightly shifted towards the red compared with the maximum in the presence of phosphate (509 nm).

In the presence of phosphate the shift of the emission maximum is more pronounced than in the absence, but the position of the maximum continues to shift at high NADP⁺ concentrations. The shape of the fluorescence emission peak in the presence of 10 mM phosphate and 0.7 mM NADP⁺ differs from that in the presence of 0.7 mM NADP⁺ alone. In the first case an inhomogeneous emission peak is observed with a maximum at 498 nm and a shoulder around 515 nm while in the absence of phosphate the emission peak is centered around 508 nm and no shoulder is visible (Fig. 6.2).

Fluorescence lifetime studies in the presence of phosphate and NADP⁺ with either a cut off filter (in the emission light path) of 495 nm or 530 nm did not show a significant difference between the values measured. If the inhomogeneous emission peak would be composed of two different flavins a difference in lifetime could be expected. It therefore seems reasonable at the moment to accept that the newly formed species has different emission characteristics than the original species.

The protein fluorescence as found upon excitation at 295 nm and at the emission peak at 340 nm remains virtually unaltered upon the addition of NADP⁺. The protein-sensitized flavin fluorescence (295 nm excitation), however, decreases somewhat more than that excited directly at 440 nm (Fig. 6.3). This effect, which is not due to optical inner filter effects since free FAD fluorescence upon excitation at 295 nm is unaltered over this concentration range of NADP⁺, probably reflects a change in energy transfer from tryptophan towards the

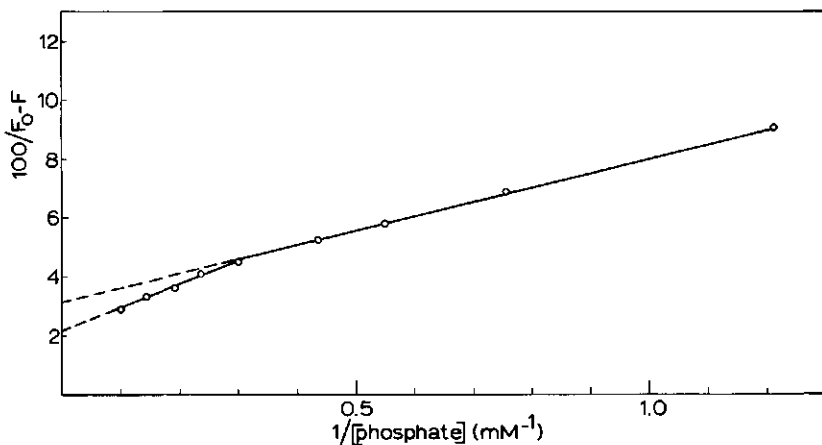


Fig. 6.4 Quenching effect of phosphate on the transhydrogenase flavin fluorescence. Excitation wavelength 440 nm, emission wavelength 510 nm. The enzyme was dissolved in 50 mM Tris-HCl pH 7.6. Temp. 22°C.

flavin (see also 6.2.4).

From Fig. 6.1 (a, b) it can be calculated that the K_D for the first molecule NADP^+ bound is about 0.4 μM in the presence of phosphate whereas in the absence a much higher dissociation constant is found, $K_D = 7.5 \mu\text{M}$. From the effect induced by the high concentrations of NADP^+ (Fig. 6.1b) K_D can be calculated to be larger than 200 μM . These values are in accordance with the results of Van den Broek et al. (1971). These authors reported a value of 2-5 μM for the first molecule of NADP^+ bound (in 0.1 M phosphate buffer, pH 7.5), but the actual value as can be derived from their results is an order of magnitude lower. The addition of phosphate and sulphate to the oxidized enzyme also results in a decrease in the fluorescence emission intensity (30-45%) as is shown in Fig. 6.4. The value of the dissociation constant of phosphate, 2-8 mM, and the magnitude of its quenching effect (30-45%), however, varies somewhat. Often a biphasic titration showing two phosphate binding sites (Fig. 6.4) is found. Saturation of the high affinity site ($K_D \approx 2 \text{ mM}$) leads to a quenching of 30%, while saturation of the low affinity site ($K_D \approx 5-8 \text{ mM}$) gives a total quenching of about 40-45%.

The flavin fluorescence quenching is the same when either 440 nm or 295 nm is used as excitation wavelength (see also section 6.2.6). The values of the dissociation constants (phosphate 2-8, sulphate 7 mM) are in the same order of magnitude as the kinetic inhibition constants (Chapter 3) obtained for the

competition with NADH binding. Nitrate has only a very small negligible quenching effect on the protein-bound flavin fluorescence. No clear shift of the emission maximum is observed upon the addition of either of these salts.

It thus can be concluded that the quenching effect of salt has a rather specific character and probably reflects the neutralization of a positive charge on the protein. The effect that NADP^+ is more tightly bound to the enzyme in the presence of phosphate indicates that a positive charge is close to the binding site of NADP^+ and especially near the nicotinamide ring of the nucleotide.

It is of interest to relate these observations to those of the lag found in the reaction of $\text{NADH} + \text{NADP}^+ \rightleftharpoons \text{NAD}^+ + \text{NADPH}$. The decline in lag after dilution takes several hours, total disappearance needs dialysis (Chapter 3).

After addition of phosphate to the enzyme in Tris-HCl, it takes 10-15 sec. before the fluorescence quenches to a constant level. In view of the observed K_D 2 mM the slow process of phosphate dissociation after dilution is explicable.

Lifetime measurements revealed that 10 mM phosphate hardly influences the lifetime of the enzyme-bound FAD fluorescence. Subsequent addition of NADP^+ clearly decreases the lifetime to a constant level (Table 6.1).

A similar pattern is observed after addition of 1 mM NADP^+ to enzyme in Tris-HCl. Again no significant change in lifetime is observed, but after addition of 10 mM phosphate again an instantaneous decrease in lifetime is observed.

Table 6.1 Fluorescence lifetime of the transhydrogenase bound flavin. Transhydrogenase (5 μM) was dissolved in 50 mM Tris-HCl pH 7.6. Excitation wavelength 440 nm, emission filter Scott-Jena OG 530, temp. 22°C.

Addition	lifetime τ in nsec
none	2.26
10 mM P_i	2.10
" + 1.1 μM NADP^+	2.08
" + 3.8 "	1.89
" + 7.6 "	1.87
" + 50 "	1.59
" + 130 "	1.61
" + 740 "	1.62

Upon observing a decrease in fluorescence intensity one can expect that the lifetime of the excited state becomes lower. In case of the formation of a so-called dark-complex between oxidized enzyme and NADP^+ or anorganic phosphate no decrease in lifetime has to be found.

The combination of NADP^+ plus phosphate results in a clear decrease in lifetime accompanied by a decrease in the fluorescence intensity. In this case the decrease in lifetime is due to a dynamic quenching of the fluorescence by a group within the protein that becomes mobile during the addition of NADP^+ or to changes in polarity around the flavin moiety. The latter view is supported by the fact that the emission characteristics of the newly formed species are quite distinct from the original fluorescence characteristics and the change in shape of the fluorescence emission peak. It is also noteworthy that the fluorescence lifetime of the enzymebound flavin (2.26 nsec) does not differ very much from that of free FAD in aqueous solution (about 2.0 nsec). This is very surprising in view of the fact that the enzymebound flavin has a much higher fluorescence yield than the free nucleotide since this would imply a more open form of the enzyme-bound FAD and thus a longer lifetime. This discrepancy can, however, be explained by the fact that substitution at the 7, 8 or 9 position of the nucleus in model flavin compounds drastically changes the fluorescence lifetime (Visser et al, to be published). In transhydrogenase interactions of the protein with the flavin at one of these positions could result in a drastic change in fluorescence lifetime without affecting the fluorescence yield that much. An alternative possibility is that the protein-bound FAD is in a totally unfolded form. In that case the system can be considered identical in fluorescence characteristics as FMN ($\tau \approx 4$ nsec). Taking into consideration a lower quantum yield with respect to FMN in solution, the shorter lifetime of the protein-bound chromophore is easily explained.

Furthermore, these studies do not rule out the possibility that the enzyme contains nonhomogeneous flavin binding sites with a different lifetime as proposed for the pig heart lipoamide dehydrogenase (Visser et al., 1974). This can also result in an average lifetime close to the value of the free flavin. An indication for this possibility could be found in the presence of more than one phosphate binding site. However, the technique used in this study does not allow analysis and discrimination between non-identical sites and multiple lifetimes.

Louie et al. (1972) reported a twofold increase in the fluorescence emission intensity of the *Pseudomonas* enzyme upon the addition of 1 mM NADP^+ totally

contrasting the results of Van den Broek (1971), where a decline was observed. It can be demonstrated that this increase is, however, only observed in the case that the fluorescence emission of the oxidized enzyme is first strongly quenched by the addition of phosphate plus β -mercaptoethanol. It is found that β -mercaptoethanol quenches the emission of the protein-bound flavin to about 40%. No shift of the flavin emission is observed (Fig. 6.5). A quenching effect of β -mercaptoethanol is also found on a free flavin (FMN). Surprisingly the enzyme-flavin fluorescence is quenched somewhat more than the free flavin emission presumably due to binding of the β -mercaptoethanol to the enzyme. With the free flavin a straight Stern-Volmer plot (1919) is obtained, indicating pure dynamic quenching of the free flavin fluorescence, this in contrast with the quenching of the enzyme-flavin emission. The view that binding of β -mercaptoethanol to the enzyme is mainly responsible for quenching of the enzyme-flavin emission comes from a straight Benesi-Hildebrand plot (1949) from which $K_D = 17$ mM can be calculated.

If to the enzyme in 50 mM Tris-HCl pH 7.6 containing 0.14 M β -mercaptoethanol and 10 mM potassium phosphate NADP^+ is added (10 μM - 1 mM) an increase in fluorescence intensity is observed together with a shift of the emission maximum towards shorter wavelengths (see also 6.2.2).

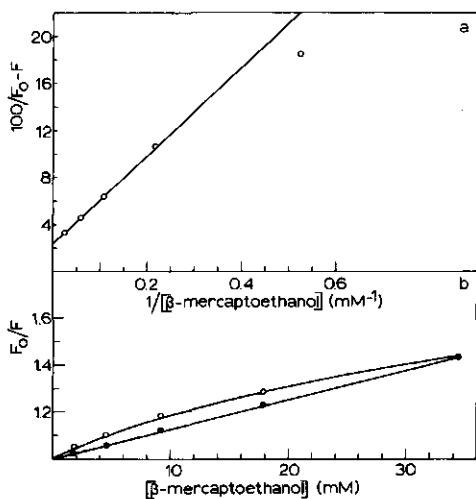


Fig. 6.5 Quenching effect of β -mercaptoethanol on the transhydrogenase flavin fluorescence and on FMN. Transhydrogenase and FMN were dissolved in 50 mM Tris-HCl pH 7.6. Excitation wavelength 440 nm, emission 510 nm. Temp. 22°C.

- a. $1/(F_0 - F)$ vs. $1/[\beta\text{-mercaptoethanol}]$, transhydrogenase flavin fluorescence quenching
- b. F_0/F vs. $[\beta\text{-mercaptoethanol}]$
- transhydrogenase flavin fluorescence quenching
- FMN fluorescence quenching

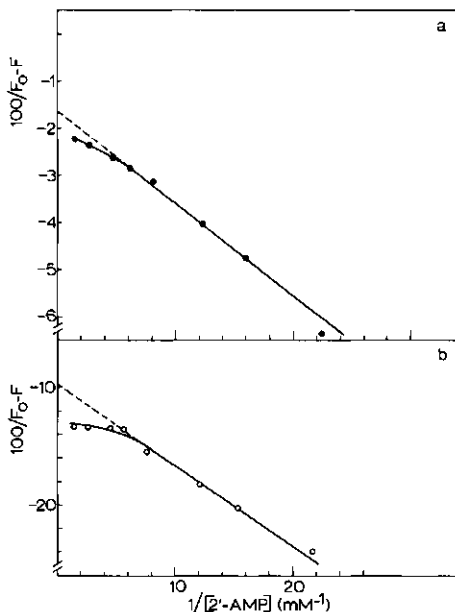


Fig. 6.6 Effect of the 2'-AMP on the transhydrogenase flavin fluorescence in presence of different phosphate concentrations. The enzyme was dissolved in 50 mM Tris-HCl pH 7.6. Excitation wavelength 440 nm, emission wavelength 510 nm. Temp. 22°C.

a. $1/(F_0 - F)$ vs. $1/[2'-AMP]$, in the presence of 15 mM potassium phosphate

b. $1/(F_0 - F)$ vs. $1/[2'-AMP]$, in the presence of 1.7 mM potassium phosphate.

In both cases the fluorescence intensity after the addition of phosphate was taken as 100. The fluorescence intensity before the titration was 160 for (a) and 113 for (b) respectively.

6.2.2 Effect of 2'-AMP on the flavin fluorescence

The addition of 1 mM 2'-AMP to the oxidized *Pseudomonas* enzyme results in a 3-4 fold enhancement of the flavin fluorescence and a distinct increase in the degree of fluorescence polarization. Van den Broek et al. (1971) reported that 2'-AMP has no effect on the spectral properties of the *Azotobacter* enzyme. As will be reported here, the effect of 2'-AMP strongly depends, however, on the experimental conditions. When 2'-AMP is added to the enzyme in the presence of phosphate an increase in the flavin fluorescence is observed; no shift of the flavin emission peak is found. No effect of 2'-AMP is observed in the absence of phosphate in agreement with Van den Broek et al. (1971). Extrapolation of the linear part of a Benesi-Hildebrand plot (1949) relating $1/F_0 - F$ vs $1/[2'-AMP]$ suggests that the initial quenching effect of phosphate could be completely reversed at infinite 2'-AMP concentration (Fig. 6.6). At high concentrations of 2'-AMP deviation from linearity is observed, but total reversal of the phosphate induced fluorescence quenching is not obtained by addition of 2'-AMP. The kinetic data show that the phosphate induced inhibition of the reaction $NADH + S-NAD^+ \rightarrow S-NADH + NAD^+$ in fact is also only partially reversed by the addition of 2'-AMP (Chapter 3). Assuming a competitive binding between phosphate and 2'-AMP it can be calculated (see appendix) that the K_D for 2'-AMP in the

linear part of the curve is about 12 μM in the presence of 15 mM phosphate and about 50 μM in the presence of 1.7 mM phosphate. These results indicate that 2'-AMP binding is promoted by phosphate. Addition of 2'-AMP to a mixture containing enzyme in 50 mM Tris-HCl pH 7.6, 0.14 M β -mercaptoethanol, 10 mM phosphate results in an increase of the fluorescence intensity. However, in the presence of NADP^+ , the fluorescence emission intensity does not increase as much as in the absence of NADP^+ (Table 6.2).

The effect of binding 2'-AMP to the oxidized enzyme differs from the binding of NADP^+ in several respects. Firstly, in the absence of phosphate no effect of 2'-AMP indicating binding is observed, while binding of NADP^+ induces a clear effect. The fact that no influence of 2'-AMP on the flavin fluorescence in the absence of phosphate is found does, however, not completely exclude the possibility that this compound is bound. It is, however, unlikely in view of the absence of any effect on this easily affectable system.

Secondly, 2'-AMP causes in the presence of phosphate an increase in the flavin fluorescence while NADP^+ causes a decrease and subsequently an increase. In the presence of phosphate and β -mercaptoethanol both induce a clear increase in the fluorescence. Thus binding of β -mercaptoethanol clearly induces a different conformation around the active centre of the protein.

Thirdly, NADP^+ causes a shift of the emission maximum while 2'-AMP does not. From the difference in effects induced it can be concluded that in spite of the

Table 6.2 Effect of 2'-AMP on the transhydrogenase flavin fluorescence in the presence of NADP^+ . The enzyme (20 μM) was dissolved in 50 mM Tris-HCl pH 7.6 containing 0.14 M β -mercaptoethanol and 10 mM potassium phosphate. Excitation wavelength 440 nm, emission wavelength 510 nm, temp. 22°C.

Species	Relative fluorescence intensity (%)	Relative fluorescence intensity at infinite [2'-AMP] (%)
1 Enzyme in Tris-buffer containing P_i and β -mercaptoethanol	100	182
2 I + 1 mM NADP^+	154	154
3 I + 100 μM NADP^+	130	152
4 I + 10 μM NADP^+	110	156

partial structural analogy between 2'-AMP and NADP^+ quite distinct spectral intermediates are formed upon binding of either of these compounds. These differences must be centered as can be concluded from kinetic studies, around the binding center of the donor since phosphate is a competitive inhibitor towards the donor. At this place NADP^+ presumably exerts its inhibitory action; NADP^+ inhibits competitively towards NADH (Cohen et al., 1970), non-competitively according to Van den Broek et al. (1971).

Furthermore, the promotion of the binding of NADP^+ by phosphate indicates that this effect is due to neutralization of a repelling positive charge, probably followed by an increased attraction between the positive nicotinamide group of NADP^+ and the partially negative phosphate ions. Binding of 2'-AMP occurs presumably at the same positive charge as binding of phosphate but with increased affinity by the presence of the adenine ribose parts of the molecule. Since 2'-AMP does not influence the fluorescence emission it is reasonable to conclude that the nicotinamide ring of NADP^+ must be close to the FAD inducing either changes in conformation of the protein or polarity changes around the flavin. Another indication that 2'-AMP binds around the donor site but not at the NADP^+ site is found from the kinetic picture as in the absence of phosphate the initial velocity is the same in the presence and absence of 2'-AMP. The effect of NADP^+ on the polymerization of the enzyme also contrasts the effect of 2'-AMP (Chapter 5).

The results of Table 6.2 indicate that 2'-AMP is not able to remove both NADP^+ molecules which can be bound to the enzyme, thus explaining the partially quenched fluorescence in the presence of NADP^+ with respect to the results in its absence. The same is true for the phosphate binding: fluorescence quenching is never completely abolished by 2'-AMP. Although one could conclude (from Fig. 6.6) that more than one 2'-AMP site is present on the enzyme such a conclusion misses justification. At least one could expect that in the absence of phosphate quenching by 2'-AMP is observed which is not the case. The small but consistent quenching of the fluorescence is undoubtedly depending on the presence of phosphate.

6.2.3. *Effect of anorganic phosphate and 2'-AMP on the absorption spectrum of the oxidized enzyme*

As already mentioned in 6.2.2 2'-AMP binds to the oxidized enzyme in the presence of phosphate inducing a change in the fluorescence emission intensity. It, therefore, can be expected that also changes in the absorption spectrum occur.

Furthermore, since phosphate quenches the flavin fluorescence, it was of interest to investigate also the influence of phosphate on the absorption spectrum, especially since the spectral studies reported by Van den Broek et al. (1971) were carried out in the presence of 0.1 M phosphate.

The spectrum of the enzyme in Tris-HCl differs considerably from the one in phosphate (see Table 6.3).

Table 6.3 Survey of the spectral characteristics observed with fluorescence and absorption studies. The enzyme (E) is dissolved in 50 mM Tris-HCl pH 7.6. Temp. 22°C.

Fluorescence:

Species	% fluorescence yield	K_D
E_{ox}	100	
$E_{ox} + P_i \rightarrow E_{ox} - P_i$	60-70	3-8 mM
$E_{ox} + NADP^+ \rightarrow E_{ox} - NADP^+$	80	7 μ M
$E_{ox} - P_i + NADP^+ \rightarrow E_{ox} - P_i - NADP^+$	about 30	0.4 μ M
$E_{ox} - P_i + 2'-AMP \rightarrow E_{ox} - 2'-AMP$	approaches 100	dependent
$E_{ox} + 2'-AMP \rightarrow E_{ox} - 2'-AMP$	remains 100	on the P_i concentration
$E_{ox} + \beta\text{-mercapto-ethanol} \rightarrow E_{ox} - \beta\text{-mercapto-ethanol}$	60	17 mM

Absorbance:

Species	Spectral characteristics in the different spectra		
	Positive maxima (nm)	Negative maxima (nm)	Isosbestic points (nm)
$E_{ox} - P_i + NADP^+ \rightarrow E_{ox} - P_i - NADP^+$	464,434 412	483,453 383	469,460 448,398
$E_{ox} + P_i \rightarrow E_{ox} - P_i$	464,434 412	483,453 383	469,460 448,398
$E_{ox} - P_i + 2'-AMP \rightarrow E_{ox} - 2'-AMP$	483,453 383	464,434 412	469,460 448,398

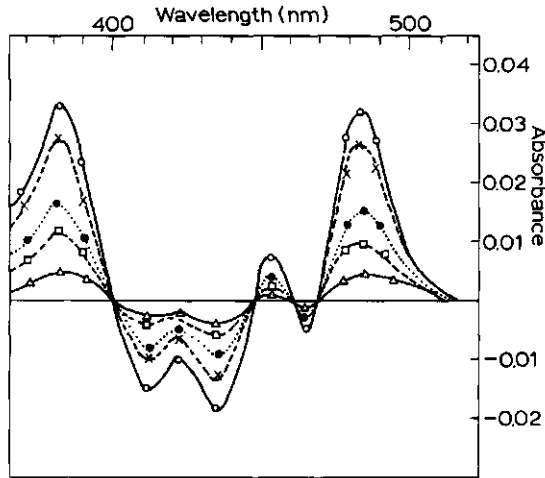


Fig. 6.7 Spectral titration of oxidized *Azotobacter* transhydrogenase with 2'-AMP in the presence of 10 mM potassium phosphate. Enzyme (36 μM) was dissolved in 50 mM Tris-HCL pH 7.6. Experiments were carried out in tandem cells as described in Chapter 2 and difference spectra were recorded after mixing. 2'-AMP additions are:

Δ — Δ 35 μM ; \square — \square 69 μM ; \bullet — \bullet 102 μM ; X—X 268 μM ; \circ — \circ 1.08 mM.

Addition of phosphate gives rise to a difference spectrum of the same pattern as found upon addition of NADP^+ to the oxidized enzyme in phosphate as published by Van den Broek et al. (1971). The difference spectrum shows isosbestic points at 469, 460, 448 and 398 nm. Positive maxima are observed at 412, 434 and 464 nm, negative maxima at 483, 453 and 383 nm. The height of the peaks especially at lower wavelengths is, however, obscured by a secondary effect of phosphate binding namely a change in scatter of the protein solution.

Addition of 2'-AMP to the enzyme in the presence of phosphate results in a difference spectrum (Fig. 6.7) that can be regarded as a mirror image of the difference spectrum obtained by phosphate addition, while no effect of 2'-AMP is found in the absence of phosphate. The isosbestic points remain unchanged but the positive peaks turn into negative peaks and the negative into positive peaks. This again indicates that a reversal of the phosphate induced spectral shift occurs by the addition of 2'-AMP and thus phosphate binding to the enzyme. It is difficult to calculate a dissociation constant for the binding of 2'-AMP in analogy of the fluorescence experiments as the calculation of the K_D and maximum change by phosphate binding are obscured by scatter effects. Similarly

it is difficult to state whether the phosphate induced effect is totally reversed by 2'-AMP. In this respect it is important to note that most of the kinetic studies of Cohen et al. (1970) on the *Pseudomonas* enzyme are performed in the presence of phosphate. Thus a 2'-AMP effect can indeed be expected under these experimental conditions.

No evidence is yet available that 2'-AMP is able to reverse the spectral shifts induced by NADP^+ . Such a reversal could be expected if the primary site of attack of 2'-AMP is the phosphate binding site. The affinity of NADP^+ is strongly dependent on the presence of phosphate. Thus removal of phosphate would lead to a diminished NADP^+ binding and reversal of the spectral and fluorescence shifts. Since this is not the case one could conclude that strong mutual cooperative binding effects occur between NADP^+ and phosphate. The drastic change in fluorescence lifetime induced by the presence of both NADP^+ and phosphate also supports this view. On the other hand, since according to the fluorimetric study 2'-AMP is able to remove but one of the two phosphates, it cannot be excluded that the phosphate which remains bound to the enzyme is the one that is responsible for the tight NADP^+ binding.

6.2.4 Excitation spectra of the oxidized transhydrogenase

At a constant emission wavelength of 510 nm excitation spectra of the oxidized enzyme were taken and compared with the excitation spectrum of free FAD (Fig. 6.8). A comparison at an excitation wavelength of 295 nm between FAD and transhydrogenase makes it clear that a pronounced energy transfer from tryptophan to the enzyme-bound flavin takes place. Scatter effects in the ultraviolet part of the absorption spectrum arising from the big polymers of transhydrogenase (see also Chapter 3) obscure a comparison between the excitation and absorption spectrum in this region. Since the excitation spectra of the enzyme and its complexes are higher than that of FAD and since it is known that effective energy transfer occurs in FAD it can be concluded that a very effective energy transfer takes place from the enzyme tryptophan towards the enzymebound flavin. This procedure is allowed when working at such protein concentrations that no inner filter effects occur. A comparison of the excitation spectra under different conditions makes it clear that addition of 10 mM phosphate has no effect on the energy transfer. Subsequent addition of either 40 μM or 400 μM NADP^+ results in a decrease of the energy transfer of about 30%. These spectra are consistent with the finding that the flavin emission obtained by excitation at 295 nm decreases more than upon excitation in the visible absorption band of

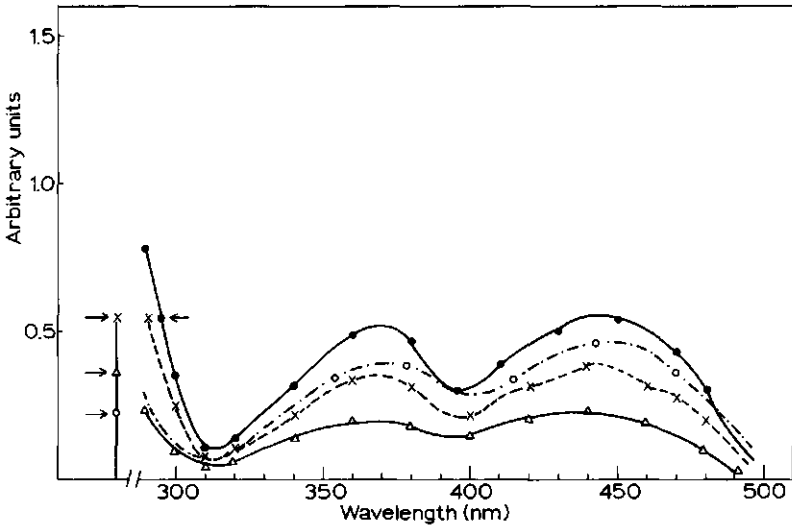


Fig. 6.8 Fluorescence excitation spectra of oxidized transhydrogenase of free FAD under different conditions. The spectra were calculated as described in Chapter 2. The enzyme and FAD were dissolved in 50 mM Tris-HCl pH 7.6. Temp. 22°C.

●—● oxidized transhydrogenase

○--○ FAD

X--X transhydrogenase plus 10 mM potassium phosphate

Δ—Δ transhydrogenase plus 10 mM potassium phosphate plus 40 μM NADP⁺

The arrows at the left side of the figure indicate the height of the spectrum at 295 nm if all spectra are normalized to the same height at 440 nm.

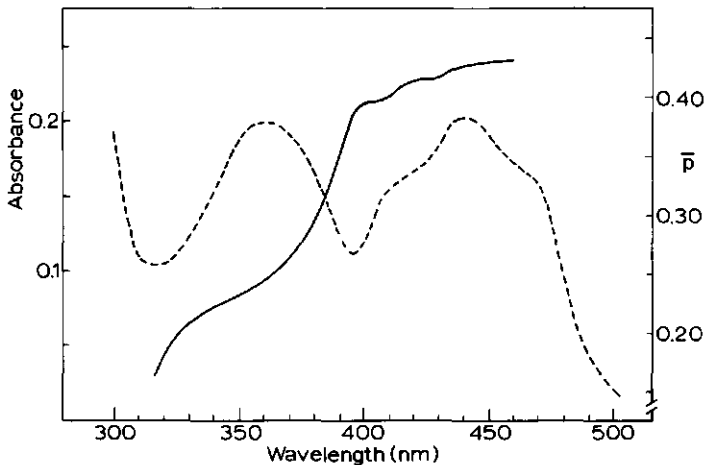


Fig. 6.9 Spectrum and flavin polarization spectrum of the oxidized transhydrogenase. The spectra were obtained as described in Chapter 2. The enzyme was dissolved in 50 mM Tris-HCl pH 7.6. Temp. 22°C.

---- absorption spectrum

— polarization spectrum

the flavin. These results also confirm the finding that quenching by phosphate does not give rise to a diminished energy transfer upon excitation at 295 nm and emission of 510 nm compared to the emission at 510 nm and 440 nm excitation.

6.2.5 Measurements of the degree of polarization

It was reported by Louie et al. (1972) that the degree of polarization of the oxidized enzyme was markedly increased by the addition of 2'-AMP. This increase thus would reflect a less mobile FAD binding to the enzyme. The degree of polarization for the *Azotobacter* transhydrogenase is higher than for the *Pseudomonas* enzyme at corresponding wavelengths (Fig. 6.9). The degree of polarization rapidly decreases between 400 and 370 nm. At wavelengths lower than 340 nm no very reliable results are obtained; the polarization remains, however, positive and becomes about 0.05-0.08 at 300 nm. It is noteworthy to see, however, the behaviour of \bar{p} in the region between 400 nm and 460 nm where there is a small although consistent increase in \bar{p} . The maximum $\bar{p} = 0.425$ is high, but not exceptionally high for a molecule of this size. The addition of about 10 mM potassium phosphate causes a small decrease in the degree of polarization. No effect of the subsequent addition of either NADP^+ or 2'-AMP is found. The higher degree of polarization of the *Azotobacter* enzyme compared to the *Pseudomonas* enzyme might reflect an essential difference in the flavin environment of the two enzymes. Addition of 2'-AMP to the *Pseudomonas* enzyme increases the maximum polarization degree of 0.38 to 0.42, a value close to the value normally found for the *Azotobacter* enzyme. This might explain that under standard assay conditions no stimulating effect of 2'-AMP is observed with the *Azotobacter* enzyme as this enzyme has already an active conformation. The decrease in polarization upon addition of phosphate seems relatively small to conclude anything about this.

The fine structure in the degree of polarization is also found in the pig heart lipoamide dehydrogenase (Visser et al., submitted for publication). It seems that due to vibrational coupling to some extent a small depolarization is induced.

From the difference in polarization values at the first and second excitation maxima an angle between the corresponding excitation vectors of 38° can be calculated. This value differs significantly from the value reported for pig heart lipoamide dehydrogenase and flavin in a solid matrix by Visser et al. (1974). So it can be concluded that this angle is depending on the environmental factors around the flavin and may be to some extent the presence of apolar or polar solvent groups.

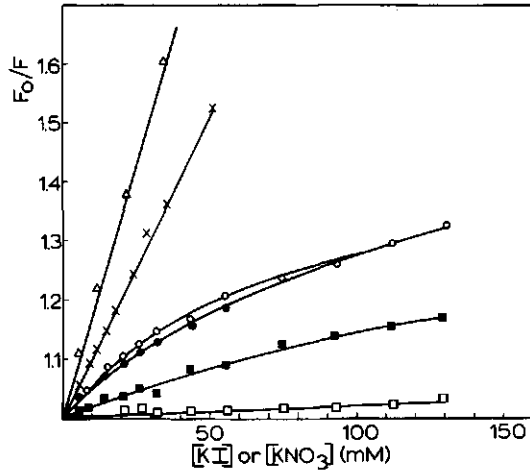


Fig. 6.10 Quenching of the protein bound flavin- and tryptophan emission by iodide and nitrate compared to the free compounds. The enzyme and FAD were dissolved in 50 mM Tris-HCl pH 7.6. Temp. 22°C.

	Excitation wavelength	Emission wavelength
Δ — Δ FAD + KI	440	510
X—X try + KI	295	350
o—o T.H. + KI	440	510
●—● T.H. + KI	295	510
■—■ T.H. + KI	295	340
□—□ T.H. + KNO ₃	440	510

6.2.6 Collisional quenching of the oxidized enzyme

Titration of the oxidized enzyme with KI (Winkler, 1968; Lehrer, 1971) shows that both fluorogenic chromophores of the enzyme (tryptophan and FAD) exhibit a small fluorescence quenching compared to the free compounds (Fig. 6.10). In order to exclude ionic strength effects, control quenching studies were also performed with KNO₃. No significant effect by this salt on the fluorescence of either the enzymebound or free flavin was observed in the concentration range used. Because of inner optical effects KNO₃ cannot be used as a quencher in the u.v. excitation experiments. The non-linear Stern-Volmer plot (1919) of the holo enzyme contrasts the straight line obtained for the free fluorogenic compounds. These results resemble those obtained by Visser et al. (1974) for the pig heart lipoamide dehydrogenase. As can be expected the quenching of the emission of the protein bound flavin by KI is the same upon excitation at 295 nm and at 440 nm.

The low quenching of the protein-bound chromophores compared to the free compounds can be explained by charge repulsion of the quencher (I^-) and the protein (Visser et al., 1974). It is, however, striking that phosphate causes a pronounced quenching of the protein-bound flavin fluorescence. Thus charge repulsion does not seem very likely. It might, therefore, also be suggested that the rather apolar environment of both the flavin and the tryptophan in the protein prevents an effective collisional quenching.

6.2.7 *Chemical reduction of the enzyme*

In order to study the groups involved in the reported four-electron reduced state of the enzyme (Van den Broek et al., 1971) anaerobic reduction studies of the enzyme were performed. The artificial electron donor dithionite and the reduced substrates NADH and NADPH were used. Titrations were carried out as described under Materials and Methods (Chapter 2). The enzyme used was freed from enzymebound $NADP^+$ by anaerobic dialysis with glucose-6-phosphate and glucose-6-phosphate dehydrogenase. Titration of the enzyme with dithionite resulted in a complete reduction of the flavin peak at one mole of reductant per mole of flavin. One clear isosbestic point at 332 nm was obtained (Fig. 6.11). After admitting air the oxidized spectrum is regained very quickly. Reduction of the enzyme with either NADH or NADPH results in a different course of the reduction. Titration curves soon deviate from linearity with both reductants (Fig. 6.12) and unreacted reductant appears in the solution as seen by the increase of absorbance at 332 nm.

Subsequent full reduction was obtained by addition of excess of dithionite. No accurate values for the stoichiometry of the reduction with NADPH or NADH can be obtained as extrapolation must be performed from a very short linear part of the titration curve. Using however the amount of unreacted reductant a correction can be made on the non-linearity of the curve. It can be calculated that full reduction is obtained by about one mole of either NADH or NADPH per mole of flavin. It must be noted that in case of the reduction by NADH and NADPH of the enzyme some scatter was present as seen in the 700-600 nm region. However, this scatter effect amounted only up to 18% of the absorbance at 440 nm. Thus the 1 : 1 stoichiometry is not significantly changed by the presence of this turbidity. These results do not confirm the stoichiometry as reported by Van den Broek et al. (1971) for the chemical reduction of the enzyme. These authors reported a 4 electron reduction per mole of flavin. It must, however, be noted that in case of the dithionite reduction no clear isosbestic point was obtained

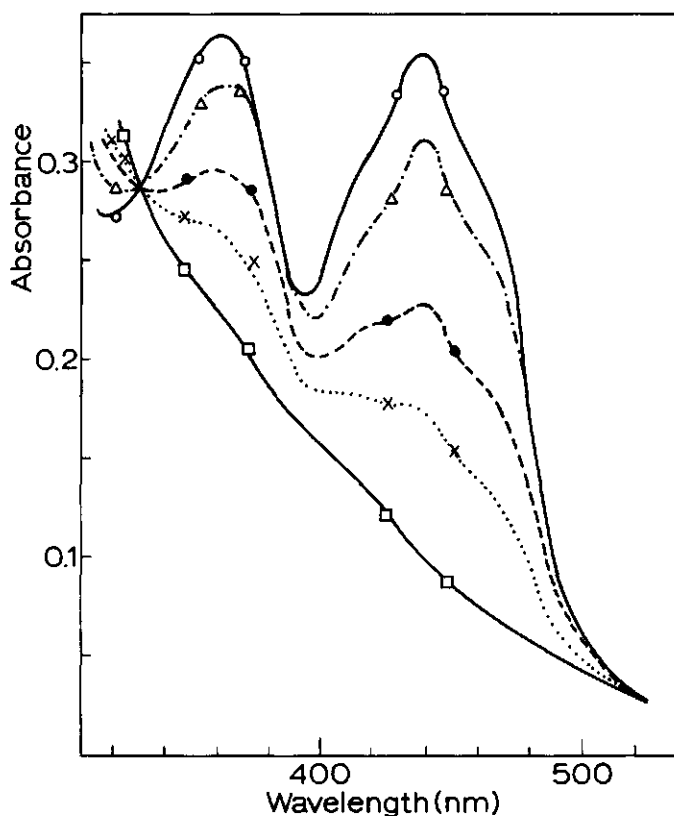


Fig. 6.11 Anaerobic reduction of *Azotobacter* transhydrogenase by subsequent additions of sodium dithionite. Enzyme in 50 mM Tris-HCl pH 7.6. The cuvette contained 6 moles of oxygen before the onset of the titrations.

○—○ oxidized enzyme; Δ---Δ 0.16 mole dithionite/mole flavin; ●---● 0.36 mole dithionite/mole flavin; X---X 0.7 mole dithionite/mole flavin; □—□ 1.0 mole dithionite/mole flavin.

After the addition of 1.0 mole dithionite/mole flavin no further decrease at 440 nm was obtained upon the addition of dithionite, and unreacted dithionite appeared as seen at 350 nm.

by these authors, and that some reduction is still present with an excess of dithionite. It might also be suggested that in case of the dithionite reduction reducing equivalents are used by tightly protein-bound NADP^+ . This would, however, imply that a clear increase in the 340 nm region would have to occur during the titration. However, such indications are not clear from the work of

Van den Broek et al. (1971). It is thus likely that the 4 : 1 stoichiometry instead of 2 : 1 is due to some impurity closely associated to the enzyme with no effect in the visible region.

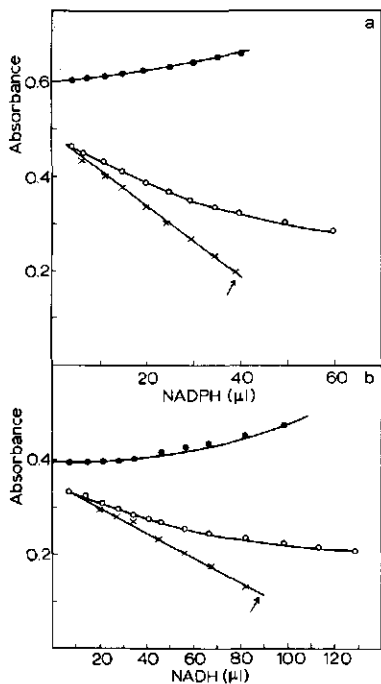


Fig. 6.12 Anaerobic reduction of Azotobacter transhydrogenase by the reduced substrates NADH or NADPH.

a. Reduction of 60 μ mole transhydrogenase flavin by NADPH (1.38 mM)

●—● unreacted reductant at 332 nm;

○—○ reduction of transhydrogenase flavin at 443 nm;

x—x calculated titration curve.

b. Reduction of 49 μ mole transhydrogenase flavin by NADH (0.53 mM).

●—● unreacted reductant at 332 nm;

○—○ reduction of transhydrogenase flavin at 443 nm;

x—x calculated titration curve.

The arrows indicate the endpoint calculated from the dithionite titration data.

Appendix

For the calculation of the dissociation constant of 2'-AMP in the presence of phosphate the following considerations were used.

The fluorescence in the presence of phosphate alone comes from free enzyme (E) and phosphate-bound enzyme (EP_i). In the presence of both phosphate and 2'-AMP the fluorescence comes from E, EP_i and E-AMP.

As 2'-AMP in the absence of phosphate does not give any change of the fluorescence it is assumed that E and E-AMP do have the same fluorescence intensity.

Thus:

$$1: E + P_i \rightarrow EP_i \text{ with } K_p = \frac{E \cdot P_i}{EP_i} \quad \text{and } E = \frac{K_p}{P_i} \cdot EP_i$$

$$2: E + AMP \rightarrow EAMP \text{ with } K_a = \frac{E \cdot AMP}{EAMP} \quad \text{and } EAMP = \frac{E \cdot AMP}{K_a}$$

substitution of E gives:

$$3: EAMP = \frac{K_p}{P_i} \cdot EP_i \cdot \frac{AMP}{K_a}$$

4: The fluorescence (F) in the presence of phosphate and 2'-AMP can be described by the sum of the fluorescence of the following compounds:

$$\begin{aligned} 5: F &= E + EAMP + EP_i \\ &= \frac{K_p}{P_i} \cdot EP_i + \frac{K_p}{P_i} EP_i \frac{AMP}{K_a} + EP_i \\ &= \frac{EP_i}{P_i} \left((K_p + P_i) + K_p \frac{AMP}{K_a} \right) \end{aligned}$$

The fluorescence can also be described by

$$F = a E_0 + b EP_{i \rightarrow \infty} \quad \text{with } a + b = 1,$$

in which E_0 is the fluorescence of the enzyme in the absence of phosphate and $EP_{i \rightarrow \infty}$ the fluorescence of the enzyme-phosphate complex at infinite P_i concentration. This makes it possible to calculate EP_i and substitution in (5) gives the value for K_a as K_p is known.

SUMMARY

Azotobacter vinelandii transhydrogenase shows a pronounced polymerizing-depolymerizing character (Chapter 3 and 5). Several factors seem to influence this phenomenon. With purified enzyme, obtained by a new purification method (Chapter 3), several parameters influencing the association-dissociation behaviour were investigated (Chapter 5).

It was found that dissociation of transhydrogenase can be obtained at a minimum concentration of 1 μM of the substrate NADP^+ . A reversal of this effect is obtained with NADPH depending on the initial concentration of NADP^+ used. No clear effect of 2'-AMP on the structure is found in contrast to the results obtained with the *Pseudomonas* enzyme (Louie et al., 1972). Increase of the pH to about pH 9.5 results in a dissociation of the polymerized structures present in purified transhydrogenase as described by Middleditch et al. (1972).

A very marked associating effect of divalent metal ions is found (Chapter 3 and 5). Large aggregates are formed, still catalytically active, that can be seen with the electron microscope and even under the phase contrast microscope (Chapter 5).

The aggregates thus formed are not soluble, and addition of EDTA does not result in a clear reversal of the effects induced by the metal. Besides an associating effect divalent metal ions also cause some dissociation of the filamentous structures into rosettes, rings and cylinders with a perpendicular striping (Chapter 5).

The effect on the highly polymerized structures of thiol reducing agents was investigated. A clear dissociating effect of β -mercaptoethanol was obtained while reduced lipoamide and dithiothreitol are much less effective (Chapter 5). Addition of ammonium sulphate to purified transhydrogenase results initially in dissociation followed by the formation of microcrystalline structures (Chapter 5). As the effects of the reagents on the morphological structure are totally different, it must be concluded that these result from a combination of different types of binding (interaction). The dissociating effect of NADP^+ at low concentration points to a strong effect of this nucleotide on the total structure of the enzyme as a very local interaction (at the catalytical side only) hardly can result in such a drastic change in appearance.

As divalent metal ions cause a pronounced association this leads to the conclusion that probably charge neutralization of negative groups within the protein causes this phenomenon. On the other hand decrease of positive charges (upon increasing the pH) results in dissociation of the enzyme.

The role of thiol reducing agents also remains obscure as only β -mercaptoethanol has a pronounced effect whereas a more powerful reducing agent as dithiothreitol has much less effect. This probably must be attributed either to a difference in steric hindrance or the differences in hydrophobicity of these agents. The significance of the different association-dissociation steps for the catalytic mechanism is not clear at this time. In the catalytic reaction it is found that divalent metal ions have a pronounced effect on the kinetic patterns (Chapter 3).

It is discussed that these effects must be due to modification of the enzyme structure rather than of the substrate structure.

A remarkable inhibition by anions is also found in the reduction of NADP^+ or S-NAD^+ by NADH . From the kinetic inhibition picture obtained with phosphate and sulphate a pingpong mechanism might be favoured but the inhibition by nitrate points to the existence of a rapid ternary complex mechanism (Chapter 3).

Spectral studies of Van den Broek et al. (1971) showed a pronounced binding of NADP^+ to the oxidized enzyme and an absence of 2'-AMP binding. It is however found (Chapter 6) that the spectral effects of NADP^+ and 2'-AMP strongly depend on the presence of phosphate. The fluorescence emission quenching by NADP^+ is much stronger in the presence of phosphate than in the absence and concomitantly the dissociation constant becomes lower in the presence of phosphate than in the absence. From the effect on the fluorescence emission it can be derived that there are two binding sites for NADP^+ . Also a more pronounced shift of the emission peak towards shorter wavelengths is observed in the presence of phosphate. No effects of 2'-AMP on the emission characteristics are found unless phosphate is present, while the quenching effect induced by phosphate is reversed by 2'-AMP.

By studying the absorption difference spectrum also binding of phosphate can be observed; addition of 2'-AMP reverses the spectral effects initially induced by phosphate (Chapter 6). The chemical reduction of the enzyme was reported to require two moles of reductant per mole of enzyme bound flavin (Van den Broek et al., 1971). Reexamination of these experiments show however that 1 mole of reductant suffices to get complete reduction of the enzyme bound flavin. (Chapter 6).

An interesting effect of the ionic strength on the equilibrium constant of the transhydrogenase catalyzed reaction was found (Chapter 4). The shift of this constant in relation to the ionic strength and hence the chemical nature of the products and substrates involved is discussed. It is concluded that the folded form of the pyridine nucleotides is responsible for the slope as obtained in the $\log K$ vs. \sqrt{I} plot. The conformation of the pyridine nucleotides was studied with N.M.R. (Chapter 4), in the absence and presence of neutral salt. No definite conclusions can be drawn from the data obtained but both electrostatics interactions and folding do attribute to the proton shifts obtained.

SAMENVATTING

Azotobacter vinelandii transhydrogenase heeft een sterke neiging tot polymerisatie-depolymerisatie, zoals beschreven wordt in hoofdstuk 3 en 5. Er zijn verschillende factoren van invloed op dit verschijnsel. Enkele van de parameters die van belang zijn bij de associatie-dissociatie zijn nader onderzocht (hoofdstuk 5).

Het bleek dat de dissociatie van transhydrogenase bewerkstelligd kon worden bij een minimum substraatconcentratie van $1 \mu\text{M NADP}^+$. Omkering van dit dissociërende effect kan verkregen worden door NADPH toe te voegen waarbij het associërende effect afhangt van de initiële concentratie NADP^+ . In tegenstelling tot de resultaten van Louie et al. (1972) met *Pseudomonas* transhydrogenase heeft 2'-AMP geen duidelijk effect op de morfologische structuur van het enzym uit *Azotobacter*. Verhoging van de pH tot ongeveer pH 9.5 resulteert in een dissociatie van de lange draden zoals die aanwezig zijn in het gezuiverde enzym bij fysiologische condities, zoals ook beschreven door Middleditch et al. (1972).

Tweewaardige metaalionen hebben een uitgesproken associërend effect op het enzym (hoofdstuk 3 en 5). Er worden grote, katalytisch nog actieve aggregaten gevormd die zowel onder de electronenmicroscopie als onder de fase contrast microscopie goed zichtbaar zijn (hoofdstuk 5). De aldus gevormde aggregaten zijn niet (of slecht) oplosbaar en toevoegen van EDTA geeft geen duidelijke omkering van het effect zoals het door metaal geïnduceerd is. Behalve dat tweewaardige metaalionen een associërend effect hebben, worden er tevens dissociatieproducten waargenomen zoals rozetten, ringen en cilindervormige strepen (hoofdstuk 5).

Het effect van thiol-reducerende agentia op de gepolymeriseerde structuur werd ook onderzocht. Hierbij werd een duidelijk dissociërend effect van β -mercaptoethanol gevonden terwijl gereduceerd lipoamide en dithiothreitol een veel minder duidelijk effect teweegbrengen (hoofdstuk 5). Toevoegen van ammoniumsulfate aan het gezuiverde enzym resulteert aanvankelijk in dissociatie waarna de vorming van microcrystalline structuren optreedt (hoofdstuk 5).

Daar het effect van de verschillende agentia op de morfologische structuur totaal verschillend is, moet wel geconcludeerd worden dat dit resulteert uit

een combinatie van verschillende soorten binding (interactie). Het dissociërende effect van NADP^+ bij lage concentratie wijst op een duidelijk effect van dit nucleotide op de totale structuur van het eiwit, aangezien een zeer lokale interactie (alleen bij het katalytisch centrum) nauwelijks kan resulteren in zo'n duidelijk verschil in aggregatietoestand.

Daar tweewaardige ionen een duidelijk associërend effect hebben, kan geconcludeerd worden, dat ladingsafscherming van negatieve groepen dit effect tot gevolg heeft. Het is evenwel ook zo dat een toename van de positieve lading van de aminozuren onder invloed van pH-verhoging resulteert in een dissociatie van het enzym.

Het effect van de thiol-reducerende agentia is niet geheel duidelijk, aangezien dithiothreitol - dat een krachtiger reductiemiddel is dan β -mercaptoethanol - geen duidelijk effect heeft. Waarschijnlijk moet het verschil in effect meer gezocht worden in een verschil van sterische hindering en/of verschil in hydrophobiciteit van deze agentia. Het belang van de verschillende associatie-dissociatie toestanden voor het katalytisch mechanisme is nog niet duidelijk. Wel wordt een duidelijk effect van de tweewaardige metaalionen op het kinetisch gedrag van het enzym gevonden (hoofdstuk 3). Het wordt hierbij aannemelijk gemaakt dat deze effecten eerder toe te schrijven zijn aan een verandering van het eiwit dan aan een verandering van het substraat.

Een heel duidelijke remming door anionen wordt gevonden in de reductie van NADP^+ of S-NAD^+ door NADH . De remmingspatronen die verkregen worden met fosfaat en sulfaat wijzen op een ping-pong-mechanisme, maar de nitraat remmingspatronen wijzen eerder in de richting van een snel-ternair-complex mechanisme (hoofdstuk 3).

Spectrale studies van Van den Broek et al. (1971) geven een duidelijke binding van NADP^+ aan het geoxideerde enzym te zien, terwijl 2'-AMP niet bindt. In hoofdstuk 6 zal echter worden aangetoond dat de bindingskarakteristieken van NADP^+ en 2'-AMP sterk afhangen van de aanwezigheid van fosfaat. De fluorescentie emissie doving door NADP^+ is veel sterker in de aanwezigheid van fosfaat dan in de afwezigheid daarvan, en hierbij is tevens de dissociatie constante lager in de aanwezigheid van fosfaat, dan in de afwezigheid. Uit het effect van de fluorescentie emissie quenching kan geconcludeerd worden dat er twee bindingsplaatsen voor NADP^+ zijn. In de aanwezigheid van fosfaat treedt onder invloed van NADP^+ ook een opmerkelijke verschuiving van de fluorescentie emissiepiek

op naar kortere golflengten. Er werd geen effect van 2'-AMP alleen op de fluorescentie emissie karakteristieken gevonden. In aanwezigheid van fosfaat werd echter de door fosfaat geïnduceerde fluorescentie doving nagenoeg ongedaan gemaakt door 2'-AMP toe te voegen. Ook uit studies van het absorptie spectrum blijkt een binding van fosfaat aan het enzym, en toevoegen van 2'-AMP keert de spectrale effecten die geïnduceerd zijn door fosfaat om (hoofdstuk 6).

Bij het bestuderen van het effect van ATP op de ligging van het evenwicht van de pyridine nucleotiden werd gevonden dat de ligging van dit evenwicht (de evenwichtsconstante) afhankelijk was van de gebruikte ionsterkte (hoofdstuk 4). De verschuiving van deze constante in relatie tot de ionsterkte en dientengevolge in relatie tot het chemische karakter van de producten en substraten wordt besproken. Hierbij wordt geconcludeerd dat de gevouwen vorm van de pyridine nucleotiden verantwoordelijk is voor de helling zoals deze gevonden wordt in de $\log K$ vs \sqrt{I} grafiek. De conformatie van de pyridine nucleotiden werd met de n.m.r. bestudeerd waarbij vooral de verschillen die optraden als gevolg van de aan- en afwezigheid van zout van belang waren (hoofdstuk 4). De aldus verkregen n.m.r.-gegevens leveren niet genoeg zekerheid om hieraan vergaande conclusies te verbinden. Het werd evenwel duidelijk dat zowel vouwing als electrostatische interacties van belang zijn bij de protonen shifts die waargenomen werden.

REFERENCES

- Apps, D.K., *Biochim.Biophys.Acta*, 320 (1973) 379.
- Asano, A., Imai, K. and Sato, R., *Biochim.Biophys.Acta*, 143 (1967) 477.
- Ball, E.G. and Cooper, O., *Proc.Natl.Acad.Sci. U.S.*, 43 (1959) 357.
- Benesi, H.A. and Hildebrand, J.A., *J.Amer.Chem.Soc.*, 71 (1949) 2703.
- Bergmeyer, H.U., *Methods of Enzymatic Analysis*, Academic Press, London, (1963) p. 1029.
- Bielmann, J.F. and Samana, J.P., *FEBS Letters*, 38 (1973), 175.
- Blumenstein, M. and Raftery, M.A., *Bioch.*, 11 (1972) 1643.
- Blumenstein, M. and Raftery, M.A., *Bioch.*, 12 (1973) 3585.
- Bragg, P.D., Davies, P.L. and Hou, C., *Biochem.Biophys.Res.Commun.*, 47 (1972) 1248.
- Bragg, P.D. and Hou, C., *FEBS Letters*, 28 (1972) 309.
- Brønsted, J.N., *Z. Physik.Chem.*, 102 (1922) 169.
- Catterall, W.A., Hollis, D.P. and Walter, C.F., *Biochem.*, 8 (1969) 4032.
- Chen, R.F., *Anal.Biochem.*, 20 (1967) 339.
- Chung, A.E., *J. Bacteriol.*, 102 (1970) 438.
- Chung, A.E. and Middleditch, L.E., *Arch.Biochem.Biophys.*, 152 (1972) 539.
- Cleland, W.W., *Biochim.Biophys.Acta*, 67 (1963) 104.
- Cohen, P.T., *Dissertation Brandeis University Microfilms Inc.*, Ann Arbor, No. 67-16542.
- Cohen, P.T., and Kaplan, N.O., *J.Biol.Chem.*, 245 (1970) 2825.
- Colman, R.F., *Anal.Biochem.*, 46 (1972) 358.
- Colowick, S.P., Kaplan, N.O., Neufeld, E.F. and Giotti, M.M., *J.Biol.Chem.*, 195 (1952) 95.
- Danielson, L. and Ernster, L.: *In Energy-linked functions of mitochondria.* Edited by B. Chance. Academic Press Inc., New York 1963, p. 157.
- Dixon, M. and Webb, E.C.: *In the Enzymes.* Edited by Academic Press Inc., New York, 1964, second edition, p. 361.
- Donohue, J. and Trueblood, K.N., *J.Mol.Biol.*, 2 (1960) 363.
- Donovan, J.W.: *in Physical principles and techniques of protein chemistry,* part A (1969), ed. Sydney J.Leach.Academic Press New York, p. 164.
- Durham, A.C.H. and Finch, J.T., *J.Mol.Biol.*, 67 (1972) 307.
- Ellis, P.D., Fishee, R.R., Dunlap, R.B., Zens, A.P., Bryson, T.A. and Williams, T.J., *J.Biol.Chem.*, 248 (1973) 7677.
- Ellman, G.L., *Arch.Biochem.Biophys.*, 82 (1959) 70.

- Engel, P.C. and Dalziel, K., *Bioch.J.*, 105 (1967) 691.
- Estabrook, R.W., Hommes, F. and Gonze, J.: In *Energy-linked functions of mitochondria*. Edited by B. Chance. Academic Press Inc., New York (1963) p. 143.
- Estabrook, R.W., Fugman, U. and Chance, E.M., *5th Int.Congr.Bioch., Mosc.* 9 522 (1961).
- Fisher, R.J. and Sanadi, D.R., *Biochim.Biophys.Acta*, 245 (1971) 34.
- Fisher, R.J., Lam, K.W. and Sanadi, D.R., *Biochem.Biophys.Res.Comm.*, 39 (1970) 1021.
- Fisher, R.R. and Guillory, R.J., *J.Biol.Chem.*, 246 (1971a) 4679, 246 (1971b) 4687.
- Fisher, R.R. and Kaplan, N.O., *Biochemistry*, 12 (1973) 1182.
- Foust, G.P., Burleigh, B.D., Jr., Mayhew, S.G., Williams, C.H., Jr. and Massey, V., *Anal.Biochem.*, 27 (1969) 530.
- Freed, S., Neyfalth, E.A. and Tumerman, L.A., *Biochem.Biophys.Acta*, 143 (1967) 432.
- Frost, A.A. and Pearson, R.G., In *Kinetics and Mechanism*, John Wiley and Sons (1965) p. 151.
- Gornall, A.G., Bardawill, C.J. and David, M.M., *J.Biol.Chem.*, 177 (1949) 751.
- Griffith, P.R., Rye, M.J. and Alexander, J.G., *Can.J.Biochem.*, 48 (1970) 947.
- Hasson, E.P. and West, C.A., *Arch.Biochem.Biophys.*, 155 (1973) 258.
- Hollis, D.P., *Org.Magn.Resonance*, 1 (1969) 305.
- Hommes, F. and Estabrook, R.W., *Biochem.Biophys.Res.Comm.*, 11 (1963) 1.
- Imai, T., *J.Biochem.*, 73 (1973) 139.
- Itzhaki, R.F. and Gill, D.M., *Anal.Biochem.*, 9 (1964) 401.
- Jacobus, J., *Bioch.*, 10 (1971) 161.
- Jardetzky, O., Wade, N.G. and Fisher, J.J., *Nature*, 197 (1963) 183.
- Jardetzky, O. and Wade-Jardetzky, N.G., *J.Biol.Chem.*, 241 (1966) 85.
- Jones, C.W. and Redfearn, E.R., *Biochim.Biophys.Acta*, 143 (1967) 354.
- Jones, C.W. and Redfearn, E.R., *Biochim.Biophys.Acta*, 143 (1967) 340.
- Juckes, I.R.M., *Biochim.Biophys.Acta*, 229 (1971) 535.
- Kaplan, N.O., Colowick, S.P. and Neufeld, E.F., *J.Biol.Chem.*, 195 (1952) 107.
- Kaplan, N.O., Colowick, S.P., Zatman, L.J. and Ciotti, M.M., *J.Biol.Chem.*, 205 (1953) 31.
- Kaplan, N.O., Colowick, S.P. and Neufeld, E.F., *J.Biol.Chem.*, 205 (1953) 1.
- Kaplan, N.O., Swartz, M.N., Frech, M. and Ciotti, M.M., *Proc.Natl.Acad.Sci.*, 42 (1956) 481.

- Kawasaki, T., Satoh, K. and Kaplan, N.O., *Biochem.Biophys.Res.Commun.*, 17 (1964) 648.
- Keister, D.L. and Hemmes, R.B., *J.Biol.Chem.*, 241 (1966) 2820.
- Keister, D.L. and Yike, N.J., *Biochem.Biophys.Res.Commun.*, 24 (1966) 519.
- Klingenberg, M. and Schollmeyer, P., *5th Int.Congr.Biochem.*, Mosc. 5, 41 (1961), Pergamon Press, London.
- Klingenberg, M. and Slenczka, W., *Biochem.Z.*, 331 (1959) 486.
- Laurent, T.C., *Bioch.J.*, 89 (1963) 253.
- Lee, C.P. and Ernster, L., *Biochim.Biophys.Acta*, 81 (1964) 187.
- Lee, C.P., Simard-Duquesne, N., Ernster, L. and Hoberman, H.D., *Biochim.Biophys. Acta*, 105 (1965) 397.
- Lehrer, S.S., *Bioch.*, 10 (1971) 3254.
- Louie, D.D., Kaplan, N.O. and McLean, J.D., *J.Mol.Biol.*, 70 (1972) 651.
- Louie, D.D. and Kaplan, N.O., *Fed.Proc.*, 28 (1969) 342.
- Louie, D.D. and Kaplan, N.O.,: in *Pyridine-Nucleotide Dependent Dehydrogenases* (edited by H. Sund), Springer Verlag, Berlin, Heidelberg, New York, 1970, p. 351.
- Lubin, M., *J.Mol.Biol.*, 39 (1969) 219.
- Mackler, B. and Green, D.E., *Biochim.Biophys.Acta*, 21 (1956) 1.
- Massey, V. and Veeger, C., *Biochim.Biophys.Acta*, 48 (1961) 33.
- Massey, V. and Williams, C.H. Jr., *J.Biol.Chem.*, 248 (1965) 4478.
- McDonald, G., Brown, B., Hollis, D. and Walter, C., *Bioch.*, 11 (1972) 1920.
- Mellema, J.E., Van Bruggen, E.F.J. and Gruber, M., *Biochim.Biophys.Acta*, 140 (1967) 180.
- Middleditch, L.E. and Chung, A.E., *Arch.Biochem.Biophys.*, 146 (1971) 449.
- Middleditch, L.E., Atchison, R.W. and Chung, A.E., *J.Biol.Chem.*, 247 (1972) 6802.
- Miller, R.E., Shelton, E. and Stadman, E.R., *Archiv.Biochem.Biophys.*, 163 (1974) 155.
- Murthy, P.S. and Brodie, A.F., *J.Biol.Chem.*, 239 (1964) 4292.
- Navazio, F., Ernster, B.B. and Ernster, L., *Biochim.Biophys.Acta*, 26 (1957) 416.
- Olsen, J.A. and Anfinsen, C., *J.Biol.Chem.*, 202 (1953) 841.
- Orlando, J.A., Sabo, D. and Curnyn, C., *Plant Physiol.*, 41 (1966) 937.
- Papa, S., Tager, J.M., Francavilla, A. and Quagliariello, E., *Biochim.Biophys. Acta*, 172 (1969) 20.
- Polson, A., Potgieter, G.M., Largier, J.F., Mears, G.E.F. and Joubert, F.J., *Biochim.Biophys.Acta*, 82 (1964) 463.
- Quagliariello, E., Papa, S., Meyer, A.J. and Tager, J.M., *Proc.5th Meeting Fed. Europ.Biochem.Soc. Prague 1968*, Academic Press, London and New York, p. 335.

- Rydström, J., Teixeira da Cruz, A. and Ernster, L., *Eur.J.Bioch.*, 17 (1970) 56.
- Rydström, J., Teixeira da Cruz, A. and Ernster, L., *Eur.J.Bioch.*, 23 (1971) 212.
- Rydström, J., *Eur.J.Bioch.*, 31 (1972) 496.
- Rydström, J., Panov, A.V., Paradies, G. and Ernster, L., *Bioch.Biophys.Res. Commun.*, 45 (1971) 1389.
- Rydström, J., Hoek, J.B. and Höjeberg, B., *Biochem.Biophys.Res.Comm.*, 52 (1973) 421.
- Sarma, R.H. and Kaplan, N.O., *Biochem.Biophys.Res.Comm.*, 36 (1969) 780.
- Sarma, R.H. and Kaplan, N.O., *Bioch.*, 9 (1970^a) 539.
- Sarma, R.H. and Kaplan, N.O., *Bioch.*, 9 (1970^b) 557.
- Schwartz, E.R., Old, L.O. and Reed, L.J., *Biochem.Biophys.Res.Comm.*, 31 (1968) 495.
- Schweizer, M.P., Broom, A.D., Ts'o, P.O.P. and Hollis, D.P., *J.Amer.Chem.Soc.*, 89 (1968) 1042.
- Shen, M., Tagawa, K. and Arnon, D.L., *Bioch.Z.*, 338 (1963) 84.
- Song, P.S.: In *Flavins and Flavoproteins*. Edited by Henry Kamin, University Park Press, Baltimore (1971) Butterworths, London, p. 56.
- Spencer, R.D. and Weber, G., *Ann.N.Y.Acad.Sci.*, 158 (1969) 361.
- Stein, A.M., Kaplan, N.O. and Ciotti, M.M., *J.Biol.Chem.*, 234 (1959) 973.
- Stern, O. and Volmer, M., *Z.Physik*, 20 (1919) 183.
- Svedberg, T. and Pederson, K.O.: *The Ultracentrifuge*, Oxford University Press, New York, 1940.
- Sweetman, A.J. and Griffiths, D.E., *Bioch.J.*, 121 (1971) 125.
- Tchan, Y.T., Birch-Andersen, A. and Jensen, H.L., *Arch.Mikrobiol.*, 43 (1962) 50.
- Teixeira da Cruz, A., Rydström, J. and Ernster, L., *Eur.J.Bioch.*, 23 (1971) 203.
- Tissières, A., Hovenkamp, H.C. and Slater, E.C., *Biochim.Biophys.Acta*, 25 (1957) 336.
- Torreilles, J. and Crastes de Paulet, *Biochimie*, 55 (1973) 1077.
- Valentine, R.C., Shapiro, B.M. and Stadtman, E.R., *Bioch.*, 7 (1968) 2143.
- Van den Broek, H.W.J. and Veeger, C., *FEBS-Letters*, 1 (1968) 301.
- Van den Broek, H.W.J. and Veeger, C., In *Pyridine Nucleotide Dependent Dehydrogenase*, Edited by H. Sund, Springer Verlag, Berlin, Heidelberg, New York, 1970, p. 335.
- Van den Broek, H.W.J., Santema, J.S., Wassink, J.H. and Veeger, C., *Eur.J.Bioch.*, 24 (1971) 31.
- Van den Broek, H.W.J., Van Breemen, J.F.L., Van Bruggen, E.F.J. and Veeger, C., *Eur.J.Bioch.*, 24 (1971) 46.

- Van den Broek, H.W.J., Santema, J.S. and Veeger, C., *Eur.J.Bioch.*, 24 (1971) 55.
- Van den Broek, H.W.J., Veeger, C., *Eur.J.Bioch.*, 24 (1971) 63.
- Van den Broek, H.W.J., *Mededelingen Landbouwhogeschool Wageningen Nederland*, 71 (1971).
- Veeger, C., Krul, J., Bresters, T.W., Haaker, H., Wassink, J.H., Santema, J.S. and Kok, A., in *Enzymes: Structure and Function* (editors J. Drenth, R.A. Oosterbaan en C. Veeger), North-Holland/American Elsevier, Amsterdam, 29 (1972) 217.
- Velick, S.F.: in *Light and Life*, Edited by William D. McElroy and Bentley Glass, Baltimore. The Johns Hopkin Press 1961 p. 133.
- Velick, S.F., *J.Biol.Chem.*, 233 (1958) 1455.
- Vinograd, J., Brunner, R., Kent, R. and Weige, J., *Proc.Natl.Acad.Sci Washington*, 49 (1963) 902.
- Visser, A.J.W.G., Grande, H.J., Müller, F. and Veeger, C., *Eur.J.Bioch.*, 45 (1974) 99.
- Weber, G., *Nature* 180 (1957) 1409.
- Weber, G. and Bablouzian, B., *J.Biol.Chem.*, 241 (1966) 2258.
- Weber, K. and Osborn, M., *J.Biol.Chem.*, 244 (1969) 4406.
- Winkler, M.H., *Bioch.*, 8 (1969) 2586.
- Wyss, O., Neumann, M. and Socolofsky, M.D., *Biophys.Biochem.Cytol.*, 10 (1961) 555.
- Zanetti, G. and Williams, C.H. Jr., *J.Biol.Chem.* 242 (1967) 5232.